STUDIES OF CONNEXINS AND CONNEXIN-ASSOCIATED PROTEINS IN MOUSE RETINA

By

CRISTINA C. CIOLOFAN

A Thesis Submitted to
The Faculty of Graduate Studies
In Partial Fulfillment of the Requirements
For the Degree of

MASTER OF SCIENCE

Department of Physiology
University of Manitoba
Winnipeg, Manitoba, Canada

The Faculty of Graduate Studies
500 University Center, University of Manitoba
Winnipeg, Manitoba R3T 2N2

Phone: (204) 474 9377
Fax: (204) 474 7553
graduate_studies@umanitoba.ca

THE UNIVERSITY OF MANITOBA

FACULTY OF GRADUATE STUDIES

*****

COPYRIGHT PERMISSION PAGE

Studies of Connexins and Connexin-Associated Proteins in Mouse Retina

BY

Cristina C. Ciolofan

A Thesis/Practicum submitted to the Faculty of Graduate Studies of The University of Manitoba in partial fulfillment of the requirements of the degree

of

MASTER OF SCIENCE

TABLE OF CONTENTS

I. ACKNOWLEDGEMENTS

I have been once asked about the most important challenge of my life, and instead of considering a reply, I changed the subject. These days, the same question was brought to my attention and this time I took a moment to analyze it more carefully. Although pursuing an MD career back home was no easy deal, I think the greatest challenge was that of coming to Canada to finish my post-universitary studies. Leaving everything and everyone you know behind, coming half way across the world to start over in a perfectly strange country, with a different culture, different life-style, different language and let's not forget the different winters, proved to be a unique experience that could be hardly expressed in words.

Now that I am towards the end of my program here at the University of Manitoba, I would like to take this moment to thank all those who helped and inspired me in these two years.

First of all I would like to thank my supervisor Dr. James I. Nagy and my committee members, Dr. Elissavet Kardami, Dr Larry Jordan and Dr. Gunnar Valdimarsson. You have shown me what research really means, you have provided constant guidance and support.

My appreciation also goes to my colleagues Xinbo Li, Carl Olson, Brett McLean, Nora Nolette and Mihai Penes as well as to Dr. Janice Dodd, Mrs. Gail McIndless and Mrs. Judy Olfert.

Finally, I would like to thank my family for being there when I needed them the most.

II. ABSTRACT

Gap junctions are formed by astrocytes, oligodendrocytes and neurons in mammalian retina, and identification of the connexins expressed by these cell types has been the subject of numerous investigations. In particular, connexin 36 (Cx36) and connexin 45 (Cx45) expression has been previously reported in various types of retinal neurons, and connexin 57 (Cx57) expression has been reported in mouse horizontal cells based on lacZ reporter activity linked with the Cx57 promoter. Using newly developed antibodies, we examined Cx57 localization in mouse retina, association of Cx45 with zonula occludens-1 (ZO-1), and localization of Cx36 in relation to ZO-1 and Y-box transcription factor 3 (MsY3). The canine ortholog of MsY3 (ZONAB) was previously reported to interact with ZO-1 in canine MDCK cells. By immunofluorescence, immunolabelling of Cx57 in wild-type mice was restricted to the outer plexiform layer, where it was co-localized with the horizontal cell marker calbindin, and labelling was absent in Cx57 knockout mice. Cx57-positive puncta were almost always found in close proximity or adjacent to labelling of the protein bassoon, which is a marker of ribbon synapses at rod spherules and cone pedicles. Cx57 was also found in close proximity to, but lacking overlap with, Cx36-positive puncta, particularly at bassoon-positive rod spherules. No overlapping association was found between Cx57 and ZO-1. Cx45 was distributed only in the inner plexiform layer (IPL), where it was partially co-localized with ZO-1, but exhibited little overlap with Cx36. Antibody against MsY3/ZONAB produced punctate fluorescence immunolabelling restricted to IPL. Double labelling indicated substantial Cx36/ZO-1 co-localization, as we previously reported, as well as Cx36/ZONAB co-localization and ZO-1/ZONAB co-localization. There was little association of Cx45 with ZONAB. In Cx36

knockout mice showing an absence of labelling for Cx36, immunolabelling of ZO-1 and ZONAB in most regions of the IPL was reduced compared to that seen in wild-type mice, except in the outer part of this layer, where ZO-1/ZONAB labelling and co-localization persisted. These results indicate differential distributions of connexins and connexin-associated proteins in mammalian retina.

III. LIST OF ABBREVIATIONS

aa, amino acids

Ab, antibody

β, beta

CNPase, monoclonal anti-2,'3'-cyclic nucleotide 3' phosphodiesterase

CNS, central nervous system

Cx, connexin

E, extracellular loop of a multi-pass transmembrane protein

EM, electron microscopy

FITC, fluorescein isothiocyanate

FL, full length

FRIL, freeze-fracture replica immunogold labelling

GCL, ganglion cell layer

GJIC, gap junction intercellular communication

GST, glutathione-S-transferase

IHC, immunohistochemistry

INL, inner nuclear layer

IP, immunoprecipitation

IPL, inner plexiform layer

kDa, kilodalton

KO, knock out

LM, light microscopy

M, molar

MAGUK, membrane associated guanylate kinase

MDCK, Madin–Darby Canine Kidney

ml, milliliter

mM, millimolar

mRNA, messenger ribonucleic acid

MsY3, mouse Y-box transcription factor 3

MsY4, mouse Y-box transcription factor 4

NGS, normal goat serum

OLM, outer limiting membrane

ONL, outer nuclear layer

OPL, outer plexiform layer

PAGE, polyacrylamide gel elecrophoresis

PB, phosphate buffer

PDZ, postsynaptic protein PSD-95/Drosophila junction protein Disc-large/tight junction protein ZO-1

pH, potential of hydrogen

PVDF, polyvidinylidene difluoride

SDS-PAGE, sodium dodecylsulphate polyacrylamide gel electrophoresis

TBS, 50 mM Tris-HCl, pH 7.4 with 1.5% sodium chloride

TBSTr, 50 mM Tris-HCl, pH 7.4, 1.5% NaCl, 0.3% Triton X-100

TBSTw, 20 mM Tris-HCl, pH 7.4, 150 mM NaCl with 0.2% Tween-20

Tr, truncated

μm, micron

WT, wild type

ZO-1, zonula occludens-1

ZONAB, ZO-1 associated nucleic acid-binding protein

IV. GENERAL INTRODUCTION

IV.1. Gap junctions

If for the rapid progress of modern society, technology has given us the internet, for the development and survival of multicellular organisms, evolution has given us other intricate means of communication resulting in exquisite coordination of intercellular activity. One such way of direct communication is achieved by the sharing of informational molecules through intercellular channels called gap junctions.

Gap junctions are dynamic structures, involved in growth control, regulation of development, metabolic coordination and synchronization of cellular physiological activities. Gap junctions exist in both invertebrates and vertebrates and similar communicating pathways have been described in higher plants (Kumar and Gilula, 1996). Ions, metabolites and second order messenger molecules are selectively allowed to pass between neighbouring cells via functional gap junction channels (Bruzzone et al., 1996; Goodenough et al., 1996). Each of the intercellular channels is formed by the docking of two hemichannels or connexons contributed by the two adjacent cells. The connexon is a hexameric structure resulting from the oligomerization of protein subunits called connexins, which are characterised by selective cell type expression patterns.

At certain intercellular locations, gap junctional channels tend to aggregate, forming gap junctional plaques, which can be visualised by means of freeze-fracture EM or freeze-fracture replica immunogold labelling (FRIL). Not every cell that expresses connexins capable of assembling into connexons can form functional communicating

channels with its neighbours. Functional gap functional intercellular communication (GJIC) can be determined through certain techniques including intercellular movement of dyes, tracers or current. Different channels formed from different connexin types exhibit a wide range of conductances and are selectively permeable to the intercellular passage of molecules (Bruzzone et al., 1996; Goodenough et al., 1996).

IV.2. Family of connexins

To date, 20 different connexin genes have been described in the murine genome, compared to 21 connexin genes found in the human genome (Eiberger et al., 2001; Willecke et al., 2002; Sohl and Willecke, 2004). Connexins are transmembrane proteins containing a well-conserved amino-terminal domain, four transmembrane domains termed M1-M4, one cytoplasmic loop, two extracellular (E1 and E2) domains and one carboxy- terminal domain (Goodenough, 1996; Sohl and Willecke, 2004). E1 and E2 are involved in connexon-connexon recognition and interaction, and contain three conserved cysteine residues capable of forming important disulfide bridges (Kumar and Gilula 1996; Evans and Martin, 2002). The cytoplasmic and the C-terminal regions have been suggested as important regulatory domains since they have the highest variation among connexins. The hemichannels can be formed from a single type of connexin (homomeric) or different types (heteromeric), while the gap junctions are divided into homotypic (containing identical connexins on each side of coupled cells) or heterotypic (connexons composed of different connexins in each of two coupled cells).

Gap junctions formed between the same cell types are called homologous, while those between different cell types are referred to as heterologous.

This provides diversity, allowing the formation of a wide variety of gap junctions, with distinct size-dependent junctional permeability and conductance properties (Veenstra, 1996; Kumar and Gilula, 1996; Willecke et al., 2002).

Gap junctional communication is essential in physiological processes such as electrical coupling in the nervous and cardiovascular systems, metabolic cooperation during embryonic development and adaptive tissue response (Paul, 1996; Evans and Martin, 2002; Rohr, 2004). Although still controversial, recent studies have indicated that non-junctional hemichannels have important functions as well; they can open under certain conditions and may help mediate paracrine and/or autocrine signalling (Bennett et al., 2003; Saez et al., 2003).

Mutations in connexins have been associated with the occurrence of numerous diseases. Charcot-Marie-Tooth disease is a severe peripheral neuropathy resulting from mutations in Cx32, while, skin diseases, genetic deafness, cataract and cardiovascular malformations are associated with mutations in Cx26, Cx30, Cx31, Cx46, Cx50 and Cx43 (Kumar and Gilula, 1996; Evans and Martin 2002; Wei et al., 2004).

Downregulation of Cx43 and Cx45, measured as mRNA and levels of protein, have been shown to be present in the end-stage heart failure, while in post-ischemic myocardium, a decrease in cardiac gap junctional communication was observed (Kieval et al., 1992; De Maio et al., 2002).

Furthermore, changes in connexin expression and function are associated with diverse brain pathologies including Alzheimer, Huntington and epilepsy (Nagy et al., 1996; Vis et al., 1998; Sohl et al., 2000).

IV.3. Gap junctions in retina

Three types of synapses are found in retina: ribbon/invaginating synapses, conventional/flat synapses and electrical synapses (gap junctions).

Electrical coupling in the retina is achieved by means of gap junctional communications between various members of all five major classes of retinal neurons (Söhl *et al.*, 2000), which are classified into rod and cone photoreceptors, ON and OFF cone bipolar cells, rod bipolar cells, horizontal cells, different classes of amacrine cells and ON and OFF ganglion cells. The diagram representing the cellular architecture of the retina is presented in Figure 1.

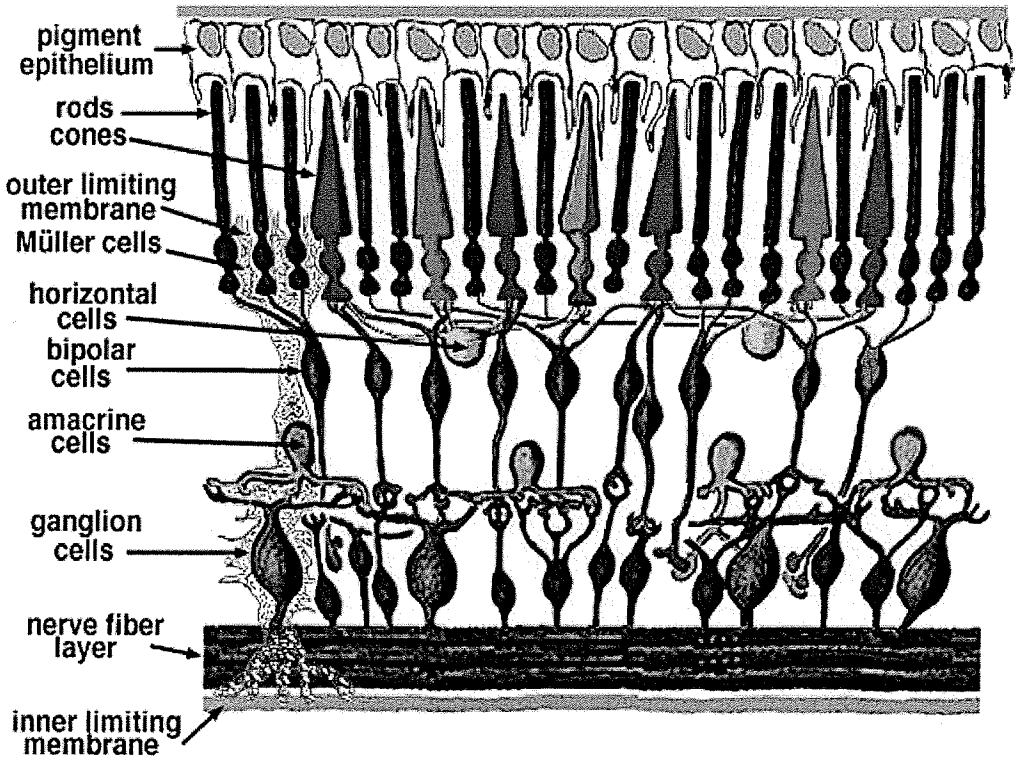

Fig.1

The presence of gap junctions in neurons and supporting cells of the vertebrate retina has been intensely studied by tracer injection methods, physiological recordings and electron microscopy (Kolb, 1970, 1974, 1977, 1979; Vaney, 1994, 1997; Cook and Becker, 1995; Xin and Bloomfield, 1997), but the identity of all the connexin proteins that comprise these gap junctions is still unknown. There is considerable data regarding the distribution and electrical properties of retinal gap junctions as well as their regulation by neurotransmitters and levels of ambient illumination (Vaney, 1994, 1996; Cook & Becker, 1995; Sterling, 1995; Baldridge et al., 1998). Xin and Bloomfield (1999) demonstrated that horizontal cells were coupled maximally under conditions of dim scotopic illumination and that the coupling was significantly reduced in either the dark-adapted retina or with increasing mesopic illumination. Various studies have shown that the coupling between A-type horizontal cells can be reduced by application of either dopamine (Hampson et al., 1994), nitric oxide (Xin and Bloomfield, 1999), or retinoic acid (Weiler et al., 1999), in agreement with earlier studies on non-mammalian horizontal cells (for review, see Baldridge et al., 1998). The release of dopamine increases with ambient illumination in the mammalian retina (Boelen et al., 1998; Godley and Wurtman, 1988). The coupling of the B-type horizontal cells was apparently unaffected by exogenous dopamine (Mills and Massey, 1997), suggesting that the light-induced uncoupling of these cells is not mediated by dopamine. Intracellular recordings in the rat retina have shown that exogenous dopamine narrows the receptive field of the horizontal

cells, consistent with a decrease in gap junctional permeability (Hankins and Ikeda, 1991).

Tracer coupling experiments (Vaney, 1991) have shown that gap junctional communication is established more often between neurons of the same type, but they are also present between different neuronal types in the retina. Homologous gap junctions are present between cone pedicles, rod spherules, cone bipolar cells, horizontal cells, same types of amacrine cells and same types of ganglion cells (Raviola and Gilula, 1975; Kolb, 1977, Kolb and Nelson, 1984, 1986; Tsukamoto et al., 2001; Mills et al., 2001; Lee et al., 2003; Hu and Bloomfield, 2003; Schubert et al., 2005). Heterologous gap junctions are established between rods and cones, between ON-cone bipolar cells and the AII amacrine cell, between different types of amacrine cells, between different types of bipolar cells and between some types of ganglion cells and various amacrine cell subtypes (Raviola and Gilula, 1973; Vaney, 1991, 1994; Penn et al, 1994; Vaney et al., 1998; Vaney and Weiler, 2000; Tsukamoto et al., 2001; Feigenspan et al., 2001, 2004). Nevertheless, some cell types do not have gap junctions; rod bipolar cells and starburst amacrine cells are two examples (Vaney, 1994; Feigenspan et al., 2004).

Gap junctions mediating homologus and heterologus coupling have also been described between retinal glia cells (Vaney, 1994; Mobbs et al., 1988; Robinson et al., 1993; Dermietzel and Spray, 1998; Zahs et al., 2003), as well as between pigment epithelial cells in the vertebrate retina (Janssen-Bienhold et al., 1998).

In the mammalian retina, extensive processing of chromatic and spatiotemporal information occurs. The visual information is transmitted from the photoreceptors to the ganglion cells in separate parallel channels, the ON (detecting light areas on dark

backgrounds) and OFF-channels (detecting dark areas on light backgrounds), involved in the transmission of light and dark signals through the retina, respectively. The outer plexiform layer (OPL) of the mammalian retina is the region where synaptic interplay between horizontal, bipolar and photoreceptor cells occurs (Missotten, 1965; Kolb, 1970, 1974, 1977), whereas in the inner plexiform layer (IPL), the synapses are formed between bipolar, amacrine and ganglion cells (Kolb, 1979; Maxeiner et al., 2005; Schubert et al., 2005). In the retina, photoreceptor, bipolar and ganglion cells are responsible for spreading the information from rods and cones using vertical pathways, whereas horizontal and amacrine cells are involved in lateral distribution of information.

The classical pathway for rod signals in the mammalian retina is: rods-rod bipolar cells-AII amacrine cells-ON cone bipolar cells- ganglion cells, and the key element of this pathway is gap junctional coupling between AII amacrine cells and ON-cone bipolar cells (Strettoi et al., 1992; Feigenspan et al., 2001; Deans et al., 2002). An alternative pathway for rod signals is the direct signal transmission from rods to cones via gap junctions and then to the inner retina via cone bipolar cells (Smith et al., 1986; DeVries et al., 1995). A third pathway for rod signals has recently been described (Tsukamoto et al., 2001; Hack et al., 2001), with the putative OFF-cone bipolar cells making flat contacts at the rod spherules present in the innermost part of OPL (accounting for 5-20% of the total spherules), therefore transmitting the scotopic information to OFF-ganglion cells, thus bypassing the rod bipolar cells.

IV.4. Functions of retinal electrical synapses

The wide variation of coupled cell networks suggests that gap junctions have diverse roles in retinal processing. Coupling has been shown to play an essential role in visual

processing, allowing the retina to operate efficiently in various lighting conditions. Electrotonic coupling mediated by gap junctions has been proposed to be responsible in retina for neuronal adaptation (Sterling, 1995; Weiler, 1996, Weiler et al., 2000). Also, the coupling is important for the establishment of receptive field size in some neurons, such as horizontal cells (Teranishi et al., 1983; Piccolino et al., 1984) and some amacrine cells (Bloomfield et al., 1997), for noise reduction, synchronizing neuronal firing, and for the transmission of rod signals to the ganglion cells in mammals. In photoreceptor cells, coupling plays important roles in spatial processing and noise filtering.

The importance of electrical coupling in retina has been demonstrated by using Cx36- and Cx45-deficients mice. It has been shown that gap junctional coupling between Cx36-positive-AII amacrine cells and Cx45-positive ON cone bipolar cells represent a key element of the rod pathway, through which scotopic signals from rod photoreceptor cells are transmitted to ganglion cells. This pathway was impaired in Cx36- and Cx45-deficient mice (Güldenagel et al., 2001; Deans et al., 2002; Maxeiner et al., 2005), demonstrating the important role of the two proteins in the mouse visual pathway, without which perception of light is severely impaired.

IV.5. Connexins in retina

The identity of all of connexin proteins that form gap junctions between retinal neurons and glia cells is unknown.

So far, mRNAs for Cx26, Cx31, Cx32, Cx36, Cx37, Cx40, Cx43, Cx45, Cx50 and Cx57 (Jones et al., 1992; Yancey et al., 1992; Johansson et al., 1997; Condorelli et al., 1998; Janssen-Bienhold et al., 1998; Gao and Spray, 1998; Schutte et al., 1998; Shöl et

al., 1998, 2000; Manthey et al., 1999; Güldenagel et al., 2000; Deans and Paul, 2001; Matesic et al., 2003; Huang et al., 2005) has been reported in mammalian retina, and immunoblot and immunofuorescence analyses using specific anti-connexin antibodies indicated the presence of Cx36, Cx37, Cx40, Cx43 and Cx45 proteins (Güldenagel et al., 2000, 2001; Sohl et al., 2000; Reed et al.,1993; Matesic et al., 2003; Maxeiner et al., 2005).

Several different glial connexins have been identified in the mammalian retina, with Cx43 and Cx45 associated with astrocytes and Müller cells (Zahs et al., 2003). Immunofluorescence and EM data demonstrate that Cx43 is not a neuronal connexin, but it is expressed by astrocytes in the CNS (Rash et al., 2000; Nagy et al., 2004), this result being confirmed by immunofluorescence data in mammalian retina (Janssen-Bienhold et al., 1998; Zahs et al., 2003). Cx37 immunoreactivity was found in retinal endothelial cells (Reed et al.,1993).

Three neuronal connexins have been described so far in mammalian retina: Cx36, Cx45 and Cx57, with Cx36 being the first connexin described in neurons of various regions of brain and the retina (Condorelli et al., 1998; Rash et al., 2000; Teubner et al., 2000; Feigenspan et al., 2001). In retina, Cx36 immunoreactivity was detected in homologous gap junctions between cone photoreceptors (Lee et al., 2003; Feigenspan et al., 2004), between dendrites of OFF-cone bipolar cells (Feigenspan et al., 2004) and between neighbouring dendrites of AII-amacrine cells in the most vitreal region of the inner plexiform layer (IPL) (Feigenspan et al., 2001; Mills et al., 2001). β-galactosidase reporter gene activity for Cx36 also suggested the presence of Cx36 in rods (Deans et al., 2002). Recent studies, using transgenic rod-less and cone-less mice (Dang et al., 2004)

confirmed expression of Cx36 in cones, but did not exclude the possibility of Cx36 expression in rods. Furthermore, Cx36 expression was detected in heterologous gap junctions between AII-amacrine cells and ON-cone bipolar cells (Feigenspan et al., 2001; Mills et al., 2001; Güldenagel et al., 2001). Recent studies (Hidaka et al., 2004; Schubert et al., 2005) also report the presence of Cx36 in alpha-retinal ganglion cells.

The distribution of Cx45 was analyzed following the expression of LacZ and EGFP reporter genes in Cx45-deficient mice and the expression of Cx45 was attributed to amacrine cells, ON- and OFF-cone bipolar cells and horizontal cells (Güldenagel et al., 2000; Maxeiner et al., 2005), these reports being inconsistent with the presence of Cx45 at glial cells (Zahs et al., 2003).

Cx57-deficient reporter mice revealed that tracer coupling was disrupted between horizontal cells and that LacZ signals are present exclusively in horizontal cells (Hombach et al., 2004), suggesting that Cx57 is present and restricted at this particular cell type. Also, Cx50 and Cx57 mRNA detection has been reported in A-type horizontal cells of rabbit retina (Massey et al., 2003; Huang et al., 2005).

Güldenagel et al. (2000) showed evidence for Cx40 mRNA expression in the mouse retina, but immunofluorescence analyses could not demonstrate the retinal presence of this protein. Detection of Cx40 immunoreactivity was found in bovine and rat retinal sections (Matesic et al., 2003), where Cx40-positive puncta were seen in the INL and ONL layers. The exact cellular expression of Cx40 is not clear yet, and it was suggested that Cx40 may be expressed by the photoreceptors in the ONL or by the amcrine cells or other neuronal cells in the INL. Also, it is possible that Cx40 is expressed by Müller cells (Matesic et al., 2003).

IV.6. Connexin associated proteins

At intercellular gap junctions, connexins have been shown to interact with multiple key proteins, including occludins, kinases and zonula occludens proteins (Duffy et al., 2002; Giepmans, 2004; Herve et al., 2004; Li et al., 2004a,b,c). Among these, zonula occludens-1 (ZO-1), a scaffolding protein known to associate with tight (Stevenson et al., 1986; Gonzales-Mariscal et al., 2003) and adherens junctions (Itoh et al., 1991, 1993; Howarth et al., 1992), is of particular interest, as previous studies in our laboratory have shown association between ZO-1 and neuronal Cx36 (Li et al., 2004a,b) and glial Cx47, Cx43 and Cx30 (Li et al., 2004c; Penes et al., 2005). Besides these proteins, ZO-1 has also been shown to directly interact with Cx31.9, Cx43, Cx45, Cx46 and Cx50 (Giepmans et al., 1998; Toyofuku et al., 1998; Kausalaya et al., 2001; Laing et al., 2001; Kojima et al., 2001; Giepmans et al., 2001; Nielsen et al., 2001, 2002, 2003). The presence of ZO-1 at gap junctions and its interaction with many connexins suggests its involvement in gap junctional regulation, but its precise function at gap junctions remains to be determined.

ZO-1, a member of the membrane-associated guanylate kinase (MAGUK) family of proteins is characterized by a modular organization, having three PDZ, one SH3 and one guanylate kinase domain (Fig.2).

Fig. 2

Each PDZ domain can interact with short PDZ binding motifs located at the C-terminus of their target proteins. Therefore, with different proteins binding to its different domains, ZO-1 is capable of recruiting structural and /or signalling proteins to plasma membranes, where it is considered to have a scaffolding role. Also, ZO-1 interacts with cytoskeletal components, the cellular cytoskeleton is functionally connected to gap junctions, and gap junctional stability depends on cytoskeleton integrity (Wang and Rose, 1995; Thomas et al., 2002; Johnson et al., 2002). Speculations on possible roles of ZO-1 in GJIC include modulation of coupling and sequestration of regulatory proteins to gap junctions.

In our attempt to describe gap junction associated proteins in retina, we investigated ZO-1-associated nucleic acid binding protein (ZONAB), a Y-box transcription factor previously described to bind to the SH3 domain of ZO-1 in canine MDCK cells (Balda and Matter, 2000; Balda et al., 2003). ZONAB and its mouse ortholog have two isoforms resulting from alternate splicing, which are referred to as MsY3 (ZONAB A) for the short isoform, and MsY4 (ZONAB B) for the long isoform. ZONAB interacts with proteins like cell division kinase 4 (CDK4) and RalA (a member of the Ras family of GTPases involved in signalling pathways for cytoskeleton remodeling and cellular transformation) as well as with the SH3 domain of ZO-1 (Balda et al., 2003; Frankel et al., 2005).

In MDCK cells, by binding to the Erbb2 promoter, ZONAB controls levels of ErbB2, a tyrosine kinase receptor involved in the regulation of epithelial cell proliferation and cell density (Balda and Matter, 2000; Balda et al., 2003). ZONAB has been shown to inhibit the ErbB2 promoter. Over-_expression of ZO-1 in cultured MDCK has the effect of binding ZONAB at the plasma membrane, preventing it from shuttling to the nucleus

and therefore preventing its repressor activity. In the CNS, ErbB2 acts as the major receptor for neuregulin (NRG) and the NRG/ErbB2 ligand/receptor signaling is crucial for oligodendrocyte differentiation in vivo and for the myelination process (Kim et al., 2003). In addition, ZO-1/ZONAB interaction has been shown to control paracellular permeability and, by controlling the nuclear accumulation of CDK4, it is involved in the regulation of epithelial cell cycle.

Besides the importance of ZO-1/ZONAB-mediated signalling pathways in MDCK cultures, their close interaction is thought to be part of more complex regulatory platforms present at intercellular junctions (Balda and Matter, 2000; Balda et al., 2003; Zahraoui, 2004; Penes et al., 2005). Recently, ZONAB has been reported to be expressed in mouse CNS in vivo, co-associated with astrocytic Cx43, oligodendrocytic Cx47 and Cx32 and with ZO-1 (Penes et al., 2005).

IV.7. Rationale for investigations undertaken

Due to its highly organised architecture, the retina was called "nature's brain slice" (Vaney, 1999), and it has been proven to be an excellent structure for studying electrical synapses between neuronal as well as between glial cells.

It is well established that all five types of retinal neurons are electrically coupled in various patterns and exhibit networks of homologous and heterologous gap junctional communication (reviewed in Vaney, 1994, 1999), and studies in retina demonstrate the importance of inter-neuronal gap junctions in retinal processing of visual information (Söhl et al., 2000; Güldenagel et al., 2001; Vaney and Weiler, 2000; He et al., 2000, 2003; Maxeiner et al., 2005). Although not completely elucidated, some of the implications of electrical synapses in visual processing have been described, including

coordination of network voltage response to light stimulus (Lamb and Simon, 1976; Devries and Baylor, 1993) and modulation of signal-to-noise ratio to improve visual resolution (Devries et al., 2002). Neighboring horizontal cells in the mammalian retina are electrically coupled through gap junctions, with the result that each cell receives photoreceptor input over receptive field that is much wider than the cell's dendritic field (Nelson et al., 1975; Dacheux and Miller, 1981; Dacheux and Raviola, 1982; Bloomfield and Miller, 1982; Bloomfield et al., 1995).

Previous research on retinal neuronal coupling through gap junctions has been focused on electrophysiological and dye-coupling experiments as well as on extensive high resolution investigative methods such as FRIL and EM, but the knowledge and the identity of connexins involved in forming GJIC remained largely unknown. It is believed that cellular coupling in CNS, including retina, requires each cell type to be selectively coupled to its partners, with specific connexin proteins assigned to distinct cell types (Nagy and Rush, 2000; Nagy et al., 2003).

In the mammalian retina, Cx36, Cx45 and Cx57 are the major neuronal connexins identified so far, with Cx36 being the first neuronal connexin described in various regions of brain and the retina (Condorelli et al., 1998; Rash et al., 2000; Teubner et al., 2000; Feigenspan et al., 2001).

In the retina, Cx36 expression was demonstrated by IHC studies using different anti-Cx36 antibodies, which showed Cx36 protein presence in the IPL and OPL (Teubner et al., 2000; Sohl et al., 2000; Güldenagel et al., 2000; Rash et al., 2000; Feigenspan et al., 2001, 2004; Mills et al., 2001; Li et al., 2004a). Additionally, the availability of Cx36-deficient mice, the use of different cell-type specific markers and the dye-injection of has

lead to the conclusion that Cx36 is expressed in all five retinal neuronal types, except horizontal cells (Deans and Paul, 2001; Feigenspan et al., 2001; Lee et al., 2003). Also, it has been shown that Cx36 binds to the first of the three PDZ domains of ZO-1 at gap junctions between neurons as well as in peripheral tissue (pancreatic islets and adrenal gland) (Li et al., 2004a,b).

Cx45 promoter activity was demonstrated by β-galactosidase staining in neurons in several regions of mouse brain (Maxeiner et al., 2003) and in the GCL and INL of retina (Güldenagel et al., 2000). IHC studies using a polyclonal rabbit anti-mouse Cx45 antibody characterised by Butterweck et al. (1994) indicated that immunolabelling in IPL was due to expression of Cx45 in amacrine cells whereas Cx45 labelling in OPL was accredited to its presence at gap junctions between bipolar or horizontal cells (Güldenagel et al., 2000). Additional IHC studies using different anti-Cx45 antibodies as well as a variety of cell-type specific markers, associated expression of Cx45 in rat retina with astrocytes and Müller cells (Zahs et al., 2003), therefore indicating a glial origin for Cx45. A recent report analysed Cx45 expression in mouse retina based on LacZ reporter gene activity and EGFP expression in two lines of Cx45 deficient mice (Maxeiner et al., 2005). This study indicates a neuronal origin for Cx45. The discrepancy regarding the neuronal or glial origin of Cx45 is due to the fact that, the available antibodies against Cx45 are not suitable for ICH in retina.

The interaction of Cx45 with ZO-1 was demonstrated in Cx45-transfected MDCK cells and in cultured osteoblastic cells (Kausalya et al., 2001; Laing et al., 2001), but the PDZ domain involved in mediation of Cx45/ZO-1 interaction was not clearly determined.

Cx57 was the first connexin shown to be expressed in mouse horizontal cells (Manthey et al., 1999). Studies on Cx57 have been few and so far, weak Cx57 mRNA expression has been reported in several mouse tissues including retina (Manthey et al., 1999). Also, in a recent study, Huang et al. (2005) reported Cx57 mRNA expression in A-type horizontal cells of rabbit retina. Furthermore, it has been shown that in Cx57 KO mice, where the Cx57 gene has been replaced by LacZ reporter gene, β-galactosidase signals were present and restricted to horizontal cells (Hombach et al., 2004), but the presence of Cx57 protein could not be demonstrated, because no specific antibodies were available.

Project 1 : In this study, we examined the spatial relationship of Cx36 and Cx45 with each other and with ZO-1 and ZONAB by using newly developed anti-Cx45 and anti-ZONAB antibodies. Immunofluorescence, immunoprecipitation (IP) and pull-down approaches were used to establish direct interaction of Cx45 with the second PDZ domain of ZO-1 in Cx45-transfected HeLa cells and mouse retina.

Taking into consideration ZO-1/ZONAB interaction and its vital functional implications in MDCK cells as well as their close association at glial gap junctions in vivo, we further investigated ZONAB relationships with zonula occludens in retina, where extensive ZO-1 expression has been described (Williams and Rizzolo, 1997; Inoko et al., 2003; Li. et al., 2004a). By using a newly developed anti-ZONAB antibody, and several anti-ZO-1 antibodies in different combinations with antibodies against retinal connexins, our aim was to identify cellular types in retina expressing ZONAB and ZONAB co-localization with Cx36 and Cx45, and to provide evidence for neuronal expression of ZONAB in mouse retina. Another important point of our studies was to employ newly developed Cx45 antibodies to confirm Cx45 protein expression in IPL of

retina. Based on previous studies which indicated Cx36/Cx45 co-localization (Maxeiner et al., 2005), we wanted to investigate the spatial relationship between Cx36 and Cx45 and their possible co-expression.

Hypotheses: 1. Cx36 and Cx45 are expressed and co-localized to some extent in subpopulations of retinal neurons.

2. ZONAB is present at gap junctions composed of Cx36 and Cx45 and is associated with ZO-1 at these gap junctions.

Project 2 : In this study, our aim was to investigate the expression and distribution of Cx57 in mouse retina by using newly developed anti-Cx57 antibodies. Specificity of these antibodies was examined by comparisons of Cx57 detection in retinas of wild-type and Cx57 KO mice. Double immunofluorescence labelling was undertaken to determine expression patterns of Cx57 in relation to that of Cx36. Having previously shown the association of Cx36 with ZO-1 in the IPL of mouse retina (Li et al., 2004a), we examined cellular associations of Cx57 and Cx36 with ZO-1 in the OPL. In addition, the spatial deployment of Cx57 and Cx36 was examined in relation to the protein bassoon, which is known to be associated with ribbon synapses at cone pedicles and at rod spherules.

Hypotheses: 1. Cx57 is expressed in horizontal cells of mouse retina and is co-localized to some extent with Cx36.

2. Cx57 and Cx36 are associated with ZO-1 at gap junctions in retina.

Personal contribution to the Projects:

Project 1: I have provided data presented in Figures 1-6. All molecular data presented in Fig. 7-10 was provided by Xinbo Li.

Under the supervision of Dr. J. I. Nagy, I was responsible for writing the first draft of the Material and Methods and Results sections related to the experiments conducted by myself, as well as parts of the Discussion section.

Project 2: I have provided data for all the figures presented, except for Fig. 8, which represents a diagrammatic representation of a rod terminal spherule and was provided by our technician Brett McLean under Dr. J. I. Nagy's supervision.

I was responsible for writing the first draft of the manuscript, in collaboration with Dr. J. I. Nagy.

Together with the other authors, I was responsible for making sure that all suggested corrections are included in the final version of both submitted manuscripts.

V. PROJECT I

Association of Connexin36 and ZO-1 with the MsY3 transcription factor ZO-1-associated nucleic acid-binding protein (ZONAB) and interaction of connexin45 with ZO-1 in mouse retina

C. Ciolofan, Xinbo Li, C. Olson and J.I. Nagy

Neuroscience (submitted)

ABSTRACT

Gap junctions between neurons in the mammalian retina are known to be formed by connexin36 and connexin45, and we have previously reported the association of connexin36 with the scaffolding protein zonula occludens-1 (ZO-1) at these junctions. We used immunofluorescence microscopy to determine relationships between connexin36, connexin45, ZO-1 and the ZO-1-interacting Y-box transcription factor MsY3 (ZONAB) in the retina of wild-type and connexin36 knockout mice, and molecular methods to examine the interaction of connexin45 with ZO-1. Immunolabelling for each of these proteins appeared exclusively as puncta distributed in the inner plexiform layer and the outer plexiform layer, although connexin45 was absent in the latter. Connexin36, ZO-1 and ZONAB were extensively co-localized in both of these layers, whereas connexin45 showed substantial co-localization with ZO-1, and only minor co-localization with connexin36 and ZONAB. In connexin36 knockout mice, labelling of ZO-1 and connexin45 was slightly to moderately reduced, while that of ZONAB was markedly decreased in the inner part of the inner plexiform layer, but persisted in the outer region of this layer, where it remained co-localized with ZO-1. As in retina, connexin45 was co-localized and co-immunoprecipited with ZO-1 in connexin45-transfected HeLa cells, and pull-down assays indicated binding of connexin45 to the second PDZ domain of ZO-1. These results demonstrate ZONAB expression and association with connexin36 and ZO-1 in retina, connexin45 association with ZO-1, and direct connexin45/ZO-1 interaction. It appears that connexin36 and connexin45 are contained partly in the same, but largely separate retinal gap junctions, which display distinct patterns of association with ZO-1 and ZONAB, and exhibit

different responses to connexin36 gene deletion, suggesting differential regulatory roles of these gap junctionlly-localized accessory proteins. Further, the persistence of ZO-1/ZONAB co-localization in connexin36 knockout mice and in a pattern matching that in wild type mice suggest the possible association of these proteins with gap junctions composed of an as yet unidentified connexin in retina.

INTRODUCTION

Interneuronal gap junctions at cell-cell plasma membrane contacts are the structural correlate of electrical synapses, allowing electrical coupling as well as passage of ions and small molecules between cells (Bennett, 1997). The intercellular channels at these junctions are composed of various members of the twenty or more identified gap junction-forming connexin (Cx) family of proteins (Goodenough et al., 1996; Kumar and Gilula, 1996; Willecke et al., 2002). Among the diverse structures in which electrical synapses have now been identified in the mammalian CNS (Bennett and Zukin, 2004; Connors and Long, 2004), the retina has been considered an ideal model system in which to study the contribution of such synapses to the processing of signals in neural pathways (Vaney, 1999). This tissue contains a high density of gap junctions that produce complex patterns of circuitry interlinking arrays of photoreceptor cells as well as specific classes of neurons (Becker et al., 1998; Sharpe and Stockman, 1999; Janssen-Bienhold et al., 2001). Connexins that form electrical synapses via gap junctions between various cell types in rodent retina include Cx36, Cx45 and Cx57 (Sohl et al., 2000; Guldenagel et al., 2000; Feigenspan et al., 2001, 2004; Hombach et al., 2004; Ciolofan et al., 2005; Schubert et al., 2005), and expression of Cx50 was additionally found in rabbit retina (Massey et al., 2003; Huang et al., 2005). The retina is an ideal system also for analyses of the regulation of gap junctional electrical synapses by ambient illumination, neurotransmitters and intracellular signalling pathways (Vaney, 1999; Weiler et al., 1999, 2000; He et al., 2000). Such regulation occurs almost certainly via gap junction-associated accessory proteins that may govern gap junctional conductance state and/or connexin trafficking via various signalling processes (Giepmans, 2004; Herve et al.,

2004). The multi-functional PDZ domain-containing protein zonula occludens-1 (ZO-1) has been found at gap junctions and interacts with the c-terminus of several different connexins (Giepmans and Moolenaar, 1998; Toyofuku et al., 1998; Kausalya et al., 2001; Laing et al., 2001; Nielsen et al., 2002, 2003; Penes et al., 2005). However, the regulatory and/or structural role of connexin/ZO-1 interaction remains obscure.

We have previously reported Cx36 co-localization with ZO-1 at interneuronal gap junctions in mouse brain and retina, and direct interaction of the c-terminus of Cx36 with the first of the three PDZ-domains in ZO-1 (Li et al., 2004a; Rash et al., 2004). In a search for proteins that interact with ZO-1 at gap junctions and that, together with ZO-1, may serve regulatory roles at these junctions, we recently found association of Y-box transcription factor 3 (MsY3) with ZO-1 at gap junctions between glial cells in mouse brain (Penes et al., 2005). MsY3, also referred to as ZONAB (ZO-1-associated nucleic acid binding protein), was previously reported to interact with ZO-1 at tight junctions in canine MDCK (Balda and Matter, 2000, 2003; Balda et al., 2003). In the present studies, we provide evidence for neuronal expression of ZONAB in mouse retina, and we used immunfluorescence approaches to examine spatial relationships of Cx36 and Cx45 with each other and with ZO-1 and ZONAB. In addition, immunofluorescence, immunoprecipitation (IP) and pull-down approaches were used to establish direction interaction of Cx45 with ZO-1 in Cx45-transfected HeLa cells and mouse retina.

EXPERIMENTAL PROCEDURES

Antibodies and animals

Antibodies used in this study, together with sequence specificity, dilutions employed and source, are presented in Table 1. Affinity-purified rabbit polyclonal and mouse monoclonal antibodies were obtained from Zymed Laboratories (South San Francisco, CA, USA), including recently available polyclonal antibodies generated against peptides corresponding to sequences within mouse Cx45 and ZONAB, the specificity of which are shown in this report. The specificity of the anti-Cx36 and anti-ZO-1 antibodies used has been demonstrated elsewhere (Li et al., 2004a,b; Penes et al., 2005). The polyclonal anti-ZONAB antibody was developed against the mouse ortholog of canine ZONAB, referred to in the GenBank as mouse Y-box transcription factor 3 (MsY3), or alternatively, cold shock domain protein. The peptide epitope orecognized by anti-ZONAB is contained within a region of ZONAB that is present in both the long (ZONAB B) isoform of this protein, as well as its shorter (ZONAB A) alternatively spliced isoform, several versions of which are listed in GeneBank database (ZONAB A, accession No. AAF72335; ZONAB B, accession No. AAF72336; MsY-box 3 short form, accession No. AAG14419; MsY-box long form, accession No. AAG14418; cold shock domain protein A short form, accession No. AAH62377; cold shock domain protein A long form, accession No. AAH48242). Mouse monoclonal anti-Cx45 and goat polyclonal anti-calretinin Ab1550 were purchased from Chemicon International (Temecula, CA, USA). Rabbit anti-GST antibody 06-332 for detection of GST-PDZ domain fusion proteins was obtained from Up State Cell Signalling Solutions (Lake Placid, NY, USA). A total of thirty-five adult male CD1 mice, ten male C57BL/6 wild-type mice and five C57BL/6 Cx36 KO mice obtained

from animal facilities at our institution were used in this study, according to protocols approved by Animal Care Committees, with minimization of stress to animals.

Light microscope immunohistochemistry

Mice deeply anaesthetised with equithesin (3 ml/kg) were transcardially perfused with 3 ml of cold "pre-fixative" solution (50 mM sodium phosphate buffer, pH 7.4, 0.9% NaCl, 0.1 sodium nitrate and 1 unit/ml heparin). This was followed by perfusion with 40 ml of cold 0.16 M sodium phosphate buffer, pH 7.6, containing either 1%, 2% or 4% formaldehyde and 0.2% picric acid. Animals were then perfused with 10 ml of 25 mM sodium phosphate buffer, pH 7.4, containing 10% sucrose. After removal, eyes were stored at 4°C for 24-72 h in cryoprotectant consisting of the final perfusate with the addition of 0.04% sodium azide. Vertical sections of retina were cut at a thickness of 10 µm on a cryostat, collected on gelatinized glass slides, and used for immunohistochemistry. All sections were washed for 20 min in 50 mM Tris-HCl, pH 7.4, containing 256 mM sodium chloride (TBS) and 0.3% Triton X-100 (TBSTr). Primary antibodies were diluted in TBSTr containing 5 or 10% normal goat or normal donkey serum.

For single immunofluorescence labelling, sections were incubated for 24 h at 4°C with either monoclonal anti-Cx45, polyclonal anti-Cx45, polyclonal anti-ZONAB or polyclonal anti-calretinin, then washed for 1 h in TBSTr, and incubated with secondary antibodies for 1.5 h at room temperature. Various secondary antibodies used included FITC-conjugated horse anti-mouse IgG diluted 1:100 (Vector Laboratories, Burlingame, CA, USA), Cy3-conjugated goat anti-mouse IgG diluted 1:200 (Jackson ImmunoResearch Laboratories, West Grove, PA, USA), Alexa Flour 488-conjugated

goat anti-rabbit IgG diluted 1:1000 (Molecular Probes, Eugene, Oregon), Cy3-conjugated donkey anti-rabbit diluted 1:200 (Jackson ImmunoResearch Laboratories), and Alexa Flour 488-cojugated donkey anti-goat IgG diluted 1:1000 (Molecular Probes).

For double immunofluorescence labelling involving Cx36, sections were incubated as above with monoclonal anti-Cx36 antibodies and simultaneously with one of the following antibodies: polyclonal anti-ZO-1, polyclonal anti-Cx45, polyclonal anti-ZONAB or polyclonal anti-calretinin. Conversely, polyclonal anti-Cx36 was incubated simultaneously with either monoclonal anti-ZO-1 or monoclonal anti-Cx45. For double-labelling involving ZO-1, sections were incubated with monoclonal anti-ZO-1 and simultaneously with one of the following: polyclonal anti-ZONAB, polyclonal anti-calretinin or polyclonal anti-Cx45. For double-labelling involving ZONAB, sections were incubated with rabbit polyclonal anti-ZONAB and simultaneously with either goat polyclonal anti-calretinin or monoclonal anti-Cx45. For triple immunofluorescence labelling, sections were incubated simultaneously with combinations of antibodies against the following: Cx36, ZO-1 and calretinin; Cx36, ZONAB and calretinin; or ZONAB, ZO-1 and calretinin. Primary antibody incubations were followed by washes in TBSTr for 1 h at room temperature, and then incubations for 1.5 h at room temperature simultaneously with appropriate combinations of the secondary antibodies described above. For triple labelling, the secondary antibody combinations were AlexaFlour 488-cojugated donkey anti-goat IgG diluted 1:1000, Cy3-conjugated donkey anti-rabbit IgG 1:200 and Cy5-conjugated goat anti-mouse IgG diluted 1:200. After secondary antibody incubations, all sections were washed in TBSTr for 20 min, and then in 50 mM Tris-HCl buffer, pH 7.4 for 30 min. Sections used for single labelling with anti-Cx36, anti-Cx45,

anti-ZONAB and anti-ZO-1 were counterstained with either red Nissl fluorescent NeuroTrace (stain N21482) or green Nissl NeuroTrace (stain N21480) (Molecular Probes). All sections were then covered with antifade medium and coverslipped. Control procedures were performed for each of the antibody combinations used and included omission of one of the primary antibodies with inclusion of each of the secondary antibodies for each combination of labelling to establish absence of inappropriate cross-reactions between primary and secondary antibodies or between different combinations of secondary antibodies.

For immunolabelling of HeLa cells transfected with Cx45 or empty vector, cells grown on poly-L-lysine-treated glass coverslips were fixed with ice-cold 1 or 2% formaldehyde for 5 min. Cultures were incubated for 16 h at 4°C simultaneously with rabbit anti-Cx45 and mouse anti-ZO-1 in TBSTr containing normal donkey serum. Cultures were then washed in TBSTr for 1 h, and incubated for 1 h at room temperature simultaneously with FITC-conjugated donkey anti-rabbit IgG diluted at 1:200 and Cy3-conjugated goat anti-mouse IgG diluted at 1:400, or alternatively, with FITC-conjugated horse anti-mouse IgG diluted 1:200 and Cy3-conjugated donkey anti-rabbit IgG diluted 1:400. Slides were then washed for 1 h in TBSTr, covered with anti-fade medium and coverslipped.

Fluorescence was examined on a Zeiss Axioskop2 fluorescence microscope with image capture using Axiovision 3.0 software (Carl Zeiss Canada, Toronto, Ontario, Canada). Confocal immunofluorescence analysis for double and triple labelling was performed on an Olympus Fluoview IX70 confocal microscope with image capture using Olympus Fluoview software. Images were finally assembled according to appropriate size and contrast using Adobe Photoshop CS (Adobe Systems, San Jose, CA, USA),

Corel Draw 12, and Northern Eclipse software (Empix Imaging, Mississauga, ON, Canada).

Cx45 and MsY3 pcDNA3 expression vector construction

Cx45 cDNA was obtained by reverse transcription of total RNA isolated from adult mouse brain, as previously described (Li et al., 2004a,b), and the Cx45 coding sequence was amplified using oligonucleotide primers and materials purchased from Gibco BRL Life Technologies (Burlington, Ontario, Canada). Primers chosen for PCR were designed according to mouse Cx45 sequence (Genbank accession number: NM_008122) and were:

sense primer, 5′-ATGAGTTGGAGCTTCCTGACTCGC-3′;

antisense primer: 5′-TTAAATCCAGACGGAGGTCTTCC-3′.

PCR conditions were: initial denaturation at 94 °C for 5 min; 35 cycles of amplification with denaturation at 94 °C for 60 s, annealing at 52 °C for 60 s, and elongation at 72 °C for 90 s; and final extension at 72 °C for 10 min for T-A cloning. Amplification of Cx45 cDNA by PCR was carried out in 20 μl of solution containing 2 μl of 10 × PCR buffer, 0.8 μl of 50 mM $MgCl_2$, 200 μM dNTP, 100 ng sense and antisense primers, one unit of *Taq* DNA polymerase and 1 μl of template cDNA. PCR products were separated by electrophoresis in a 1.5% agarose gel prepared using TAE buffer (40 mM Tris-HCl, 0.1% acetic acid, 1 mM EDTA pH 8.0, and 0.0004% ethidium bromide). Separated PCR products were isolated and excised under UV illumination and purified using a gel purification kit (Qiagen Inc, Mississauga, Ontario, Canada). PCR products were subcloned into the PCR 2.1 vector, digested with BstX I, and ligated into the pcDNA3 expression vector (Invitrogen Life Technologies, Burlington, Ontario, Canada) using T4 DNA ligase (Invitrogen Life Technologies) according to the manufacturer's instructions.

Cx45 recombinant plasmids were extracted and digested with Xba I to confirm insert orientation and sequenced with M13 forward and reverse primers for sequence confirmation.

A bacterial cDNA clone containing the full-length coding region for mouse cold shock domain protein A (I.M.A.G.E. clone ID 6530404, Genbank accession number BC062377), corresponding to MsY3 short form and the mouse ortholog of canine ZONAB A, was obtained from American Type Culture Collection (ATCC) (Rockville, MD, USA) ATCC number 10470249. Selected colonies were incubated overnight at 37 °C in LB media supplemented with 50 μg/ml penicillin. Plasmid DNA was extracted using the QIAprep Spin Miniprep Kit (Qiagen Inc.), cut with ApaI enzyme and separated by electrophoresis (as above) to confirm ZONAB coding region orientation. Plasmid DNA was digested using XbaI and EcoRV enzymes and the ZONAB coding region was ligated into the pcDNA3.1 expression vector (Invitrogen Life Technologies) using T4 DNA ligase. DH5α *E.coli* cells (Invitrogen Life Technologies) were transformed with ZONAB-pcDNA3 recombinant plasmid according to manufacturer's instructions then plated on ampicillin containing agar plates and incubated overnight at 37 °C. Transformed colonies were selected and amplified overnight at 37 °C in LB media supplemented with 50 μg/ml penicillin. The ZONAB-pcDNA3 recombinant plasmid was extracted (as above), and an aliquot was digested with XbaI and EcoRV and separated by electrophoresis for recombinant product verification.

Cell culture and HeLa cell transfection

HeLa cells (ATCC), grown in Dulbecco's Modified Eagle's Medium supplemented with 10% fetal bovine serum and 1% penicillin-streptomycin, were transiently transfected with

pcDNA3 vector, Cx45-pcDNA3 plasmids or ZONAB-pcDNA3.1 plasmids using LipofectAMINE 2000 reagent, as previously described (Li et al., 2004a,b). Transiently transfected HeLa cells were analyzed after a 24 h transfection period. For selection of clones stably transfected with Cx45, cells were passaged after a 24 h transfection period at 1:40 dilution with fresh Dulbecco's Modified Eagle's Medium containing 1.5 mg/ml of G418, and individual clones expressing Cx45 were isolated after 3 weeks in culture.

Western blotting

Mice were deeply anaesthetized using equithesin (3 ml/kg) (Scadding, 1981) followed by decapitation and removal of the eyes. Retinas were dissected, rapidly frozen and stored at -80 °C until future use. Transfected and vector-control HeLa cells rinsed with PBS buffer (50 mM sodium phosphate buffer, pH 7.4, 0.9% saline) and retinas were homogenized in IP buffer (20 mM Tris-HCl, pH 8.0, 140 mM NaCl, 1% Triton X-100, 10% glycerol, 1 mM EGTA, 1.5 mM $MgCl_2$, 1 mM dithiothreitol, 1 mM phenylmethylsulfonyl fluoride and 5 μg/ml each of leupeptin, pepstatin A and aprotinin) and sonicated. Retinal samples were cleared of cellular debris by centrifugation at 20,000 x g for 5 min and the supernatants were collected and taken for protein determination using a kit (Bio-Rad Laboratories, Hercules, CA, USA). Western blotting was performed as previously described (Li et al., 2004a,b). Briefly, 50-100 μg of protein per lane was separated electrophoretically by SDS-polyacrylamide gel electrophoresis (SDS-PAGE) using 12.5% gels followed by transblotting to polyvinylidene difluoride membranes (PVDF) membranes (Bio-Rad Laboratories) in standard Tris-glycine transfer buffer, pH 8.3, containing 0.5% sodium dodecylsulfate (SDS). Membranes were blocked for 2 h at room temperature in TBSTw (10 mM Tris-HCl, pH 8.0, 150 mM NaCl, 0.2% Tween-20)

containing 5% non-fat milk powder, briefly rinsed in TBSTw, and then incubated overnight at 4 °C with either monoclonal anti-Cx45 or polyclonal anti-ZONAB in TBSTw containing 1% non-fat milk powder. Membranes were then washed in TBSTw for 40 min, incubated with horseradish peroxidase-conjugated donkey anti-rabbit IgG or anti-mouse IgG diluted 1:3000-1:5000 (Sigma-Aldrich Canada, Oakville, Ontario, Canada) in TBSTw containing 1% non-fat milk powder, washed in TBST for 40 min and resolved by chemiluminescence (ECL, Amersham PB, Baie d'Urfe, Quebec, Canada).

Immunoprecipitation (IP)

Mouse retinas and Cx45-transfected HeLa cells were homogenized in IP buffer, sonicated and centrifuged at 20,000 x g for 10 min at 4°C. Following protein determination of sample supernatants, volumes corresponding to 1 mg of mouse retina protein and 2 mg of Cx45- transfected HeLa cell protein were pre-cleared for 1 h at 4°C using 20 µl of protein A-coated agarose beads (Santa Cruz BioTech, Santa Cruz, CA, USA), centrifuged at 20,000 x g for 10 min at 4°C, and then incubated with 2 µg of monoclonal anti-ZO-1 antibody for 16 h at 4°C. The mixture was then incubated for 1 h at 4°C with 20 µl of protein-A coated agarose beads, centrifuged at 20,000 g for 10 min, and the pellet was washed five times with 1 ml of wash buffer (20 mM Tris-HCl pH 8.0, 150 mM NaCl, and 0.5% NP-40). Samples were then mixed with an equal volume of SDS-PAGE loading buffer (125 mM Tris-HCl, pH 6.8, 20% glycerol, 0.3 mM bromophenol blue, 0.14 M SDS, 20% β-mercaptoethanol), then boiled for 5 min, and taken for immunoblotting with polyclonal anti-Cx45 antibody. Control samples were precipitated with the omission of anti-ZO-1 antibody.

GST-PDZ domain fusion proteins and in vitro pull-down assays

Three pGEX-3X plasmids each containing one of the three GST-linked PDZ domains of ZO-1 (Nielsen et al., 2002, 2003) were kindly provided to us by Dr. B. Giepmans (University of California, San Diego, CA, USA). Preparation of GST-PDZ fusion proteins from these plasmids expressed in *E. Coli* DH5α and binding of fusion proteins to glutathione-agarose beads was conducted as previously described (Li et al., 2004a,b). Beads containing PDZ domain fusion proteins were incubated for 16 h at 4 °C with retina or Cx45-transfected HeLa cells that had been homogenized in IP buffer. After extensive washing in PBS buffer containing 1% Triton X-100, proteins from the agarose beads were eluted with SDS-PAGE loading buffer, separated by SDS-PAGE, transferred to PVDF membrane and analysed by western blotting with anti-Cx45 or anti-GST antibody.

RESULTS

Distribution of Cx36, Cx45, ZO-1 and ZONAB in mouse retina

The general distributions Cx36, Cx45, ZO-1 and ZONAB were compared in low magnification images of vertical retinal sections labelled by immunofluorescence for each of these proteins individually and simultaneously counterstained with Nissl fluorescent Neurotrace (Fig. 1). Immunolabelling of each of the proteins consisted exclusively of fluorescent puncta, except in the case of ZO-1, which was also evident as continuous labelling along blood vessels (Fig. 1E). Labelling of Cx36 was restricted to the inner plexiform layer (IPL) and outer plexiform layer (OPL), and in the IPL was considerably more intense than that of the other three proteins, often obscuring visualization of individual puncta at low magnification (Fig. 1A). The intensity of Cx36 labelling was greater in the inner compared with the outer half of the IPL (Fig. 1A).

Labelling of Cx45 was present only in the IPL, where Cx45-positive puncta were consistently distributed at low density in the inner half of this layer, and at even lower density in the outer half (Fig. 1C). Labelling of ZO-1 was of moderate density throughout the IPL, except in a narrow band in the middle of this layer, where it was of slightly higher density (Fig. 1E). Punctate labelling of ZO-1 was also evident in OPL, but was partly obscured by ZO-1-positive blood vessels in this layer (Fig. 1E). Labelling of ZONAB was restricted to the plexiform layers and was characterised by dispersed ZONAB-positive puncta in the IPL and a continuous band of puncta in the OPL (Fig. 1G). In the IPL, ZONAB tended to be more concentrated in the outer and inner third than in the middle third of this layer (Fig. 1G). In Figures 1E and 1G, intense fluorescence was also present at the outer limiting membrane, consistent with previous findings (William and Rizzolo, 1997; Tserentsoodol et al., 1998).

Confocal microscopy of Cx36, ZO-1 and ZONAB

Double immunofluorescence confocal microscopy was used to examine sublaminar distributions and co-localization relationships of Cx36, ZO-1 and ZONAB in vertical sections through the IPL of mouse retina. Each of the images in Figures 2A-C represent z-stacks of five scans, and Figure 2D was taken as a single scan. Cx36-positive puncta in the inner half of the IPL were of larger size on average than those in the outer half of the IPL, which may have contributed to the appearance of a greater intensity of labelling for Cx36 in the inner half seen in Figure 1A. In addition, small aggregates of Cx36-positive puncta were occasionally seen along a thin band in the mid-region of IPL, and this region was flanked by bands of sparse labelling for Cx36, with the upper band evident in Fig. 2A1 and 2B1, and the lower band better seen in Fig. 2A1. Labelling of ZO-1 appeared as

small puncta of relatively uniform size, which were generally of finer grain (Fig. 2A2) compared with Cx36-positive puncta (Fig. 2A1). As in the case of Cx36, small aggregates of ZO-1-positive puncta were seen in the mid-region of the IPL, below which was located a band of sparse labelling (Fig. 2A2). Image overlays of double immunofluorescence labelling for Cx36 and ZO-1 indicated that nearly all Cx36-positive puncta were labelled for ZO-1, whereas not all ZO-1-positive puncta were labelled for Cx36, including labelling of ZO-1-puncta alone in the inner and more so in the outer half of IPL (Fig. 2A3). The above double labelling was conducted using monoclonal anti-Cx36 37-4600 and polyclonal anti-ZO-1 61-7300, and the same results were obtained by double labelling with polyclonal anti-Cx36 36-4600 and monoclonal anti-ZO-1 33-9100.

Various distinguishing features of punctate labelling for ZONAB (Fig. 2B2) included sparse labelling within the extreme inner region of the IPL, with increasing density towards a band almost devoid of ZONAB, corresponding to a band nearly devoid of Cx36 (Fig. 2B1). Beyond this band in the outer region of the IPL was a concentration of ZONAB-positive puncta, a proportion of which were distinctly larger in size than most of the other ZONAB-positive puncta observed in the IPL (Fig. 2B2). Double labelling for Cx36 and ZONAB (Fig. 2B3) indicated a high degree of their co-localization in mid-regions of the IPL, and especially within the band containing large ZONAB-positive puncta (Fig. 2B3). Cx36-positive puncta devoid of labelling for ZONAB were most concentrated in the extreme inner part of IPL, whereas ZONAB-positive puncta lacking Cx36 were most concentrated in the extreme outer part of the IPL (Fig. 2B3). Double labelling of ZONAB and ZO-1 (Fig. 2C) indicated that a high proportion of ZONAB-positive puncta were labelled for ZO-1, whereas many ZO-1-positive puncta, particularly

in the mid-region of the IPL containing a greater density of ZO-1, were devoid of labelling for ZONAB.

We have reported elsewhere that the vast majority of Cx36-positive puncta in the OPL was co-localized with ZO-1(Ciolofan et al., 2005). Confocal double immunofluorescence revealed that most of the punctate labelling of Cx36 in the OPL was also associated with ZONAB (Fig. 2D). The laminar distributions and co-localization of Cx36, ZO-1 and ZONAB described above in the retina of CD1 mice were similarly observed in rat retina (not shown).

Confocal microscopy of Cx45 in relation to Cx36, ZO-1 and ZONAB

Confocal immunofluorescence analysis of Cx45 in vertical sections of mouse retina gave considerable variation in the density and size of scattered Cx45-positive puncta in the IPL. In general, however, most puncta in the inner half of IPL were larger than those in the outer half, and there appeared to be a gradual decrease in size and density of puncta form the inner to the outer part of IPL (Fig. 3A1, B1, C1). This variation in labelling was in part due to the relative sparsity of Cx45 puncta combined with high magnification analyses, making it difficult to choose uniformly representative fields of labelling. This was partly compensated by presenting images in Figure 3 as z-stacks of five scans. In addition, retinas from at least five mice were examined and similar results as described above were obtained in each. As well, labelling patterns of Cx45 in IPL obtained with Zymed polyclonal anti-Cx45 antibody (Fig. 3A1, 3B1) were similar to those obtained with Chemicon monoclonal anti-Cx45 Mab 3101 (Fig. 3C1).

Confocal double immunofluorescence revealed instances of clear co-localization of Cx45 with Cx36 in most regions of IPL, but showed that only a small proportion of

Cx45-positive puncta were labelled for Cx36 (Fig. 3A3). Counts of total Cx45-puncta per field in at least five fields indicated that about 11% were also positive for Cx36. Given the far greater density of Cx36 in the IPL, a much smaller percentage (not quantitated) of Cx36-positive puncta were labelled for Cx45. In contrast, double immunolabelling of Cx45 with ZO-1 revealed that nearly all Cx45-positive puncta were labelled for ZO-1. The differential density of labelling for the two proteins left the vast majority of ZO-1-puncta devoid of Cx45. As in the case of Cx45/Cx36, double labelling indicated that only a small proportion of Cx45-positive puncta were positive for ZONAB (Fig. 3C), and that the small number of Cx45/ZONAB-positive puncta were randomly distributed throughout the IPL.

Cx45, ZO-1 and ZONAB in retina Cx36 KO mice

Double immunofluorescence was used to examine expression and labelling patterns of ZO-1, ZONAB and Cx45 in Cx36 KO mice. Because Cx36 gene deletion was achieved in the C57BL6/129SvEv hybrid mouse strain (Deans et al., 2001), we first established that the retinal IPL distributions, relative densities and co-localization relationships of Cx36/ZO-1 (Fig. 4A), Cx36/ZONAB (Fig. 4C) and ZO-1/ZONAB (Fig. 4E) in WT mice of the C57/BCL6/129SvEv strain paralleled that described above in retina of the CD1 mice. Double immunofluorescence of Cx36 and ZO-1 in retina of Cx36 KO mice (Fig. 4B) showed an absence of Cx36 labelling (Fig. 4B1) and a slightly reduction of ZO-1 expression (Fig. 4B2) in the IPL. Double-labelling of Cx36 and ZONAB in vertical retinal sections from Cx36 KO mice showed that the absence of Cx36 in the IPL (Fig. 4D1) resulted in large reduction of ZONAB in the inner two thirds of the IPL (Fig. 4D2). However, the band of large ZONAB-positive puncta in the outer one-third region of the

IPL was still present (Fig. 4D2), and appeared similar to that observed in WT mice. Double labelling of ZO-1 and ZONAB in retina of Cx36 KO mice (Fig. 4F) showed less ZO-1/ZONAB co-localization in the inner two-thirds of the IPL (Fig. 4F3) due to the reductions labelling for these proteins in this region KO mice (Fig. 4F1,4F2). However, ZO-1/ZONAB co-localization was largely preserved in the outer third of the IPL containing the band of large ZONAB puncta (Fig. 4F3). Magnification of this band of puncta by confocal microscopy in overlay images show comparisons of Cx36/ZO-1 in WT and KO mice (Fig. 4A4 and 4B4, respectively), Cx36/ZONAB in WT and KO mice (Fig. 4C4 and 4D4, respectively), and ZO-1/ZONAB (Fig. 4E4 and 4F4, respectively), and indicate that this band of ZO-1-puncta and ZONAB-puncta labelled for Cx36 in WT mice persisted and remained co-localized in Cx36 KO mice. As in the case of ZONAB-positive puncta found to be associated with Cx36 in the OPL of retina form CD1 mice, a high degree of Cx36/ZONAB co-localization was also observed in OPL of retina from C57BL/6 mice (not shown) and, as in most regions of IPL, gene deletion of Cx36 resulted in a large reduction of punctate labelling for ZONAB in the OPL (Fig. 5A,B).

Confocal immunofluorescence double labelling of Cx36 and Cx45 in vertical sections of retina from WT C57/BCL6 mice (Fig. 5C,D) indicated that the expression pattern of Cx45 in the IPL of these mice (Fig. 5D) was identical to that observed in CD1 mice. Similar double immunofluorescence in retina of Cx36 KO mice showed a typical absence of labelling for Cx36 in the IPL (Fig. 4E) and a reduction in punctate labelling of Cx45 (Fig. 4F). Counts of Cx45 puncta in fields of the IPL of retina from WT and Cx36 KO mice indicate approximately 33% percent reduction.

Cx36, ZO-1 and ZONAB in relation to calretinin in IPL

To examine further the patterns of punctate labelling for Cx36, ZO-1 and ZONAB observed in the IPL, and particularly to assign a precise location to the Cx36/ZO-1/ZONAB-positive puncta that remain positive for ZO-1/ZONAB in the IPL of Cx36 KO mice, labelling of these proteins was examined in vertical sections of retina simultaneously labelled for calretinin. This was achieved by triple labelling for Cx36, ZO-1 and calretinin in WT mice, shown at low magnification (Fig. 6A) and at high magnification in Fig. 6B, and by triple labelling for ZONAB, ZO-1 and calretinin in WT mice (Fig. 6C) and double labelling for ZONAB and calretinin in Cx36 KO mice (Fig. 6D). Calretinin has been well documented as a marker of a subclass of amacrine cells with somata lying within the inner edge of the inner nuclear layer (INL), and displaced amacrine cells located in the ganglion cell layer (Jeon et al., 1998), all having a characteristic trilaminar distribution pattern of dendritic processes in the middle to outer half of the IPL (Fig. 6A3). Triple labelling revealed that Cx36 (Fig. 6A1,A4) and ZO-1 (Fig. 6A2,A5) were distributed sparsely along the inner calretinin-positive band, moderately in the region between the outer two calretinin-positive bands, and concentrated in a region between the inner two calretinin bands. Magnified confocal images showed a high degree of Cx36/ZO-1 co-localization in IPL sublamina encompassed by the calretinin-positive band, including those puncta between the outer two bands (Fig. 6B). Triple labelling in WT mice showed a similar distribution of ZONAB in relation to calretinin (Fig. 6C1) as observed in the case of Cx36 and ZO-1 and, as in other regions of IPL, indicated substantial co-localization of the larger ZONAB-positive puncta with ZO-1 in the region between the outer two calretinin-positive bands (Fig. 6C2). Double labelling for ZONAB and calretinin in retina of Cx36

KO mice clearly revealed that labelling for ZONAB persisting in the IPL of these mice was located between the two outer calretinin bands and partially overlapping with the outer band (Fig. 6D).

Interaction of Cx45 with ZO-1 in HeLa cells and retina

Cultured HeLa cells transfected with Cx45 were used to examine Cx45 association with ZO-1. In control, empty-vector-transfected cells, labelling of ZO-1 typically appeared as fine, intermittent puncta or as short, continuous strands of immunofluorescence at cell-cell contacts (Fig. 7A1), whereas Cx45 immunoreactivity was entirely absent (Fig. 7A2, 7A3). In HeLa cells stably transfected with Cx45, labelling of ZO-1 had a more dispersed appearance, and was localized both at cell-cell contacts as well as intracellularly (Fig. 7B1). Nearly all cells displayed labelling of Cx45 either at cell-cell contacts or intracellularly (Fig. 7B2), and double immunofluorescence labelling indicated partial Cx45/ZO-1 co-localization at both of these subcellular locations (Fig. 7B3), as better seen in the confocal image (Fig. 7C3).

Immunoblotting and co-immunoprecipitation were used to confirm polyclonal anti-Cx45 antibody specificity and to examine association of Cx45 with ZO-1. In lysates of Cx45-transfected HeLa cells, anti-Cx45 detected a doublet of bands migrating at approximately 45-48 kDa (Fig. 8A, lane 1), and a similar doublet of bands were detected after IP of Cx45 with polyclonal anti-Cx45 (Fig. 8A, lane 3) or IP of ZO-1 with monoclonal anti-ZO-1 (Fig. 8A, lane 4) from these lysates. The doublet of bands was absent in lysates of empty vector-transfected HeLa cells (Fig. 8A, lane 2). Control procedures involving omission of anti-Cx45 and anti-ZO-1 antibodies during IP indicated lack of Cx45 detection in IP material (not shown). Immunoblots of Cx45 in homogenates

of mouse retina are shown in Figure 8B. Anti-Cx45 detected a single band in retina (Fig. 8B, lane 2), corresponding to the lower Cx45 band that was seen in Cx45-transfected HeLa cells (Fig. 8B, lane 1). After IP of ZO-1 from retina using monoclonal anti-ZO-1 antibody, Cx45 was detected migrating as a band corresponding to that seen in retina or the lower band seen in Cx45-transfected HeLa cells (Fig. 8B, lane 3). Detection of Cx45 was also observed after IP of ZO-1 from retina using polyclonal anti-ZO-1 antibody (not shown). Additional bands other than Cx45 and IgG used for IP, some of which were also evident in vector-transfected HeLa cells, are of unknown identity.

Fusion proteins containing GST linked separately to each of the three PDZ domains in ZO-1 and Cx45-transfected HeLa cell lysates were used for in vitro *p*ull-down to examine direct binding of Cx45 to ZO-1. As shown by immunoblotting in Fig. 9, protein eluted from beads coupled to the GST-PDZ1 (Fig. 9, lane 1) or GST-PDZ3 (Fig. 9 lane 3) domain of ZO-1 failed to contain Cx45. However, protein eluted from beads coupled to the GST-PDZ2 domain of ZO-1 (Fig. 9 lane 2) contained Cx45, migrating as a band corresponding to detection of Cx45 in homogenate of mouse retina (Fig. 9, lane 4) and in Cx45-transfected HeLa cells (Fig. 9, lane 5), which was absent in empty vector-transfected HeLa cell (Fig. 9, lane 6).

ZONAB in retina and HeLa cells

Expression of ZONAB in retina and anti-ZONAB antibody specificity were confirmed by probing homogenates of mouse retina and lysates of ZONAB-transfected HeLa cells with anti-ZONAB. In the retina, immunoblots revealed detection of ZONAB as a band migrating at approximately 32 kDa, which was very close to the predicted molecular weight of the ZONAB A (MSY3) alternatively spliced isoform (31.8 kDa). This band

corresponded to a co-migrating protein detected in ZONAB-transfected HeLa cells (Fig. 10, lane 2). A much fainter band at this molecular weight was observed in empty vector-transfected HeLa cells, and may represent endogenous ZONAB expressed at substantially lower levels in the non-transfected cells (Fig. 10, lane 3). It is noteworthy here that the peptide sequence in mouse ZONAB used to generate anti-ZONAB is totally conserved in the human ortholog of this protein, and may thus be expected to recognize the human ortholog in HeLa cells. A band of unknown identity migrating at 30 kDa was also detected in retina and HeLa cells. We cannot rule out the possibility that the additional band detected in retina, transfected and non-transfected HeLa cells represents a modified form of ZONAB, and that the anti- ZONAB detects this form in non-transfected HeLa cells.

DISCUSSION

Cx36 and Cx45 at retinal gap junctions

The present observations of Cx36 distribution in the mouse retina are consistent with results in numerous reports on this connexin in retina of various species. To date, the dense labelling of Cx36 observed in the inner half of the IPL has been ascribed to Cx36 in terminal dendrites of AII amacrine cells and in dendrites of ON-alpha ganglion cells (Feigenspan et al., 2001; Mills et al., 2001; Hidaka et al., 2004; Schubert et al., 2005). In this region, Cx36 was shown to be contained in gap junctions between homologously coupled AII amacrine cell terminal dendrites, between heterologously coupled AII amacrine cell dendrites and ON-cone bipolar cell axon terminals, and between heterologously coupled ON-alpha ganglion cells and wide-field amacrine cells (Famiglietti and Kolb, 1975; Strettoi et al., 1992; Güldenagel et al., 2001; Feigenspan et

al., 2001; Mills et al., 2001; Deans et al., 2002; Schubert et al., 2005). Moderate labelling of Cx36 in the outer half of IPL has been ascribed to Cx36 in OFF-alpha ganglion cell dendrites, forming homologous gap junctions with each other and heterologous gap junctions with dendrites of wide-field amacrine cells (Hidaka et al., 2004; Schubert et al., 2005). The somewhat more sparse labelling of Cx36 in the OPL has been assigned to Cx36 expression in cone pedicles and OFF-cone bipolar cell dendrites (Lee et al., 2003; Feigenspan et al., 2004).

Studies of Cx45 in the retina have been fewer and somewhat contradictory. Pronounced immunolabelling of Cx45 in the innermost part of the IPL was reported to be associated with astrocytes, labelling of Cx45 throughout the retina was found along Müller cell processes, and labelling in the inner part of INL was attributed to Cx45 in amacrine cell bodies (Zahs et al., 2003). In contrast, based on Cx45 promoter driven β-galactosidase expression in the INL and GCL, immunolabelling of Cx45 in IPL was assigned to amacrine cells, and in OPL to bipolar or horizontal cells (Güldenagel et al., 2000). More recently, studies of Cx45 promoter-driven EGFP or β-galactosidase expression in Cx45-deficient mice indicated Cx45 expression in amacrine cells as well as in OFF-cone bipolar cells and ON-cone bipolar cells (Maxeiner et al., 2005). In addition, heterologous AII amacrine/ON bipolar cell gap junctions were identified to be heterotypic, containing Cx36 on the amacrine cell side and Cx45 on the ON-bipolar cell side (Maxeiner et al., 2005). The existence of these heterotypic junctions was supported by EM, electrophysiological and tracer-coupling studies showing that gap junctions between AII amacrine and ON-cone bipolar cells had structural and functional asymmetries and that tracers pass more efficiently from AII amacrine cells to ON cone

bipolar cells than in the other way (Kolb, 1979; Strettoi et al., 1992; Mills and Massey, 1995; Hartveit, 2002). Consistent with these latter findings, our results indicate expression of Cx45 restricted to the IPL, where a small proportion of Cx45 puncta was co-localized with Cx36. The low level of Cx36/Cx45 co-localization we observed was consistent with a 5-fold fewer Cx36-positive puncta observed at intersections between AII amacrine cells/ON cone bipolar cells compared with those at intersection between AII amacrine cells (Mills et al., 2001).

In Cx36 KO mice, the reduction of Cx45-puncta we observed in the IPL suggests requirement of Cx36 for the formation of Cx36/Cx45 heterotypic gap junctions, such as we reported in the case of Cx32 KO mice where absence of Cx32 at astrocyte-oligodendrocyte gap junctions resulted in the loss of Cx30 at these junctions (Nagy et al., 2003). However, the decrease in Cx45-puncta in Cx36 KO mice appeared to exceed the percentage of Cx45-puncta that was co-localized with Cx36 in WT mice, suggesting a broader loss of Cx45 than can be accounted for by its presence in heterotypic Cx36/Cx45 junctions. Gap junctional coupling between AII amacrine cells containing Cx36 and ON cone bipolar cells containing Cx45 represents a key element in the rod pathway (Maxeiner et al., 2005). Our results suggest that deficits observed in this pathway after Cx36 gene deletion (Güldenagel et al., 2001; Deans et al., 2002) may be due to loss of not only Cx36, but also to down-regulation of Cx45 at sites where this connexin forms junctions independently of Cx36, in cells where it is nevertheless co-expressed with Cx36.

Co-localization and interaction of Cx45 with ZO-1

Previous reports have described the localization of ZO-1 along blood vessels in retina, consistent with the well documented association of this protein with tight junctions in CNS vasculature (Wolburg and Lippoldt, 2002; Vorbrodt and Dobrogowska, 2003), as well as in pigment epithelium and outer limiting membrane of retina (Williams and Rizzolo, 1997; Tserentsoodol et al., 1998; Paffenholz et al., 1999; Inoko et al., 2003). However, as shown by us here and elsewhere (Li et al., 2004a; Ciolofan et al., 2005), labelling of ZO-1 was far more broadly distributed in retina than previously observed, with dense ZO-1-positive puncta evident in both the IPL and OPL of mouse retina. We previously demonstrated the association of Cx36 with ZO-1-puncta in both the IPL and OPL, and the direct binding of Cx36 to the first PDZ domain of ZO-1 (Li et al., 2004a,b). The present immunofluorescence and co-IP results extend these observations to include Cx45 as a ZO-1 associated connexin in IPL of mouse retina. Among the population of Cx45-puncta in the IPL, only a small proportion contained Cx36 but nearly all contained ZO-1, indicating Cx45/ZO-1 association at gap junctions lacking Cx36, and ZO-1 expression in cells separately expressing Cx45 and Cx36. Further, the near total Cx45/ZO-1 co-localization observed suggests that each of the above discussed candidate cell types considered to express Cx45 also express ZO-1.

The interaction of Cx45 with ZO-1 was first found by yeast two-hybridization screens using the PDZ domain-containing region of ZO-1 as bait, and it was reported that this interaction was dependent on a short c-terminus PDZ domain binding motif in Cx45 (Kausalya, et al; 2001). Association of Cx45 with ZO-1 was further demonstrated in cultured osteoblastic and Cx45-transfected MDCK cells (Kausalya et al, 2001; Laing et al., 2001), and confirmed by GST-Cx45 pull-down and mutational analysis showing that

the c-terminus isoleucine of Cx45 is required for Cx45/ZO-1 interaction (Thomas et al., 2002). However, the PDZ domain in ZO-1 responsible for mediating interaction with Cx45 was not determined. Our finding that Cx45 interacts with the second PDZ domain of ZO-1 is consistent with the similarity of the c-terminus PDZ binding motif of Cx45 (SVWI) to that in Cx47 (TVWI), which was also shown to interact with the second PDZ domain of ZO-1 (Li et al., 2004b). With now nine members of the connexin family of proteins reported to associate with ZO-1 (Giepmans, 2004; Li et al., 2004a,b,c; Penes et al., 2005), it appears that ZO-1 has functional roles at gap junctions in many cell types expressing these connexins. While the exact nature of those roles remains elusive, the regulatory importance of ZO-1 at gap junctions was recently most clearly demonstrated in ROS osteoblastic cells, where overexpression of the connexin-interacting fragment of ZO-1 disrupted Cx43/ZO-1 interaction, nearly eliminated gap junction-mediated dye-transfer and reduced junctional plaque assembly, whereas overexpresion of ZO-1 increased gap junctional coupling and Cx43 at plasma membrane appositions (Laing et al., 2005). Our results suggest that ZO-1 may exert similar regulatory influences at gap junctions composed of Cx36 and Cx45 in the retina.

In other tissues, ZO-1 expression has been reported in a variety of cell types and it is also a component of adherens junctions (Howarth et al., 1992; Itoh et al., 1991, 1993; Gonzales-Mariscal et al., 2000). Since our results indicated that a substantial proportion of ZO-1-puncta in the IPL were not co-localized with Cx36, and that ZO-1-puncta showing lack of overlap with Cx36 far out numbered Cx45-puncta, it appears that in addition to its presence at gap junctions composed of Cx36 and Cx45, ZO-1 may be associated with other subcellular structures in retina, such as observed in peripheral

tissues. Alternatively, it may be localized at glial gap junctions, as we have observed in mouse brain (Penes et al., 2005).

ZO-1 and ZONAB at retinal gap junctions

Identification of ZO-1 at numerous types of gap junctions has raised the possibility that proteins known to be associated with ZO-1 at tight junctions (Gonzalez-Mariscal, 2003) may also be anchored with ZO-1 at gap junctions. Among such proteins, we chose to examine ZONAB, which was previously shown to interact with ZO-1 at tight junctions of cultured MDCK cells (Balda and Matter, 2000). Our results demonstrate ZONAB expression in the mouse retina, and the high degree of Cx36 co-localization with both ZO-1 and ZONAB in the IPL indicates the co-association of all three proteins at individual puncta. Similarly, we have reported elsewhere that Cx36 associated with rod spherules was nearly totally co-localized with ZO-1 in the OPL (Ciolofan et al., 2005), where the substantial Cx36/ZONAB overlap observed presently indicates co-association of all three proteins also in this region of the retina. Based on these observations, together with previous freeze-fracture replica immunogold labelling studies demonstrating the presence and co-localization of Cx36 and ZO-1 in individual gap junctions between retinal neurons (Rash et al., 2004), it may be concluded that ZONAB is a component of many of these interneuronal gap junctions. As in the case of Cx36/ZO-1, however, not all ZO-1 was associated with ZONAB, indicating the presence of ZO-1 in separate structural entities lacking ZONAB. Further, despite the high incidence of Cx45/ZO-1 co-localization, ZONAB only rarely overlapped with Cx45, indicating its absence at Cx45/Cx45 homotypic gap junctions, and the low level of overlap that did occur may represent ZONAB associated with Cx36/ZO-1 on the Cx36 side of Cx36/Cx45

heterotypic junctions. We found a similar lack of ZONAB association with gap junctions composed of Cx57 in OPL (unpublished observations), which was further indicated by observations of Cx36/ZO-1 and Cx36/ZONAB co-localization in OPL, but an absence of Cx36/Cx57 or Cx57/ZO-1 co-localization in this retinal layer (Ciolofan et al., 2005).

Following its recent identification, only a few reports have appeared on ZONAB or its mouse ortholog MsY3, which has also been referred to as MsY3 (ZONAB A) for the short isoform and MsY4 for the long isoform (ZONAB B). It was found to be expressed in brain, heart, spleen, liver and muscle, with the highest levels observed in testis (Mastrangelo and Kleene, 2000; Davies et al., 2000), and was reported to cause translational repression of protamine 1 mRNA in spermatids (Giorgini et al., 2001, 2002) and transcriptional repression of the tyrosine kinase receptor ErbB2 (a.k.a. Neu or HER2) in canine MDCK cells (Balda and Matter, 2000; Balda et al., 2003). In canine MDCK cells, ZONAB was shown to interact with the SH3 domain of ZO-1, and it was suggested that sequestration of ZONAB by ZO-1 at tight junctions derepresses ErbB2 expression, thereby promoting ErbB2-mediated cell differentiation (Balda and Matter, 2000; Balda et al., 2003). It is noteworthy that neuregulins act as ligands for the ErbB2 receptor, and that neuroregulin/ErbB2 signalling is essential for a variety of cellular processes (Casalini et al., 2004; Holbro and Hynes, 2004; Marmor et al., 2004). Both erbB2 and neuregulin were found to be expressed in mammalian retina, and neuregulin promoted survival and neurite extension of retinal neurons (Bermingham-McDonogh et al., 1996; Williams et al., 1998; Lindqvist et al., 2002). Thus, we speculate that ZO-1/ZONAB may participate in local regulatory control of retinal gap junctions and contribute to far reaching regulatory processes involved in retinal function and development. However, further

biochemical and molecular studies are required to establish ZO-1/ZONAB interaction in retina and the transcriptional activities of ZONAB in retinal neurons.

ZO-1 and ZONAB in Cx36 KO retina

The spatial distribution of Cx36, ZO-1 and ZONAB in IPL was determined in relation to calretinin-positive structures to allow precise localization of ZO-1/ZONAB puncta that remain in the Cx36 KO retina. Immunocytochemical markers for AII amacrine cells include the use of parvalbumin or calretinin in retinas of various species (Gabriel and Straznicky, 1992; Wässle et al., 1993; Casini et al., 1995; Feigenspan et al., 2001; Wässle et al., 1995; Massey and Mills, 1999; Massey et al., 2001). Although these markers fail to label Cx36-containing AII amacrine cells in mouse retina, calretinin was found to be adequate for labelling of other types of amacrine cell somata in the INL and GCL, as well as the dendritic arborisation of these cells in three distinct bands of roughly equal thickness in the outer OFF-sublamina of the IPL (Haverkamp and Wässle, 2000). Among these bands, Cx36/ZO-1/ZONAB puncta were distributed between the two outer bands and intermingled with the outer band. Previous studies of Cx36-puncta in this region of the IPL excluded association of these puncta with appendages of AII amacrine cells distributed in this region, even though the dendrites of these cells are heavily coupled by Cx36 in the inner part of IPL (Feigenspan et al., 2001). A likely candidate for the origin of these Cx36-puncta are OFF-alpha-ganglion cells some of which have dendritic terminal fields distributed in the outer IPL (Famiglietti and Kolb, 1976; Nelson et al., 1978; Sun et al., 2002), in the region of the outer two calretinin-positive bands. These alpha-ganglion cells have been shown to express Cx36, and to be coupled with each other via Cx36, but they also junctionally couple with wide-field amacrine cells that were

shown to lack Cx36 expression (Vaney, 1991, 1994; Penn et al., 1994; Jacoby et al., 1996; Hu and Bloomfield, 2003; Schubert et al., 2005). It was suggested that Cx36 in alpha-ganglion cells form junctions with an as yet unidentified connexin in these wide-field amacrine cells (Schubert et al., 2005). This possibility provides a plausible explanation for the persistence of ZO-1/ZONAB co-localized puncta in the outer region of the IPL in Cx36 KO mice. Thus, these puncta may represent ZO-1/ZONAB association with hemiplaques containing an unknown connexin expressed in wide-field amacrine cells, which ordinarily couples with Cx36 in alpha-ganglion cells or, alternatively, association with an unidentified connexin that forms gap junctions between wide-field amacrine cells (Kolb and Nelson, 1984, 1985). Investigation of these possibilities will require EM analyses to establish the presence of ultrastructurally-identified gap junctions in the outer part of the IPL in Cx36 KO mice, and demonstration of the association of ZO-1/ZONAB with these junctions.

ACKNOLEDGMENTS

This work was supported by grants from the Canadian Institutes of Health Research to JIN. We thank B. McLean and N. Nolette for excellent technical assistance, and Dr. B. Giepmans for providing GST-PDZ expression vectors, and Dr. D. Paul (Harvard University) for providing Cx36 KO mice.

Table 1. Antibodies used for western blotting and immunohistochemistry

Antibody	Type*	Species	Epitope; Designation	Dilution	Source
Cx36	Polyclonal	rabbit	c-terminus; 36-4600	1 µg/ml	Zymed
Cx36	Monoclonal	mouse	mid-region; 37-4600	3 µg/ml	Zymed
Cx45	polyclonal	rabbit	c-terminus; N/A	2 µg/ml	Zymed
Cx45	monoclonal	mouse	aa 354-367; Mab3101	4 µg/ml	Chemicon
ZONAB	polyclonal	rabbit	c-terminus; 40-2800	2 µg/ml	Zymed
ZO-1	polyclonal	rabbit	aa 463-1109; 61-7300	1 µg/ml	Zymed
ZO-1	monoclonal	mouse	aa 334-634; 33-9100	4 µg/ml	Zymed
calretinin	polyclonal	goat	Protein; Ab1550	1:3000	Chemicon

aa, amino acids

Fig. 1. Overview of the laminar distribution and relative densities of Cx36, Cx45, ZO-1 and ZONAB in adult mouse retina. A-H: Each pair of images (A,B), (C,D), (E,F) and (G,H) show low magnification fields of vertical retinal sections labelled by immunofluorescence for the proteins indicted (A,C,E,G) and the same fields counterstained with fluorescence Neurotrace (B,D,F,H, respectively). Labelling of each of the proteins appears punctate in all major layers, whereas ZO-1 also displays continuous labelling along blood vessels (E, arrow). Labelling of Cx36 is very dense in the inner half of IPL (A, double arrow), dense in the outer half of IPL (A, arrowhead), and dense to moderate in the OPL (A, arrow). Labelling of Cx45 is sparse in the IPL and absent elsewhere (C, arrow). Labelling of ZO-1 is dense to moderate in both IPL and OPL (E). Labelling of ZONAB is moderate to sparse in both the IPL and OPL (G). Labelling of photoreceptors and outer limiting membrane seen with anti-ZO-1 (E, arrowhead) and anti-ZONAB antibodies (G, arrow) is of uncertain specificity. Scale bars: 100 μm.

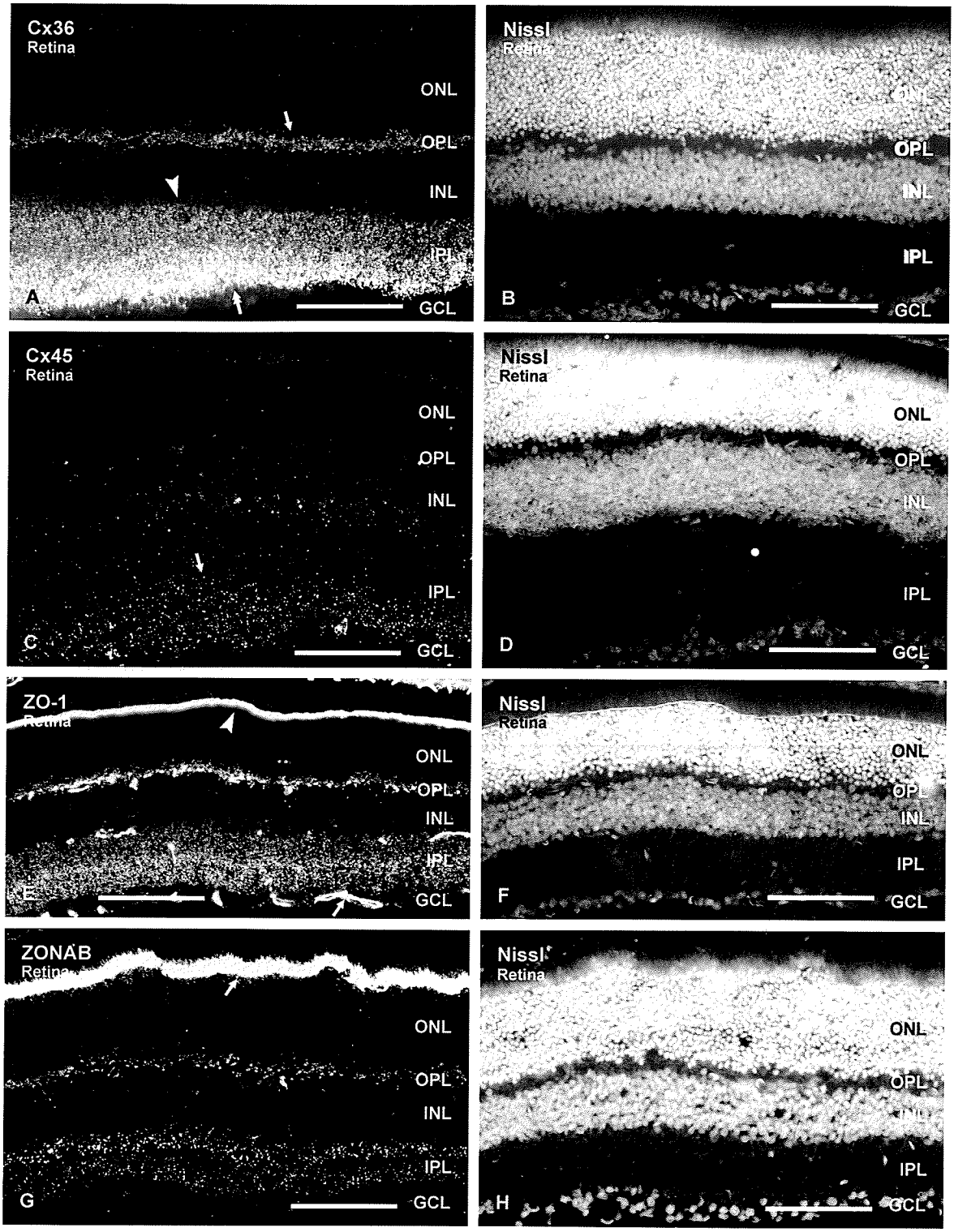
Cx36
Retina
ONL
OPL
INL
IPL
GCL
A
Nissl
Retina
OPL
INL
IPL
GCL
B
Cx45
Retina
ONL
OPL
INL
IPL
GCL
C
Nissl
Retina
ONL
OPL
INL
IPL
GCL
D
ZO-1
Retina
ONL
OPL
INL
IPL
GCL
E
Nissl
Retina
ONL
OPL
INL
IPL
GCL
F
ZONAB
Retina
ONL
OPL
INL
IPL
GCL
G
Nissl
Retina
ONL
OPL
IPL
GCL
H

Fig. 1

Fig. 2. Laser scanning confocal double immunofluorescence showing co-localization relationships between Cx36, Z0-1 and ZONAB in adult mouse retina. A-C: Images show the entire of IPL from inner (bottom) to outer (top) edge, and represent Z-stacks of five scans. Overlap of green and red labelling is seen as yellow in all images. A: Labelling of Cx36 and ZO-1 in the same field. Nearly all Cx36-positive puncta are positive for ZO-1, but not all ZO-1-puncta are positive for Cx36. B: Labelling of Cx36 and ZONAB in the same field. Most Cx36-puncta in mid-regions of the IPL are positive for ZONAB, but those in the extreme inner region lack ZONAB (B1, B3, arrow). The extreme outer region contains many ZONAB-puncta (B2, arrowhead) lacking Cx36 (B3, arrowhead). C: Labelling of ZONAB and ZO-1 in the same field. Nearly all ZONAB-puncta are positive for ZO-1, whereas many ZO-1 puncta lack ZONAB. D: Double labelling of Cx36 (D1) and ZONAB (D2) in the OPL, showing punctate labelling for both, and a high degree of co-localization (D3). Scale bars: 10 μm.

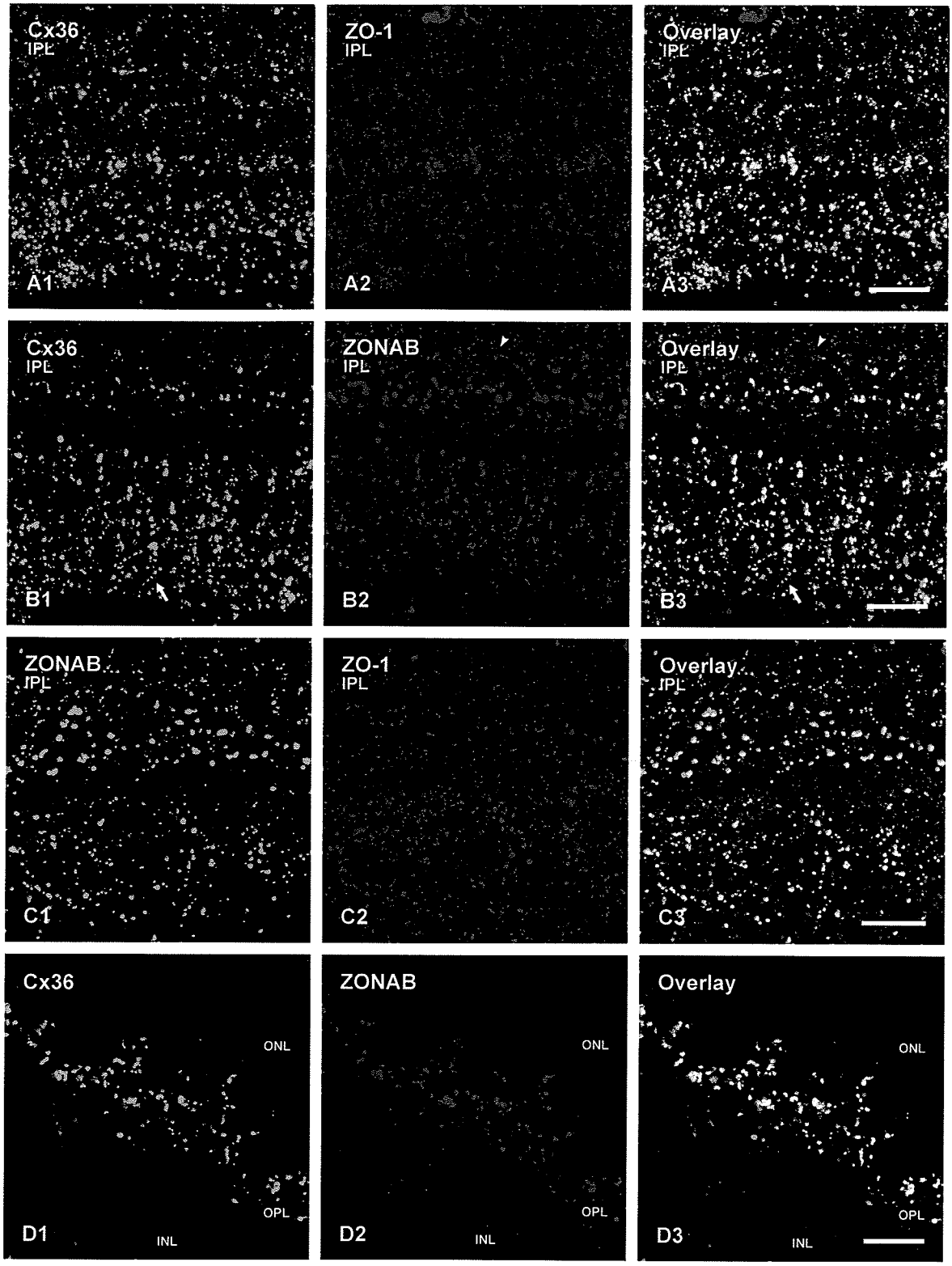
Cx36
IPL
A1
ZO-1
IPL
A2
Overlay
IPL
A3
Cx36
IPL
B1
ZONAB
IPL
B2
Overlay
IPL
B3
ZONAB
IPL
C1
ZO-1
IPL
C2
Overlay
IPL
C3
Cx36
ONL
OPL
D1
INL
ZONAB
ONL
OPL
D2
INL
Overlay
ONL
OPL
D3
INL

Fig. 2

Fig. 3. Laser scanning confocal double immunofluorescence showing co-localization relationships between Cx45, Cx36, ZO-1 and ZONAB in IPL of adult mouse retina. Images show the IPL from inner (bottom) to outer (top) edge, except A which is tilted slightly counter clockwise, and represent Z-stacks of five scans. Overlap of green and red labelling is seen as yellow in all images. A: Labelling of Cx45 and Cx36 in the same field. A small proportion of Cx45-puncta are positive for Cx36, and a very small proportion of Cx36-puncta are positive for Cx45. B: Labelling of Cx45 and ZO-1 in the same field, showing that the majority of the Cx45-puncta are positive for ZO-1, and that only a small proportion of ZO-1-puncta are associated with Cx45. C: Labelling of Cx45 and ZONAB in the same field, showing that very few Cx45-puncta are positive for ZONAB. Scale bars: 10 μm.

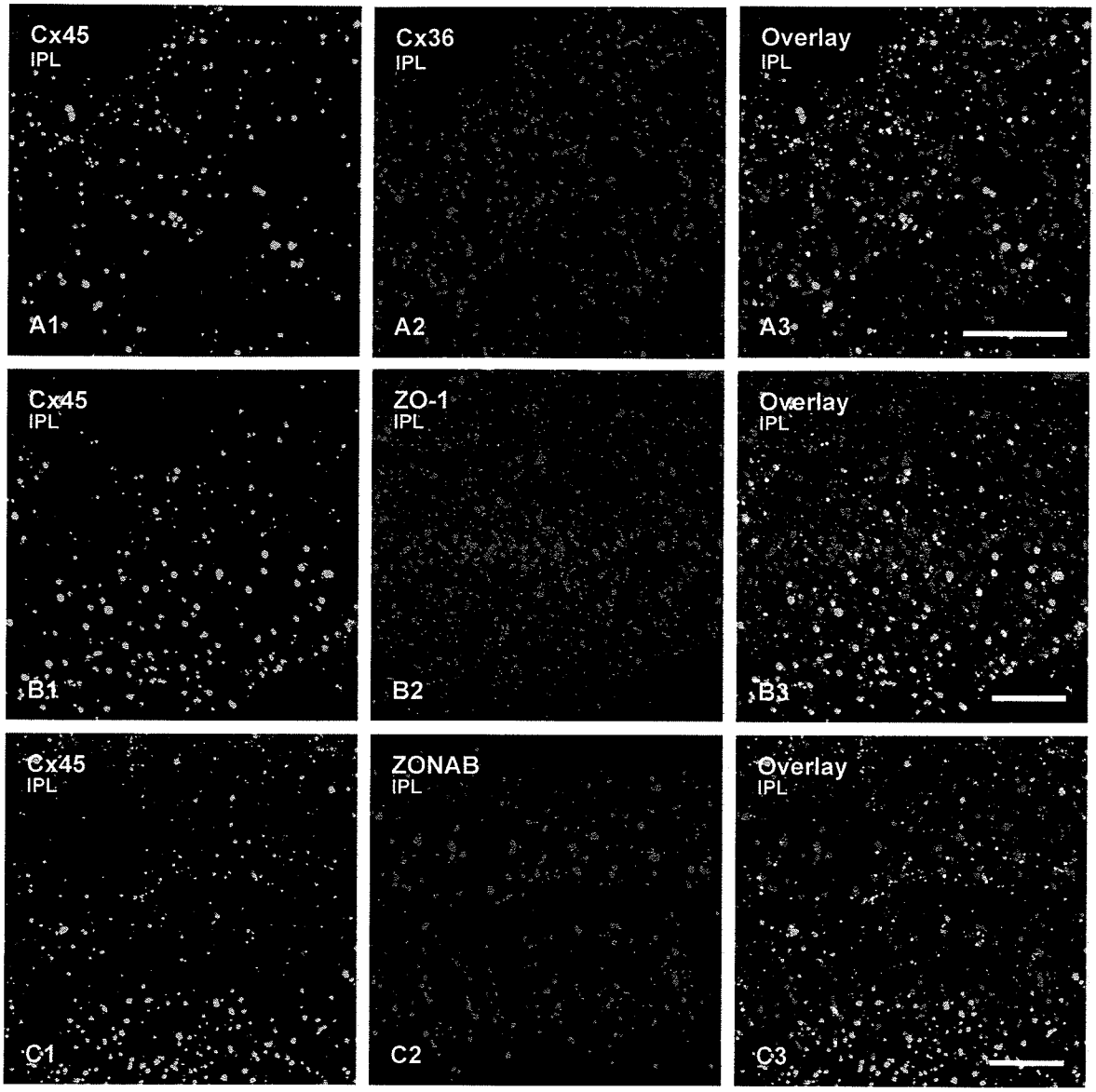
Cx45
IPL
A1
Cx36
IPL
A2
Overlay
IPL
A3
Cx45
IPL
B1
ZO-1
IPL
B2
Overlay
IPL
B3
Cx45
IPL
C1
ZONAB
IPL
C2
Overlay
IPL
C3

Fig. 3

Fig. 4. Immunofluorescence labelling of Cx36, ZO-1 and ZONAB in IPL of retina from adult WT and Cx36 KO C57/BL6 mice. The first three panels in each horizontal row of images show the same field double-labelled for the proteins indicated in IPL of WT and Cx36 KO mice. The fourth panel in each row (A4-F4) shows the outer one-third region of IPL magnified from overlays in A3-F3. Overlap of green and red labelling is seen as yellow in all images. A,B: Compared with dense punctate labelling and co-localization of Cx36 and ZO-1 in the IPL of WT mice (A), Cx36 is absent (B1) and ZO-1 is only slightly reduced (B2) in the IPL of Cx36 KO mice. C,D: Compared with dense labelling and co-localization of Cx36 and ZONAB in most regions of the IPL of WT mice (C), including the outer margin (C4), the absence of Cx36 in Cx36 KO mice (D1) is accompanied by a large reduction of ZONAB in most regions of the IPL, except the outer one-third margin (D2, arrrows, D4). E,F: As in CD1 mice, substantial ZO-1/ZONAB co-localization is seen in IPL of WT C57/BL6 mice, and punctate labelling for ZONAB that persists in the outer third of IPL in Cx36 KO mice (F2, arrows) remains co-localized with ZO-1 (F3, arrows, F4). Scale bars: A1,2,3-F1,2,3 10 μm; A4-F4, 5 μm.

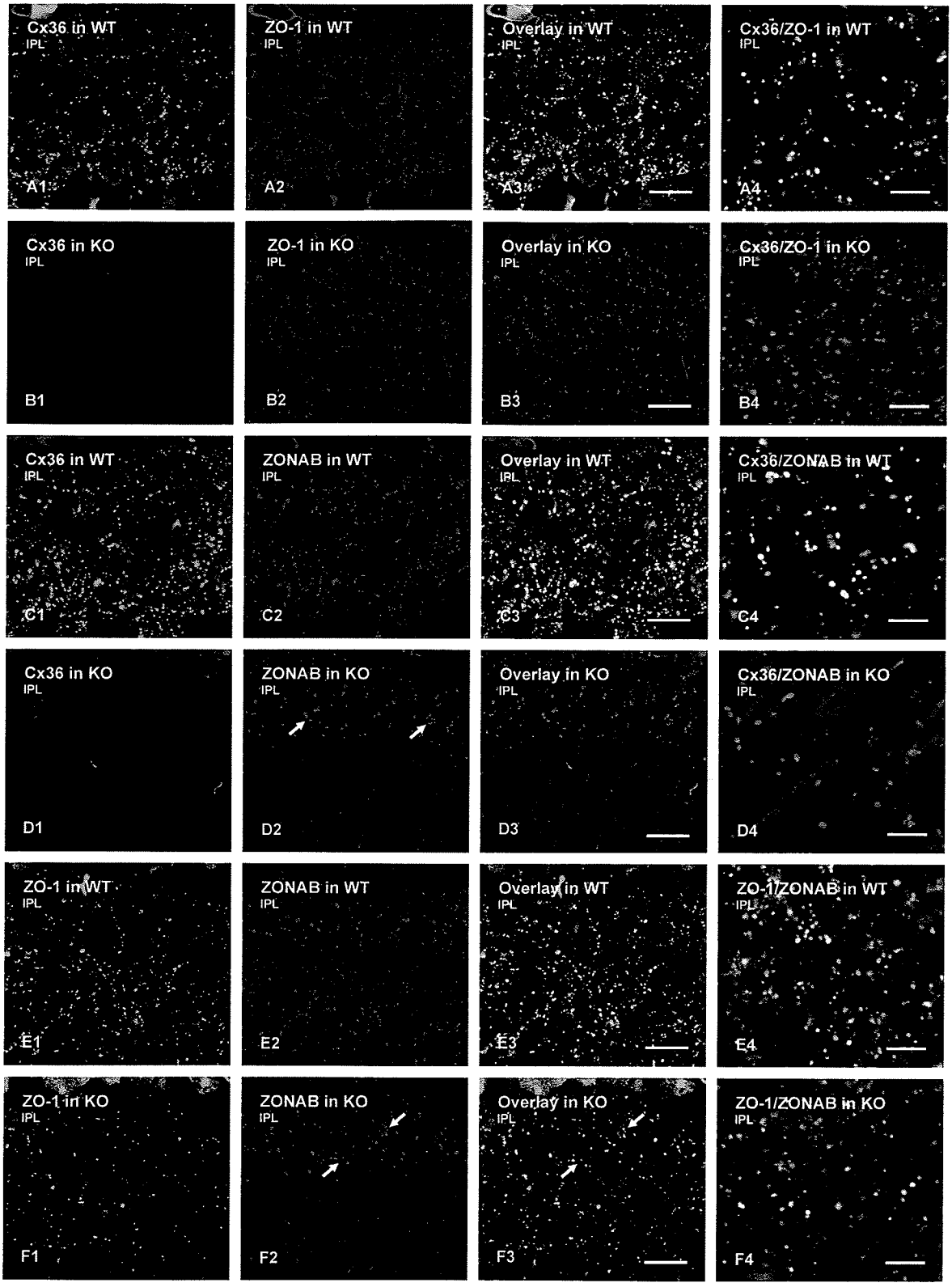
Cx36 in WT
IPL
A1
ZO-1 in WT
IPL
A2
Overlay in WT
IPL
A3
Cx36/ZO-1 in WT
IPL
A4
Cx36 in KO
IPL
B1
ZO-1 in KO
IPL
B2
Overlay in KO
IPL
B3
Cx36/ZO-1 in KO
IPL
B4
Cx36 in WT
IPL
C1
ZONAB in WT
IPL
C2
Overlay in WT
IPL
C3
Cx36/ZONAB in WT
IPL
C4
Cx36 in KO
IPL
D1
ZONAB in KO
IPL
D2
Overlay in KO
IPL
D3
Cx36/ZONAB in KO
IPL
D4
ZO-1 in WT
IPL
E1
ZONAB in WT
IPL
E2
Overlay in WT
IPL
E3
ZO-1/ZONAB in WT
IPL
E4
ZO-1 in KO
IPL
F1
ZONAB in KO
IPL
F2
Overlay in KO
IPL
F3
ZO-1/ZONAB in KO
IPL
F4

Fig. 4

Fig. 5. Laser scanning confocal double immunofluorescence of ZONAB in the OPL, and Cx36 and Cx45 in the IPL of WT and Cx36 KO adult mouse retina. A,B: Single confocal scans showing punctate labelling of ZONAB in the OPL of WT retina, and a large reduction of ZONAB-positive puncta in the OPL of retina from Cx36 KO mice. C,D: Single confocal scans showing Cx36-puncta (C) and Cx45-puncta (D) in the IPL of WT retina. E,F: Single confocal scans showing an absence of labelling for Cx36 (E) and a reduction of labelling for Cx45 (F) in IPL of retina from Cx36 KO mice. Scale bars: 10 μm.

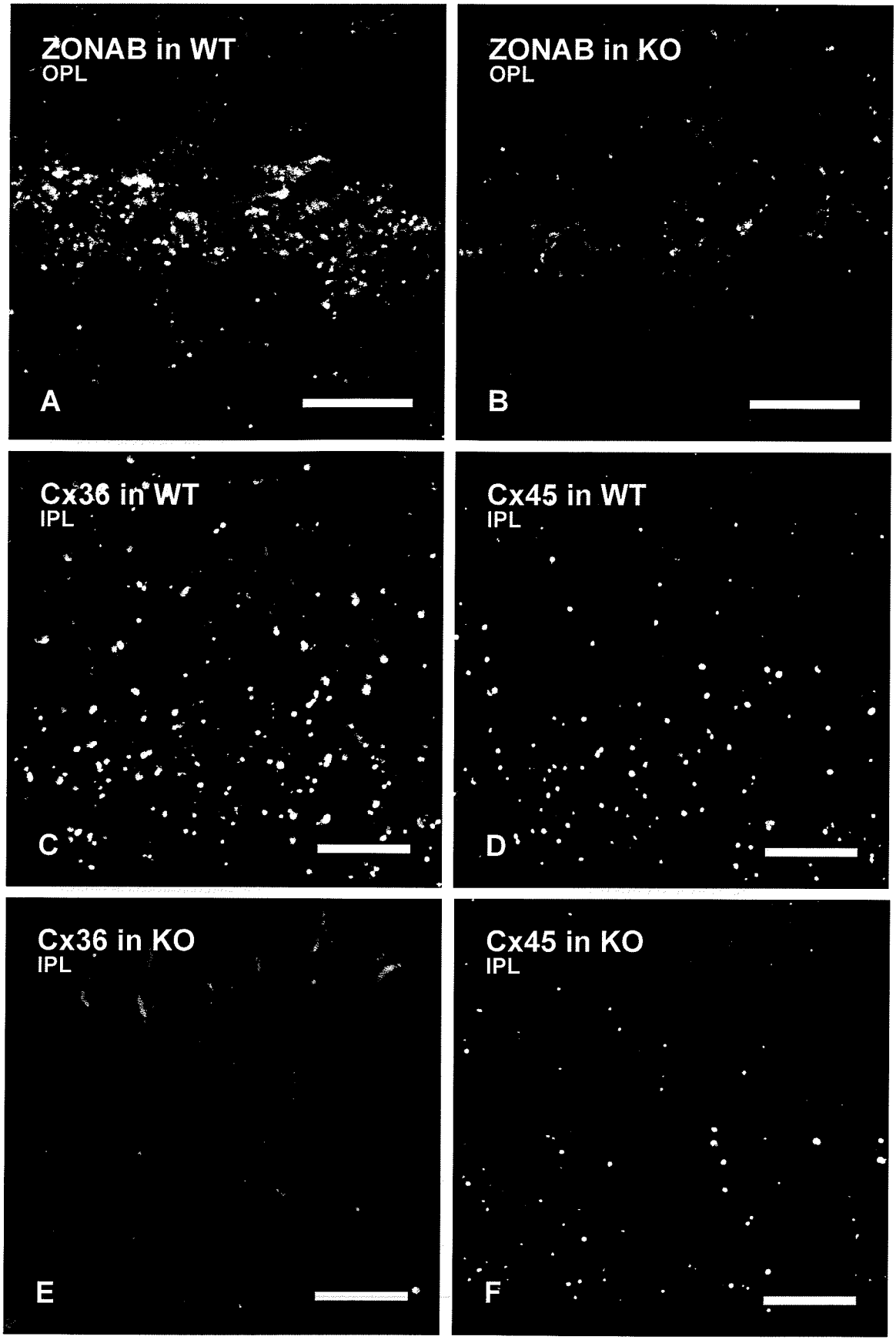
ZONAB in WT
OPL
A
ZONAB in KO
OPL
B
Cx36 in WT
IPL
C
Cx45 in WT
IPL
D
Cx36 in KO
IPL
E
Cx45 in KO
IPL
F

Fig. 5

Fig. 6. A1-A6: Triple immunofluorescence labelling showing the distribution of Cx36, ZO-1 and ZONAB in relation to the sublaminar arrangement of calretinin in the IPL of adult mouse retina. Low magnifications of the same field show Cx36 (A1), ZO-1 (A2) and calretinin (A3) in relation to the retinal layers GCL, IPL and INL, and Cx36/calretinin in overlay (A4), ZO-1/calretinin in overlay (A5) and Cx36/ZO-1/calretinin in overlay (A6). The processes of calretinin-positive amacrine cells form three parallel bands (A3, arrows) in the outer part of IPL, with the outer band located near the IPL/INL border (dotted line). Cx36 and ZO-1 are relatively sparse along the inner bands (arrowheads), and are more concentrated between the inner two bands. B,C: Higher magnifications showing Cx36/calretinin (B1), ZO-1/calretinin (B2), and Cx36/ZO-1/calretinin in overlay (B3), and ZONAB/calretinin (C1) and ZO-1/ZONAB/calretinin (C2) in overlay. Fine Cx36-puncta co-localized with ZO-1 (B, arrowheads) and larger ZONAB-puncta co-localized with ZO-1 (C, arrowheads) are seen between the outer calretinin-positive bands, as well as straddling the outer band. D: Double labelling of ZONAB and calretinin in retina of Cx36 KO mice, showing the persistence of ZONAB-positive puncta between the outer two calretinin-positive bands (arrowheads). Scale bars: A1-A6, 20 μm; B-D, 10 μm.

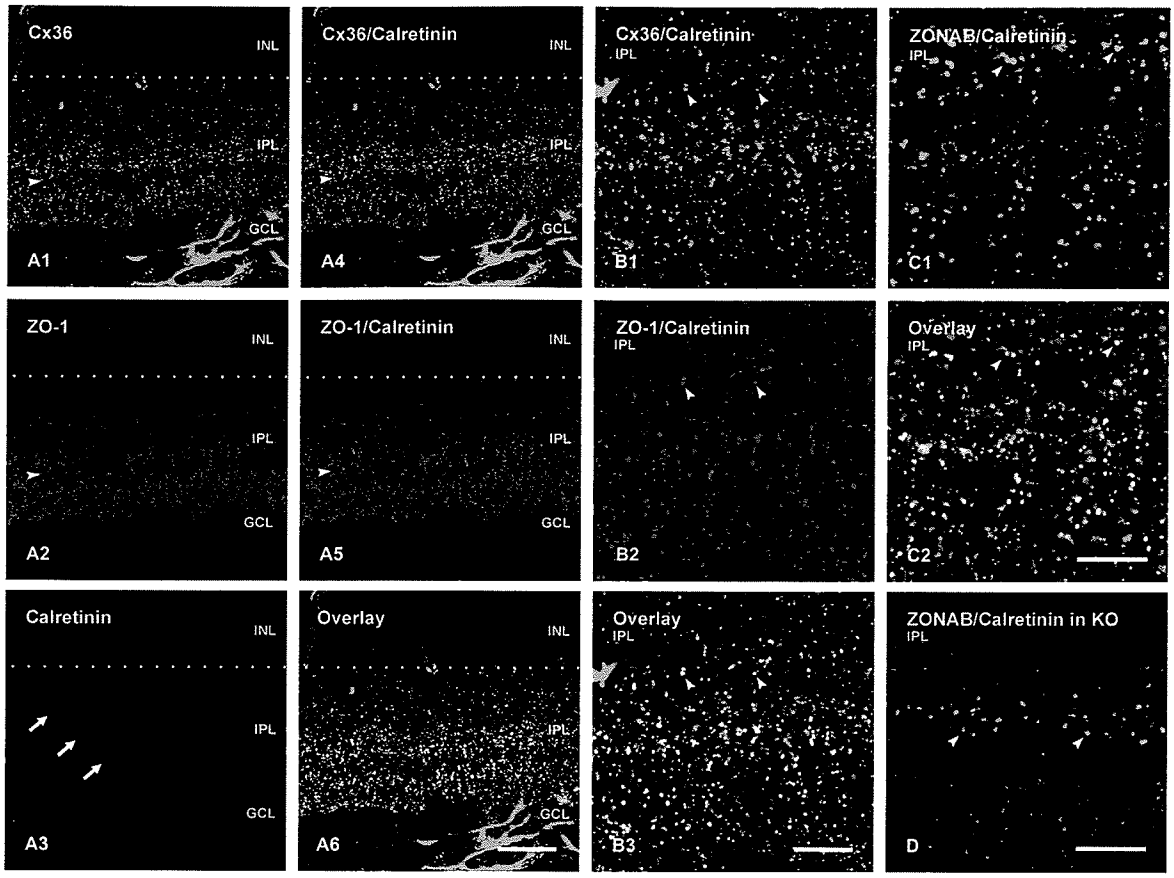
Cx36
INL
IPL
GCL
A1
Cx36/Calretinin
INL
IPL
GCL
A4
Cx36/Calretinin
IPL
B1
ZONAB/Calretinin
IPL
C1
ZO-1
INL
IPL
GCL
A2
ZO-1/Calretinin
INL
IPL
GCL
A5
ZO-1/Calretinin
IPL
B2
Overlay
IPL
C2
Calretinin
INL
IPL
GCL
A3
Overlay
INL
IPL
GCL
A6
Overlay
IPL
B3
ZONAB/Calretinin in KO
IPL
D

Fig. 6

Fig. 7. Double immunofluorescence labelling of ZO-1 and Cx45 in HeLa cells in culture. A: Control non-transfected HeLa cells showing labelling of ZO-1 at cell-cell contacts (A1, arrows), a lower level of intracellular ZO-1-puncta, and an absence of labelling for Cx45 (A2). B: HeLa cells stably transfected with Cx45. Immunolabelling is seen as linear strands of ZO-1-puncta (B1) and Cx45-puncta (B2) at cell-cell contacts (arrows), as well as collections of puncta within cells (arrowheads), and ZO-1/Cx45 co-localization is evident at both locations (B3). C: Enlarged confocal micrograph images showing same results as in B. Scale bars: 50 μm.

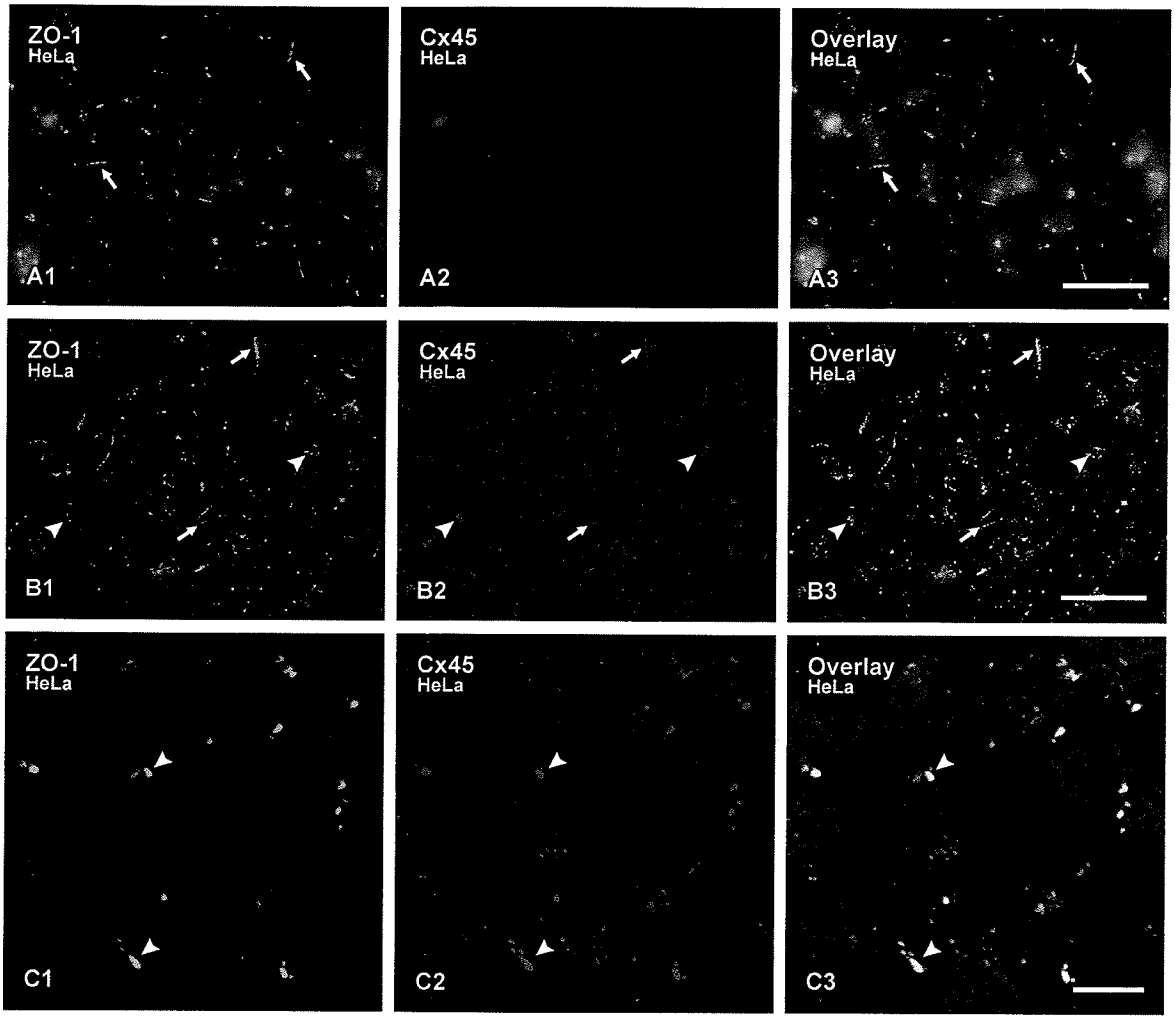
ZO-1
HeLa
A1
Cx45
HeLa
A2
Overlay
HeLa
A3
ZO-1
HeLa
B1
Cx45
HeLa
B2
Overlay
HeLa
B3
ZO-1
HeLa
C1
Cx45
HeLa
C2
Overlay
HeLa
C3

Fig. 7

Fig. 8. Immunoblot showing co-IP of Cx45 with ZO-1. A: Lanes were loaded with lysates from HeLa cells stably transfected with Cx45 (lane 1) and empty vector-transfected HeLa cells (lane 2), and anti-Cx45 IP protein (Lane 3) and anti-ZO-1 IP protein (lane 4) from Cx45-transfected HeLa cells. Anti-Cx45 antibody detects Cx45 in HeLa cells expressing this connexin (lane 1) and in IP of Cx45 from Cx45-transfected HeLa cells (lane 3), shown as positive controls for Cx45 detection, but not in vector-transfected HeLa cells (lane 2), shown as a negative control. Cx45 is also detected after IP of ZO-1 from lysates of Cx45-transfected cells (lane 4). Cx45 appears as a doublet of bands migrating between 45 and 48 kDa (arrowheads). B: Anti-Cx45 detected a band in homogenates of mouse retina (Fig. 8B, lane 2), corresponding to the lower Cx45 band that was seen in Cx45- transfected HeLa cells (Fig. 8B, lane 1). After IP of ZO-1 from retina, Cx45 was detected migrating as a band corresponding to that seen in retina or the lower band seen in Cx45-transfected HeLa cells (Fig. 8B, lane 3).

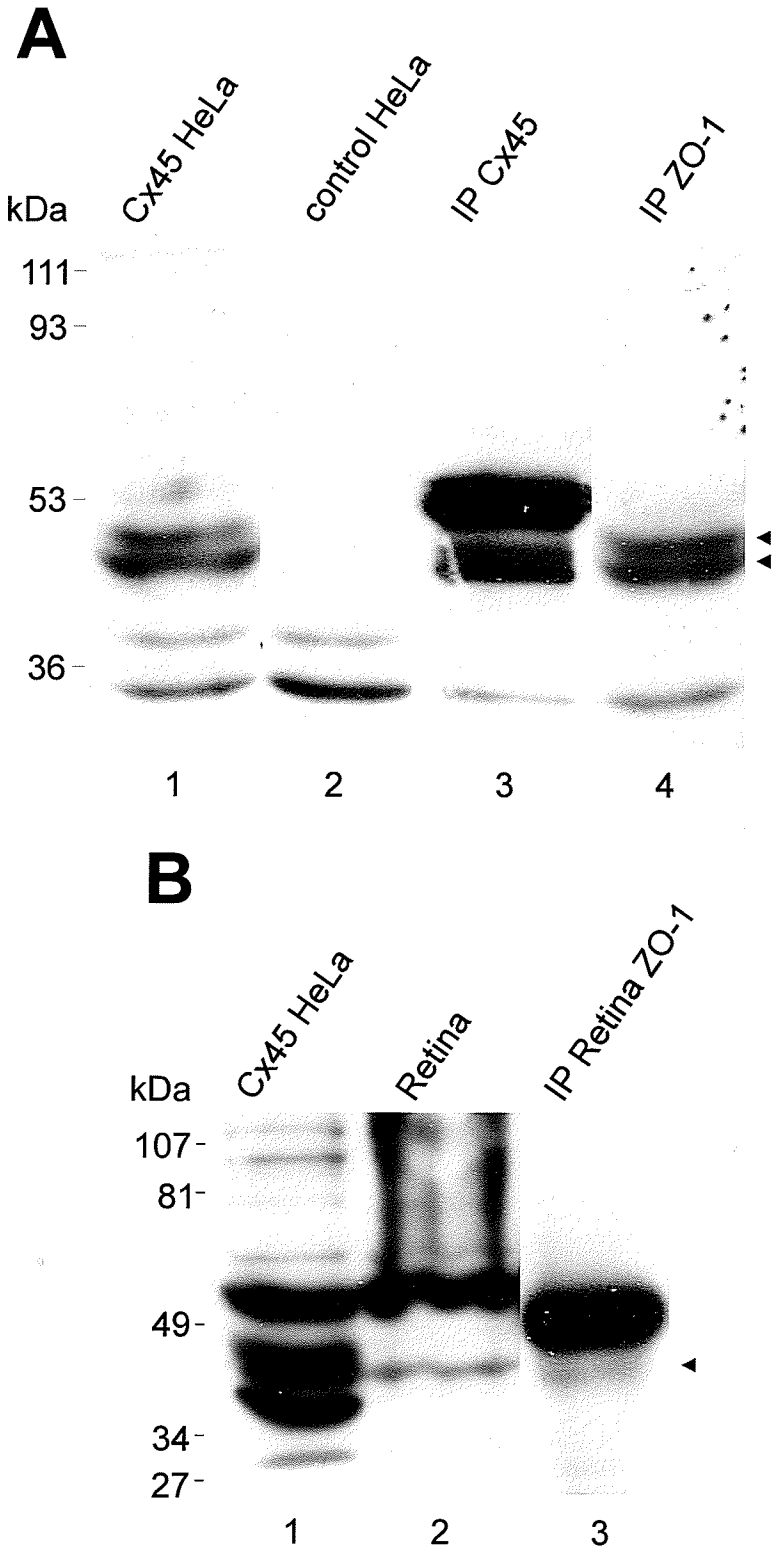
A
Cx45 HeLa
control HeLa
IP Cx45
IP ZO-1
kDa
111
93
53
36
1
2
3
4
B
Cx45 HeLa
Retina
IP Retina ZO-1
kDa
107
81
49
34
27
1
2
3

Fig. 8

Fig. 9. Pull-down assay showing Cx45 interaction with the second PDZ domain of ZO-1. Lysates of Cx45-transfected HeLa cells were incubated with GST fusion proteins containing either the PDZ1, PDZ2 or PDZ3 domain of ZO-1, and immunoblots of pull-down proteins were probed with anti-Cx45. Detection of Cx45 is seen after pull-down with the second PDZ domain of ZO-1 (lane 2), but not after pull-down with the first or third PDZ domains of ZO-1 (lane 1 and 3). The Cx45 band obtained by pull-down in lane 2 corresponds to detection of the same band in homogenates of retina (lane 4) and in lysates of Cx45-transfected HeLa cells (lane 5), which is absent in lysates of empty vector-transfected HeLa cells (lane 6).

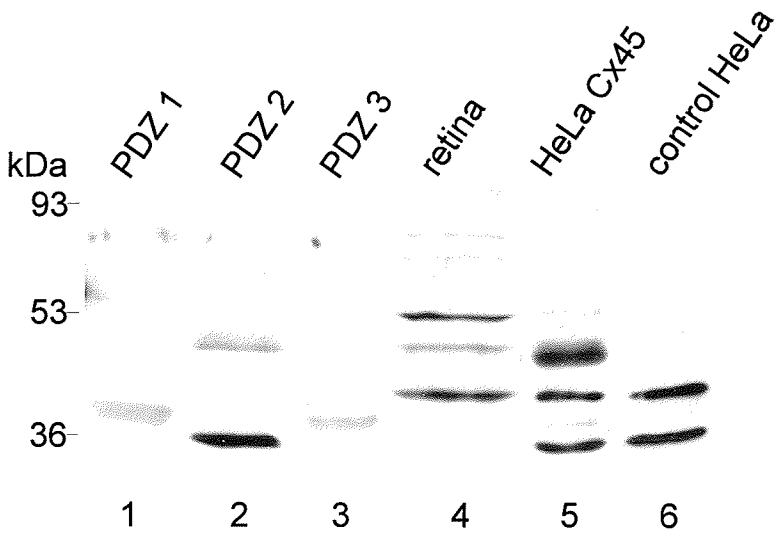
kDa
93
53
36
PDZ 1
PDZ 2
PDZ 3
retina
HeLa Cx45
control HeLa
1
2
3
4
5
6

Fig. 9

Fig. 10. Immunoblot showing detection of ZONAB in retina (lane 1) and in HeLa cells transiently transfected with ZONAB A (lane 2), and absence of a corresponding band in control empty vector-transfected HeLa cells (lane 3). ZONAB A is seen migrating at approximately 32 kDa in retina and ZONAB-transfected cells (arrowhead). An additional protein migrating slightly faster at 30 kDa is also detected by anti-ZONAB in all three tissues, and is of uncertain identity.

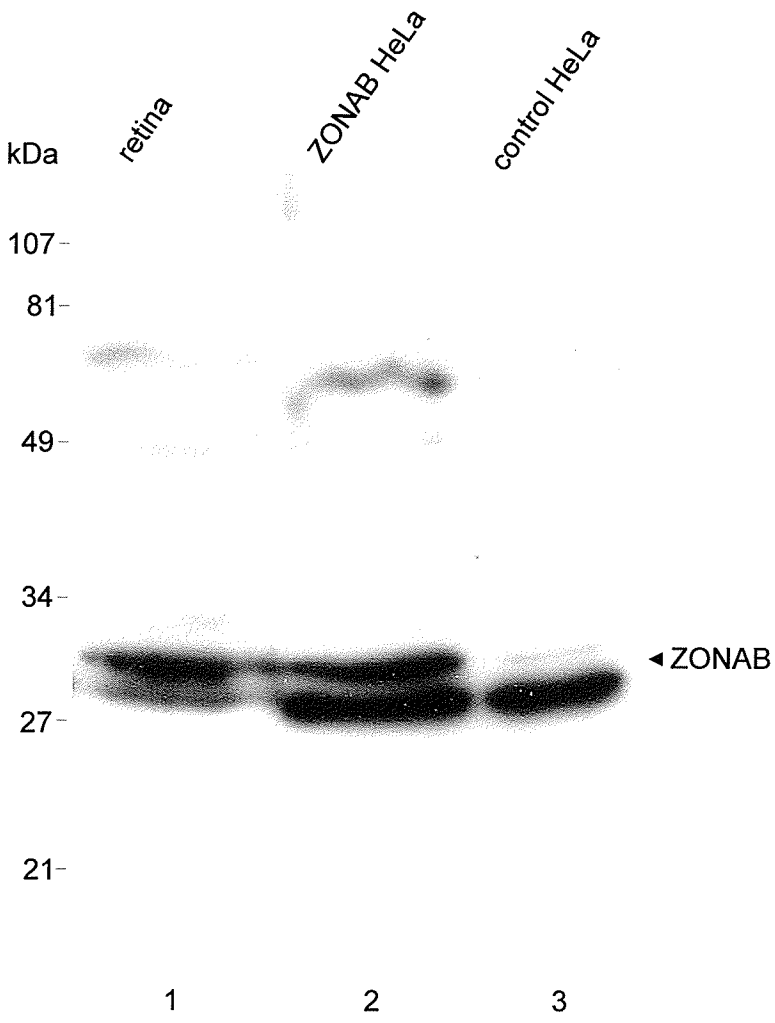
kDa
retina
ZONAB HeLa
control HeLa
107
81
49
34
27
21
ZONAB
1
2
3

Fig. 10

VI. PROJECT II

Spatial relationships of connexin57, connexin36 and zonula occludens-1 (ZO-1) in the outer plexiform layer of mouse retina

C. Ciolofan, K. Wellershaus, K. Willecke and J.I. Nagy

European Journal of Neuroscience (submitted)

ABSTRACT

Horizontal cells form extensive gap junctions with each other in mammalian retina, and lacZ reporter analyses have indicated that these cells express the gap junction forming protein connexin57 (Cx57). Using newly developed anti-Cx57 antibodies, we demonstrate punctate immunolabelling of Cx57 co-distributed with calbindin-positive horizontal cells in the outer plexiform layer (OPL) of mouse retina, with antibody specificity confirmed by absence of Cx57 immunosignals in retina of Cx57 knockout mice. We conducted double immunofluorescence labelling to determine the spatial relationships of Cx57, the gap junction protein Cx36, the gap junction-associated protein zonula occludens-1 (ZO-1) and the photoreceptor ribbon synapse-associated protein bassoon in the OPL. Cx57 in the OPL was often found immediately adjacent to, but lacking total overlap with, Cx36-positive and ZO-1-positive puncta. Cx57 was also located immediately adjacent to bassoon-positive ribbon synapses at rod spherules, and intermingled with such synapses in cone pedicles. Cx36 was substantially co-localized with ZO-1 in the OPL, and both of these proteins were frequently located in close spatial proximity to bassoon-positive ribbon synapses. These results suggest an absence of Cx57/Cx36 heterotypic gap junctional coupling in mouse retina, and ZO-1 interaction with Cx36 but not with Cx57 in the OPL. Further, an arrangement of synaptic contacts within rod spherules is suggested whereby gap junctions between horizontal cell terminals containing Cx57 occur in very close proximity to ribbon synapses formed by photoreceptors, as well as in close proximity to homotypic or heterotypic gap junctions between rods and cones.

INTRODUCTION

Visual information is transmitted from photoreceptors to ganglion cells in separate, parallel ON- and OFF-channels for processing of light and dark signals through the retina, respectively. Photoreceptor, bipolar and ganglion cells spread signals via vertical retinal pathways, whereas horizontal and amacrine cells contribute to lateral distribution of signals. These vertical and lateral channels converge in the outer plexiform layer (OPL), where synaptic interactions occur between horizontal, bipolar and photoreceptor cells (Missotten, 1965; Kolb, 1970, 1974, 1977). Gap junctions are formed by the five major classes of neurons in the mammalian retina, and allow these cells to communicate via complex networks of electrical synapses (Söhl et al., 2000). The importance of these synapses in visual information processing was indicated by observations of physiological deficits in retina of transgenic mice lacking gap junctions formed by at least one member of the connexin (Cx) family of proteins, namely connexin36 (Cx36) (Güldenagel et al., 2001; Deans et al., 2002; Maxeiner et al., 2005). In addition, regulated electrical coupling between horizontal cells contributes to retinal adaptation to stimuli under various lighting conditions (Teranishi et al., 1983; Piccolino et al., 1984; He et al., 2000). Horizontal cells as well as photoreceptors and cone bipolar cells each form gap junctions in the outer plexiform layer (OPL) of rodent retina. Horizontal cell axon terminals form the lateral elements apposing ribbon synapses within rod spherules, and horizontal cell dendrites form synaptic contacts with cones at ribbon synapses of cones pedicles (Dowling and Boycott, 1966; Kolb, 1974; Raviola and Gilula, 1975).

Ultrastructural documentation of gap junctions formed at specific sites by various classes of mammalian retinal neurons have been supplemented by the identification of connexins in particular cell types. In particular, Cx36 in retina has been well studied, and there is evidence for its expression in rod and cone photoreceptors, subclasses of bipolar cells and AII-amacrine cells (Mills et al., 2001; Güldenagel et al., 2001; Deans et al., 2002; Feigenspan et al., 2001, 2004). Following identification and characterization of mouse connexin57 (Cx57) (Manthey et al., 1999), evidence for expression of this connexin in horizontal cells was obtained in transgenic mice, where the Cx57 coding region was replaced with the LacZ coding region such that the expression of b-galactosidase is driven by the Cx57 promoter (Hombach et al., 2004).

In the present study, we used newly developed anti-Cx57 antibodies to investigate the expression and distribution of Cx57 in mouse retina. Specificity of these antibodies was examined by comparisons of Cx57 detection in retinas of wild-type and Cx57 knockout (KO) mice. Double immunofluorescence labelling was undertaken to determine expression patterns of Cx57 in relation to that of Cx36. Having previously shown the association of Cx36 with zonula occludens-1 (ZO-1) in the inner plexiform layer of mouse retina (Li et al., 2004a), we examined cellular associations of Cx57 and Cx36 with ZO-1 in the OPL. In addition, the spatial deployment of Cx57 and Cx36 was examined in relation to the protein bassoon, which is known to be associated with ribbon synapses at cone pedicles and rod spherules.

MATHERIALS AND METHODS

Antibodies and animals

Primary antibodies used in this study are listed in Table 1, with indications of source and dilutions employed. Monoclonal mouse anti-calbindin C-9848 antibody was obtained from Sigma (St. Louis, CA, USA), and monoclonal anti-bassoon VAM-PS00 antibody was purchased from Stressgen Biotechnologies Corporation (Victoria, BC, Canada). Affinity-purified anti-Cx57, anti-Cx36 and anti-ZO-1 antibodies were obtained from Zymed Laboratories Inc. (South San Francisco, CA, USA). A total of twenty-five normal adult male CD1 mice, five wild-type male C57BL/6 and four Cx57 knockout mice and two Cx36 knockout mice were used in this study in accordance with animal approval protocols at our respective universities, including minimization of stress to, and number of animals used.

Light microscope immunofluorescence

Animals were deeply anesthetised with equithesin (3 ml/kg) and perfused transcardially with 3 ml of cold (4°C) pre-fixative (50 mM sodium phosphate buffer, pH 7.4, 0.1% sodium nitrite, 0.9% NaCl and 1 unit/ml of heparin). This was followed by perfusion with 40 ml of fixative solution containing cold 0.16 M sodium phosphate buffer, pH 7.6, 0.2% picric acid and 1% or 2% paraformaldehyde. Animals were then perfused with 10 ml of cold solution containing 10% sucrose and 25 mM sodium phosphate buffer, pH 7.4). Eyes were carefully removed and stored at 4°C for 24-48 h in cryoprotectant (25 mM sodium phosphate buffer, pH 7.4, 10% sucrose, 0.04% sodium azide). Vertical and horizontal sections of retina were cut on a cryostat at a thickness of 10 μm, and collected on gelatinized glass slides. Sections were processed for immunofluorescence staining

with all antibodies diluted in TBST (50 mM of Tris-HCl, pH 7.4, containing 1.5% sodium chloride, 0.3% Triton X-100) and either 5% normal goat serum or 5% normal donkey serum.

For single labelling, sections were incubated for 24 h at 4°C with polyclonal anti-Cx57, monoclonal anti-calbindin and monoclonal anti-bassoon, then washed for 1 h in TBST and incubated with secondary antibody for 1.5 h at room temperature. Secondary antibodies used were AlexaFlour 488-conjugated goat anti-rabbit IgG diluted 1:1000 (Molecular Probes, Eugene, Oregon), Cy3-conjugated donkey anti-rabbit diluted 1:200 (Jackson ImmunoResearch Laboratories, West Groove, PA, USA), FITC-conjugated horse anti-mouse IgG diluted 1:100 (Vector Laboratories, Burlingame, CA, USA), Cy3-conjugated goat anti-mouse IgG diluted 1:200 (Jackson ImmunoResearch Laboratories), and AlexaFlour 488-conjugated goat anti-mouse IgG diluted 1:1000 (Molecular Probes). The same procedures were used for double immunofluorescence labelling, except that sections were incubated simultaneously with polyclonal anti-Cx57 and either monoclonal anti-Cx36, monoclonal anti-ZO-1, monoclonal anti-calbindin or monoclonal anti-bassoon. Conversely, polyclonal anti-Cx36 was incubated simultaneously with either monoclonal anti-ZO-1 or either monoclonal anti-bassoon, and monoclonal anti-Cx36 was incubated simultaneously with polyclonal anti ZO-1. Sections were then simultaneously incubated with appropriate combination of the secondary antibodies describe above, then washed in TBST for 20 min, followed by two times 15 min washes in 50 mM Tris-HCl buffer, pH 7.4. Vertical sections, single labelled with anti-Cx57 or anti-Cx36 antibodies were counterstained with either green Nissl fluorescent NeuroTrace (stain N21480) or red Nissl NeuroTrace (stain N21482) (Molecular Probes (Eugene, OR, USA). All sections

were coverslipped with antifade medium. Control procedures involving omission of one of the primary antibodies with inclusion of each of the secondary antibodies indicated absence of inappropriate cross-reactions between primary and secondary antibodies for all of the combinations used in this study.

Immunofluorescence was examined on a Zeiss Axioskop2 fluorescence microscope, using Axiovision 3.0 software (Carl Zeiss Canada, Toronto, Ontario, Canada) for capturing images. Laser scanning confocal analysis was conducted with a Olympus Fluoview IX70 confocal microscope. The double-labelled sections were scanned twice, using single laser excitation for each fluorochrome per scan, and images were obtained using Olympus Fluoview software. Final images were assembled according to appropriate size and adjusted for contrast using Corel Draw 8 (Corel Corp., Ottawa, Canada), Photoshop 6.0 (Adobe Systems, San Jose, CA, USA) and Northern Eclipse software (Empix Imaging, Mississauga, Ontario, Canada).

RESULTS

Immunofluorescence localization of Cx57 in mouse retina

Expression of Cx57 in mouse retina was investigated by immunofluorescence using affinity-purified antibodies (40-4800 and 40-5000) raised in rabbits against two different peptides with amino acid sequences corresponding to non-overlapping regions in Cx57. These antibodies produced qualitatively similar labelling patterns, as observed in vertical sections cut perpendicular to the retinal layers (Fig. 1A-D). Sections were counterstained with Nissl fluorescent NeuroTrace to allow visualization of the layers, including the ganglion cell layer (GCL), inner plexiform layer (IPL), inner nuclear layer (INL), outer

plexiform layer (OPL) and outer nuclear layer (ONL) (Fig. 1A-D). Labelling was characterized by a continuous band of moderate to intense immunoreactivity restricted to the OPL, and encompassing the full width of this layer. Although faint background fluorescence was observed with antibody 40-5000 in various areas of retina (Fig. 1A), neither of the antibodies produced labelling in other retinal layers comparable to that seen in the OPL. However, variable diffuse fluorescence occurred in the outer segment of photoreceptors (Fig. 1A,C, Fig. 3A) with not only anti-Cx57 antibodies, but also with a variety of other antibodies we have employed against proteins known to be absent in photoreceptors (not shown), suggesting that this layer is particularly prone to non-specific binding of antibodies. Immunofluorescence labelling in OPL was reproducibly obtained with both antibodies under optimal fixation conditions, consisting of fixative containing 1% paraformaldehyde, and was noticeably suppressed after fixation with 2% paraformaldehyde.

Specificity of Cx57 detection with the two antibodies was examined by comparison of labelling in retinas of WT and Cx57 KO mice. Antibody 40-4800 gave a typical pattern of labelling in OPL of retina from WT mice (Fig. 1E), and showed an absence of labelling in OPL of retina from Cx57 KO mice (Fig. 1F). Curiously, labelling with antibody 40-5000 persisted in Cx57 KO mice, which may be due to cross reaction of the antibody with a protein of unknown identity specifically expressed in the OPL, or incomplete knockout of Cx57, with the sequence recognized by antibody 40-5000 still present in these mice. After primary antibody omission, labelling in mouse retina was comparable to that seen in Cx57 KO mice. In view of these results, all further studies, except those shown in Figure 8, were pursued only with antibody 40-4800.

Cx57 in retina of WT and Cx36 KO mice

Possible alterations in retinal Cx57 expression were examined in mice with Cx36 gene deletion. Consistent with previous reports of Cx36 localization in mammalian retina (Feigenspan et al., 2001, 2004; Li et al., 2004a), low magnification images of vertical retinal sections immunolabelled for Cx36 (Fig. 2A) and counterstained with Nissl (Fig. 2B) revealed Cx36 to be densely and moderately distributed in the inner and outer half of the IPL, respectively. In addition, a continuous band of faint labelling was evident in the OPL, and other retinal layers were devoid of labelling. By confocal double immunofluorescence in retinas of WT mice, labelling for both Cx57 and Cx36 in the OPL consisted of fine, sparsely distributed puncta (Fig. 2C,D). Confocal double immunofluorescence in retinas of Cx36 KO mice showed persistence of Cx57 (Fig. 2E), but an absence of Cx36 in the OPL (Fig. 2F) and the IPL (not shown), as previously reported (Li et al., 2004a). Although presented in slightly different planes of section through the retina (Fig. 2C,E), no discernable differences in intensity or density of labelling for Cx57 were evident in retinas of WT compared with those of Cx36 KO mice. Fluorescent staining of cellular nuclei in the ONL of sections from both WT and Cx36 KO mice (Fig. 2D,F) was present after primary antibody omission, and was due to variable binding of some of the secondary antibodies under the weak tissue fixation conditions used.

Immunofluorescence of Cx57 and calbindin

Expression of Cx57 mRNA has been reported in retinal horizontal cells, and these cells contain an abundance of the calcium-binding protein D28K calbindin (Röhrenbeck et al., 1989; Haverkamp and Wässle, 2000). Thus, double labelling was conducted to determine cellular localization of Cx57 in relation to calbindin. As shown at low magnification, Cx57 lebelling (Fig. 3A) was closely associated with calbindin labelling of horizontal cell bodies lying at the outer margin of the INL, and with faint labelling of the processes of these cells distributed in the OPL (Fig. 2B). By confocal microscopy with antibody 40-4800, Cx57-positive puncta in the OPL (Fig. 3C) were co-distributed with calbindin-positive puncta (Fig. 3D) representing clusters of horizontal cell dendrites and axons, and some Cx57-positive puncta were co-localized with calbindin-immunoreactive processes in the OPL (Fig. 3C,D). Lack of a more substantial co-localization expected, based on the presence of Cx57 and calbindin in horizontal cells, may be due to our findings of stronger fixation conditions (>2% paraformadehyde) required to fully reveal calbindin-positive processes, and suppression of Cx57 immunoreactivity with use of 2% paraformadehyde for Cx57/calbindin double labelling.

Spatial organization of Cx57and Cx36 in OPL

Laser scanning confocal double immunofluorescence was used to examine the spatial distribution of Cx57 in relation to that of Cx36 in the OPL. In vertical sections taken perpendicular to the retinal layers (Fig. 4A), Cx57 and Cx36 appear as a thin band of sparse, dispersed puncta throughout the OPL, as well as short bars of intense labelling for Cx57, and similar bars of moderate labelling for Cx36 in the vitreal or inner part of the OPL (Fig. 4A1,A2). Image overlays indicated that Cx36-positive bars were often situated

adjacent to, and beneath, the Cx57-positive bars, which together were encompassed within a vertical distance of 1.8 ± 0.1 μm (n = 8) (Fig. 4A3). In sections slightly off the vertical plane (Fig. 4B), dispersed punctate labelling of Cx57 and Cx36 was more widely distributed (Fig. 4B), consistent with visualization of a greater expanse of the OPL. In addition, it became clear that the bars of Cx57 and Cx36 labelling shown in Figure 4A represented edge on views of round aggregates clusters of immunoreactivity in the inner part of OPL, which were more evident in the case of Cx57. On average, these aggregates had diameters of about 3.5 ± 0.2 μm. Analysis at higher confocal magnification of horizontal retinal sections through the OPL showed that round aggregates of labelling consisted of individual Cx57- and Cx36-positive puncta, containing a greater abundance of Cx57 compared with Cx36 (Fig. 4C1,C2). Image overlay (Fig. 4C3) indicated minor co-localization between Cx57 and Cx36 within in these clusters. Higher confocal magnification of dispersed punctate labelling in the OPL revealed that Cx57 and Cx36 were often in close proximity (Fig. 4D3). In particular, despite the clear separation of individual puncta labelled for either Cx57 (Fig. 4D1) or Cx36 (Fig. 4D2), Cx57-positive puncta were frequently found immediately adjacent to one or two Cx36-positive puncta (Fig. 4D3), with occasionally partial but rarely total overlap of labelling.

Immunofluorescence of ZO-1 with Cx57 and Cx36 in retina

We have reported the association of Cx36 with ZO-1 in various regions of mouse brain, including the IPL of retina (Li et al., 2004a; Rash et al., 2004). Confocal double immunofluorescence was used here to examine ZO-1 association with Cx36 and Cx57 in OPL. In vertical sections through the retina, immunolabelling of Cx36 with antibody 36-

4600 (Fig. 5A1) was similar to that described above using antibody 37-4600. The pattern of labelling of ZO-1 with antibody 33-9100 resembled the distribution of dispersed Cx36-positive puncta throughout the OPL (Fig. 5A1). In addition, distinct bar-like clusters of ZO-1-positive puncta were seen in the inner part of OPL (Fig. 5A2), which displayed little overlap with Cx36 (Fig. 5A3). In horizontal sections, Cx36 and ZO-1 associated with dispersed puncta were nearly totally co-localized throughout the OPL (Fig. 5B,E). ZO-1-positive bar seen on face in vertical sections consisted of round aggregates of large puncta (Fig. 5E2), showing only minor co-localization with Cx36 (Fig. 5E3). Similar results were obtained using a different combination of antibodies for detection of Cx36 (monoclonal 37-4600) and ZO-1 (polyclonal 61-7300) (not shown).

Vertical sections double-labelled for Cx57 and ZO-1 showed a uniform co-distribution of dispersed punctate labelling of both proteins throughout the OPL (Fig. 5C), and horizontal sections clearly revealed close spatial association of dispersed Cx57-positive puncta and ZO-1-positive puncta, as well as intermingling of immunopositive puncta concentrated in round aggregates (Fig. 5D), which in vertical sections are seen to be in close proximity that spanned a distance of 1.8 ± 0.1 μm ($n = 9$) (Fig. 5C3, inset). Higher magnifications indicated close proximity but lack of total overlap of punctate labelling for Cx57 and ZO-1 (Fig. 5F).

Spatial association of bassoon with Cx57 and Cx36

Localization of Cx57 and Cx36 was examined in relation to that of the cytomatrix protein bassoon (tom Dieck et al., 1998), which is a well established marker of presynaptic structures (Brandstätter et al., 1999). It is also a component of ribbon synapses formed by

rod photoreceptor spherules in the OPL, as well as those formed by cone photoreceptor pedicles in the inner part of OPL (Dowling and Boycott, 1966; Kolb, 1970, 1074, 1977; Raviola and Gilula, 1975; Mariani, 1984). At low magnification of vertical retinal sections, labelling of bassoon was co-distributed with Cx57 in the OPL (Fig. 6A,B), and with Cx36 in the IPL (Fig. 6C,D). Bassoon immunoreactivity consisted of densely distributed puncta in the IPL, and a more sparsely distributed continuous band of puncta in the OPL.

By confocal double immunofluorescence in vertical (Fig. 7A) and horizontal (Fig. 7B) sections, labelling of bassoon (Fig. 7A1,B1) and Cx57 (Fig. 7A2,B2) consisted of dispersed small puncta throughout the OPL (Fig. 7A1,B1), and intermittent bars of puncta in the vitreal part of the OPL (Fig. 7A1). These bars were closely apposed within a vertical distance spanning 1.4 ± 0.06 μm (n = 7), and appeared as round or rosette-like accumulations in horizontal sections (Fig. 7B2). The bar-like arrays represent bassoon localized to, on average, ten synaptic ribbons at cone pedicles (Tsukamoto et al., 2001), and the dispersed punctate labelling, appearing as semi-circular structures, represents bassoon localized to arciform active zones of individual ribbon synapses in rod spherules. Image overlays indicated close spatial association of bassoon and Cx57, with Cx57-positive linear clusters located adjacent to, and beneath, the base of bassoon-positive cone pedicles (Fig. 7A3), and dispersed Cx57-positive puncta often lying adjacent to bassoon-positive rod spherules (Fig. 7B3). Higher magnifications of bassoon-positive cone pedicles in horizontal sections labelled for Cx57 or Cx36 indicated only minor co-association of bassoon with aggregates of Cx57-positive puncta (Fig. 7C) and little

association with aggregates of Cx36-positive puncta (Fig. 7D) distributed within the area of these pedicles.

Higher magnifications of bassoon-positive spherules in horizontal sections double-labelled for either Cx57 or Cx36 are shown by overlays in Figures 7E-G. Labelling of bassoon often appeared as crescent-shaped structures having a relatively uniform distribution. Image overlays revealed that nearly all bassoon-positive crescent-shaped spherules were closely associated, but lacking total overlap, with Cx57-positive puncta, as revealed with anti-Cx57 antibody 40-4800 (Fig. 7E) and 40-5000 (Fig. 7F). Each spherule contained a single Cx57-positive puncta cradled within the crescent (Fig. 7E,F), resembling slices of a pimento-stuffed olive dissected in half along its central axis. Bassoon showed a similar close spatial association with Cx36 (Fig. 7G), except that Cx36-positive puncta were not directly apposed, but rather slightly removed from bassoon-positive spherules, and the concave side of each crescent shaped spherule encompassed one or two Cx36-positive puncta.

Additional information regarding the measurement of the distances between Cx57-, Cx36- and bassoon- positive structures are present in Table 2.

DISCUSSION

We demonstrate the expression of Cx57 protein in mouse retina, and provide evidence for its localization within horizontal cell processes distributed in the OPL. Our results are consistent those of Hombach et al. (2004), who replaced the Cx57 gene coding region with the LacZ reporter in mice and observed β-galactosidase activity in cell bodies of

retinal horizontal cells. However, as with many other connexins that fail to be detected in the somata of neural cells in which they are expressed (Nagy and Rash, 2000; Nagy et al., 2004), we found negligible immunolabelling of Cx57 in horizontal cell somata. Such lack of detection may be due to rapid transport of Cx57 from cell bodies to dendrites and axons, leaving little accumulation of the protein at sites of synthesis, or alternatively, to blockade of antibody epitopes in the course of connexin trafficking to cellular processes. Our observations of identical immunolabelling patterns in OPL with two antibodies generated against different, non-overlapping sequences in Cx57 would ordinarily support specific detection of Cx57 by these antibodies, but only one of the antibodies (40-4800) showed an absence of labelling for Cx57 in the OPL of Cx57 KO mice. It is difficult to imagine a random cross reaction of the other antibody (40-5000) with a protein coincidently having exactly the same tissue expression pattern, cellular localization within this tissue and presence in gap junction plaques as Cx57 (unpublished observations). Thus, we cannot currently explain these results, which suggest opposite conclusions concerning specificity of anti-Cx57 antibody 40-5000, but suspect that the Cx57 KO mice may have a c-terminus portion of the Cx57 gene remaining, which is translated into protein.

Expression of Cx57 appears to be highly restricted, with detection of low Cx57 mRNA levels in only a few peripheral tissues and only in retinal horizontal cells in neural tissues (Manthey et al., 1999; Homback et al., 2004). Similarly, we have found no evidence of Cx57 protein expression in mouse CNS other than in retinal horizontal cells. In other species, evidence has been obtained that type A horizontal cells in rabbit retina express Cx50 and Cx57 (Massey et al., 2003; Huang et al., 2005), and these cells in zebra fish

were reported to express Cx52.6 (Zoidl et al., 2004). In carp and turtle retina, horizontal cells express Cx26 (Janssen-Bienhold et al., 2001; Kamermans et al., 2001; Pottek et al., 2003), suggesting alternate connexin usage in these species, since Cx26 has not been detected in mouse retina (Güldenagel et al., 2000; Deans & Paul, 2001; Filippov et al., 2003).

Molecular associations of ZO-1, Cx36 and Cx57 in OPL

We previously reported direct interaction of Cx36 with ZO-1, and Cx36/ZO-1 co-localization in gap junctions formed by neurons in the IPL (Li et al., 2004a). The present results demonstrate ZO-1 expression in cells having processes distributed in the OPL, and suggest similar ZO-1/Cx36 interaction in many, if not all, gap junctions lying near bassoon-positive rod spherules. In contrast, Cx36 showed little co-localization with densely distributed ZO-1 at the base of cone pedicles, indicating the presence of ZO-1 in cellular processes or subcellular structures other than gap junctions containing Cx36 at this location. Association of ZO-1 with Cx36 at spherules was seen as complete overlap of immunofluorescence labelling for these proteins at individual puncta. Similarly, in previous studies, the presence of two different connexins mediating heterotypic coupling at gap junctions was observed as total overlap of immunofluorescence labelling for these connexins at individual gap junctions (Rash et al., 2001; Nagy et al., 2001, 2003; Li et al., 2004b). Thus, the absence of such total overlap between ZO-1 and Cx57 at rod spherules and cone pedicles indicates lack of association of these proteins. Further, absence of total immunofluorescence overlap of Cx57 with Cx36 at individual puncta, together with Cx57 expression restricted to horizontal cells and reports showing absence of Cx36 in these

cells (Deans and Paul, 2001; Feingespan et al., 2004), indicate that these two connexins do not form heterologous, heterotypic gap junctions with each other. This is consistent with findings that horizontal cells are coupled via gap junctions only to each other (McMahon et al., 1989; Vaney, 1993; Weiler et al., 1999, 2000; He et al., 2000).

Cx57 localization at rod spherules

In rodent retina, a single class of dendrite- and axon-bearing horizontal cells lie postsynaptic to photoreceptors (Suzuki and Pinto, 1986; He et al., 2000). The axons make synaptic contacts exclusively with rod spherules distributed throughout the OPL, and dendrites make synaptic contact exclusively with cone pedicles occupying the inner most portion of the OPL (Dowling and Boycott, 1966; Kolb, 1974; Raviola and Gilula, 1975). Rod spherules contain a particular geometrical arrangement of postsynaptic elements that invaginate into the spherule. In contrast to long held views (Missotten, 1965), recently 3-dimensional serial reconstruction analysis has revealed that spherules in human, monkey and cat retina contain what was defined as two "ribbon synaptic units", with each unit consisting of a rod photoreceptor presynaptic ribbon associated with a trough-shaped arciform density, two laterally apposed elements formed by horizontal cell axons and one or more central elements of bipolar cell dendrites (Migdale et al., 2003). Immunolabelling of bassoon associated with the arciform density at the base of spherule synaptic ribbons often appears as a single crescent-shaped structure (Brandstätter et al., 1999; Haverkamp et al., 2001). This is consistent with observations that the two ribbons associated with each of the "ribbon synaptic units" lie roughly in the same plane, and that two

arciform densities partly circumventing the more centrally located elements were sometimes separated by only small gaps (Migdale et al., 2003), that may be unresolved here by LM immunofluorescence.

Our results revealed a remarkable association of Cx57 with spherules, specifically showing a single Cx57-positive puncta very often immediately adjacent to a bassoon-labelled ribbon synapse. This arrangement suggests the presence of Cx57 within gap junctions at the tips of horizontal cell axons invaginating the spherules. If mouse spherules, like other species, also contain two ribbon synaptic units, each with a pair of laterally apposed horizontal cell axons, then our observation of a single Cx57-puncta within spherules suggests that gap junctions linking these axons, in some as yet unknown combinations, occur within very close proximity to each other, below the resolution (200 nm) of LM immunofluorescence. A possible site for these junctions is where the ends of the two lateral axons of one "ribbon synaptic units" abut those of the other unit, where the abutment corresponds to a gap in the arciform density evident in retinal spherules of cat and monkey (Migdale et al., 2003). Previous studies demonstrating tracer-transfer between axon terminals of horizontal cells in mammalian retina support the occurrence of gap junctions between these axons (Vaney, 1993; He et al., 2000). Moreover, small gap junctions (0.1 μm) have been observed between unidentified processes *within* spherules of monkey retina (Raviola and Gilula, 1975), and these processes were likely horizontal cell axons, since none of the other elements in spherules express either Cx57 or Cx36 that could potentially form these intra-spherule junctions.

Cx36 and ZO-1 at rod spherules

In the OPL, electrical coupling via gap junctions occurs between rod-rod, cone-cone and rod-cone photoreceptor cells (Raviola and Gilula, 1973, 1975; Nelson, 1977; Hornstein et al., 2004; Tuskamoto et al., 2001; Li and DeVries, 2004). In particular, it has been reported that gap junctions are formed between rod spherules, between rod soma and spherule, and between rod spherule and rod axons (Tuskamoto et al., 2001). In addition, the base of each rod spherule forms two gap junctions with terminal cone processes that contact opposite sides of the spherule invagination (Tuskamoto et al., 2001). Although still controversial, there is evidence for the expression of Cx36 in rods, cones or in both of these cell types (Deans et al., 2002; Lee et al., 2003; Feigenspan et al., 2004; Dang et al., 2004). Our results showing a high degree of Cx36/ZO-1 co-localization at what were inferred to be rod spherules, based on the similar close proximity of two Cx36-puncta and two ZO-1-puncta to bassoon, was consistent with the near identical close spatial association of Cx57 with both Cx36 and ZO-1 at spherules. The set of two Cx36-puncta we observed in close proximity to each bassoon-positive spherule conforms to descriptions of two gap junctions at the base of spherules (Tuskamoto et al., 2001), with Cx36 present in either or both spherules and cone processes, as previously discussed (Deans et al. 2002; Lee et al., 2003; Feigenspan et al., 2004). In addition, the innermost rod spherules in OPL (5-20% of all rods) form flat contacts with dendrites of OFF-cone bipolar cells (Hack et al., 1999; Tuskamoto et al., 2001; Li et al., 2004c), which express Cx36 (Feigenspan et al., 2004), and may also contribute a small fraction of the observed Cx36 association with spherules.

Cx57 and Cx36 at cone pedicles

The synaptic endings of cone pedicles in mouse retina contain on average ten ribbon synapses (Tsukamoto et al., 2001), with invaginating dendrites of horizontal cells forming the lateral elements and bipolar dendrites forming the central elements of each ribbon synaptic complex. Neighbouring horizontal cells are known to be coupled by gap junctions, which were sometimes located between their dendrites at the base of cone pedicles (Raviola and Gilula, 1975; Kolb, 1977; Weiler et al., 1999; He et al., 2000). Our results showing that multiple Cx57-puncta were nearly always associated with bassoon at the inner margin of OPL suggest that the majority of the gap junctions formed by Cx57 between horizontal cell dendrites are located at sites of cone pedicles. Further, the presence of Cx57 immediately adjacent to and beneath bassoon, and the presence of albeit more sparsely distributed Cx36 immediately adjacent to and beneath Cx57, suggests a laminar arrangement of elements containing these proteins at the base of cone pedicles. It is possible that Cx57 is contained in an abundance of gap junctions between horizontal dendrites that invaginate cone pedicles, and Cx36 in homologous gap junctions between dendrites of OFF-cone bipolar cells as previously shown (Feigenspan et al., 2004).

ACKNOWLEDGMENTS

This work was supported by grants from the Canadian Institutes of Health Research to J.I.N. We thank B. McLean and N. Nolette for excellent technical assistance. We thank Dr. D. Paul (Harvard University) for provision of Cx36 knockout mice, and C. Olson for help in maintaining and genotyping these mice. We also thank Dr. S. Schein (University

of California, Los Angles) for invaluable discussions on the 3-D organization of ribbon synaptic units.

Table 1. Antibodies used for immunohistochemistry

Antibody	Type	Species	Epitope*; Designation	Dilution	Source
Cx36	polyclonal	rabbit	c-terminus; 36-4600	1 μg/ml	Zymed
Cx36	monoclonal	mouse	mid-region; 37-4600	3 μg/ml	Zymed
Cx57	polyclonal	rabbit	mid-region; 40-5000	2 μg/ml	Zymed
Cx57	polyclonal	rabbit	c-terminus; 40-4800	2 μg/ml	Zymed
ZO-1	polyclonal	rabbit	aa 463-1109; 61-7300	1.25 μg/ml	Zymed
ZO-1	monoclonal	mouse	aa 334-634; 33-9100	4 μg/ml	Zymed
bassoon	monoclonal	mouse	aa 738-1035; VAM-PS00	1:1000	Stressgen
calbindin	monoclonal	mouse	whole protein; C-9848	1:500	Sigma

*aa, amino acids

Table 2. Measurements of immunolabelled elements associated with spherules

structures	measurement (μm)
bassoon arciform length	1.55 ± 0.06 (15)
Cx57 puncta diameter	0.78 ± 0.02 (15)
Cx36 puncta diameter	0.32 ± 0.01 (15)
bassoon to Cx57 distance	0.37 ± 0.02 (22)
bassoon to Cx36 distance	0.62 ± 0.02 (42)
Cx57 to Cx36 distance	0.48 ± 0.02 (38)

Values represent means ± S.E.M of the number of measurements indicated in parentheses. Distances were measured from the center-to-center of individual immunolabelled puncta, and from the apex of bassoon-positive arciform structures to the centers of puncta

Fig. 1. Low magnification immunofluorescence micrographs of labelling patterns with two different polyclonal anti-Cx57 antibodies and with anti-Cx36 antibody in fluorescent NeuroTrace Nissl counterstained vertical sections of mouse retina. (A,B) Section showing labelling of Cx57 with antibody 40-5000 (A), and the same Nissl stained section (B) showing retinal cell layers. Ganglion cell layer, GCL; inner nuclear layer, INL; outer nuclear layer, ONL; outer plexiform layer, OPL. Labelling of Cx57 is seen as continuous linear strand of puncta restricted to the OPL (arrows). (C,D) Immunolabelling of Cx57 with antibody 40-4800 (C) in a Nissl counterstained section (D), showing similar distribution of Cx57 in the OPL (arrows) as obtained in A. (E,F) Higher magnification showing labelling of Cx57 with antibody 40-4800 in OPL of retina from a WT mouse (E), and absence of labelling with this antibody in OPL of retina from a Cx57 KO mouse. Scale bars: A-D, 100 μm; E,F, 20 μm .

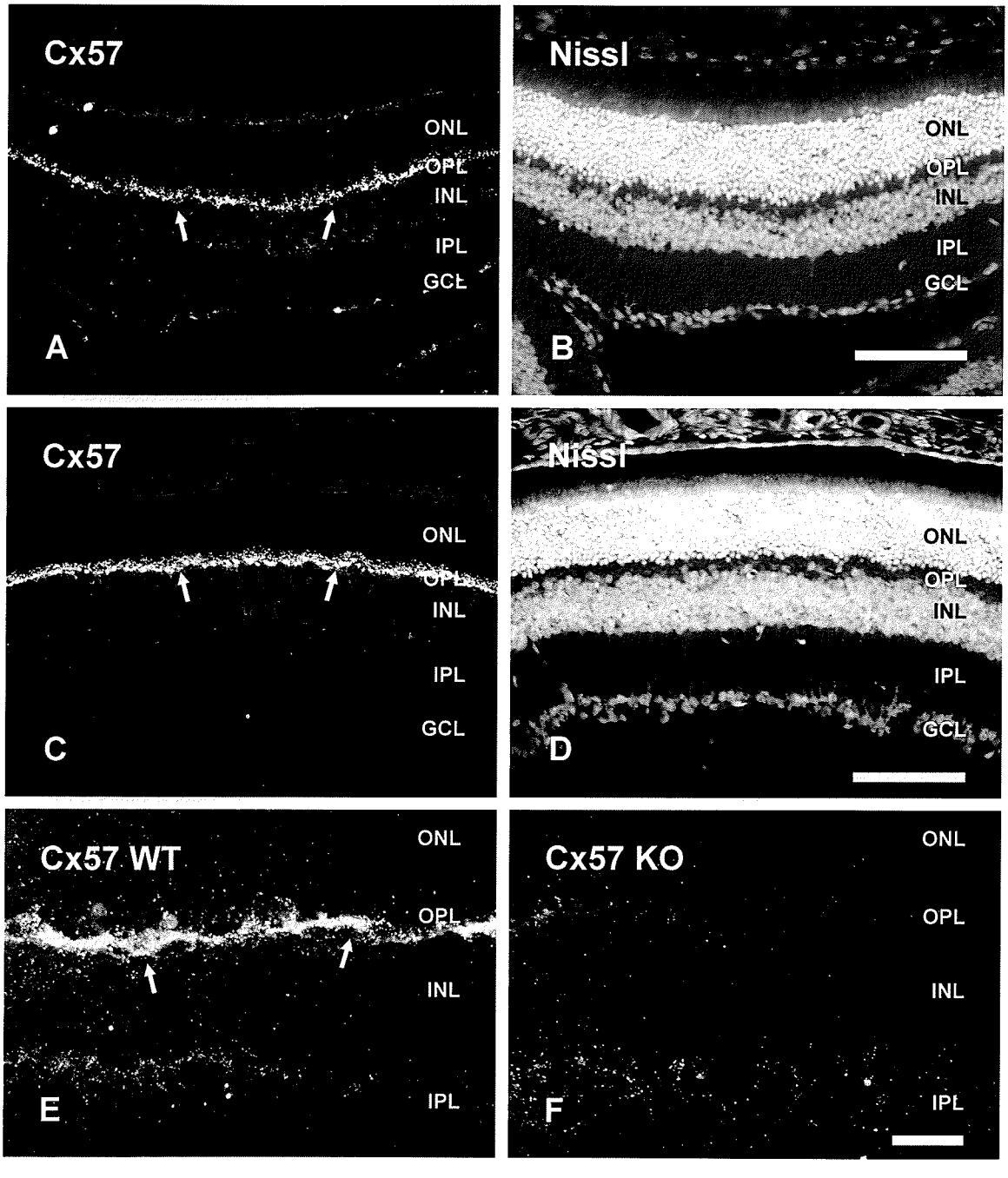
Cx57
ONL
OPL
INL
IPL
GCL
A
Nissl
ONL
OPL
INL
IPL
GCL
B
Cx57
ONL
OPL
INL
IPL
GCL
C
Nissl
ONL
OPL
INL
IPL
GCL
D
Cx57 WT
ONL
OPL
INL
IPL
E
Cx57 KO
ONL
OPL
INL
IPL
F

Fig. 1

Fig. 2. Comparison of labelling for Cx57 in retina of WT and Cx36 KO mice. (A,B) Immunolabelling of Cx36 with antibody 37-4600 (A) in a Nissl counterstained section (B). Punctate labelling is densely distributed in the inner part of IPL (large arrowhead), moderately in the outer part of IPL (small arrowhead), and sparsely in the OPL (arrows). (C,D) Laser scanning double immunofluorescence of the same field showing the distribution of punctate labelling for Cx57 (C) and Cx36 (D) in a near vertical section through the OPL of retina from a WT mouse. (E,F) Confocal double immunofluorescence of the same field showing punctate labelling for Cx57 (E) and an absence of labelling for Cx36 (F) in a vertical section through the OPL of retina from a Cx36 KO mouse. Although shown at slightly different plane of section through retina, no discernable difference in patterns or density of labelling for Cx57 was observed in retina from WT and Cx36 KO mice. Scale bars: A,B, 100 μm; C-F, 10 μm.

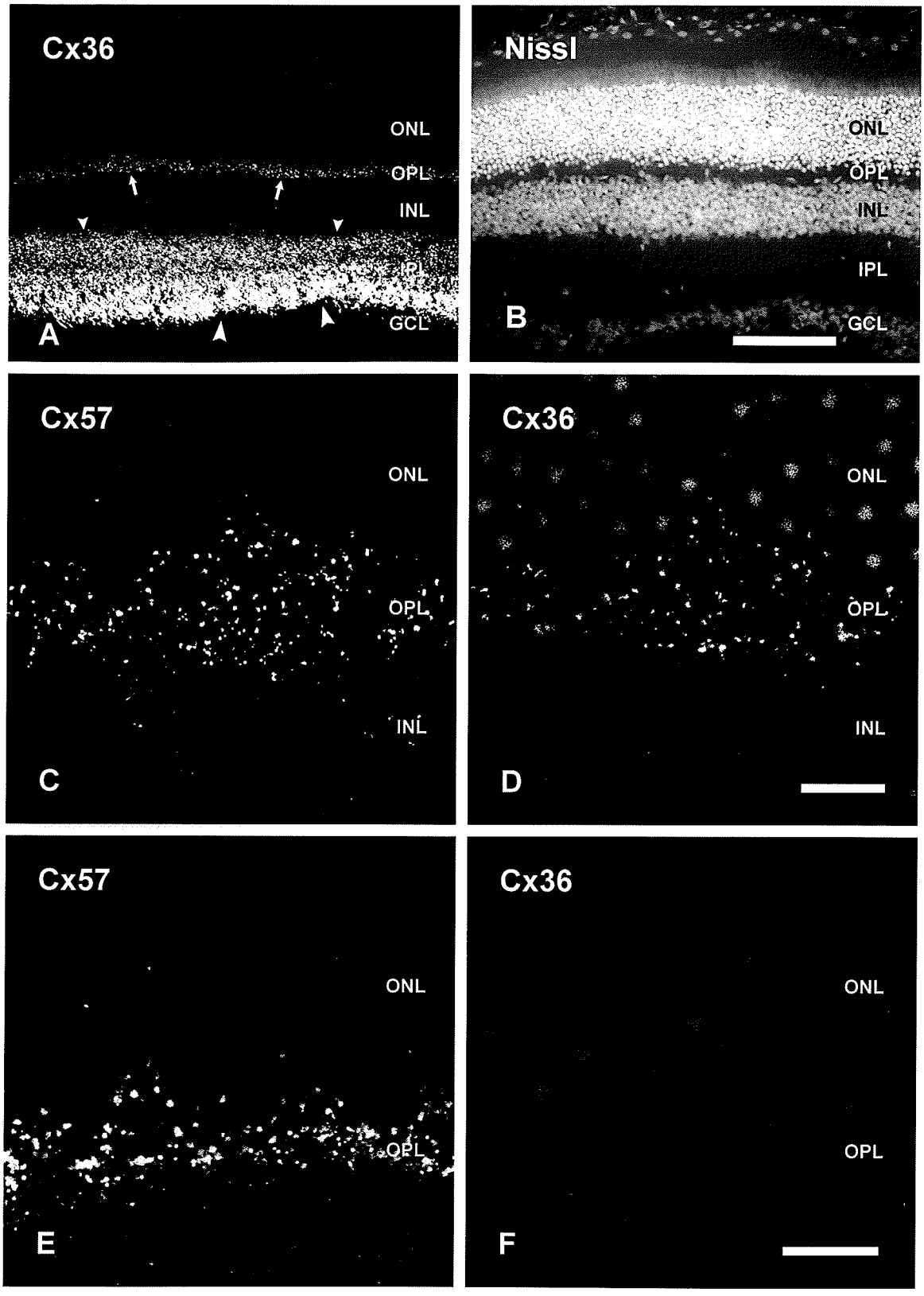
Cx36
ONL
OPL
INL
IPL
GCL
A
Nissl
ONL
OPL
INL
IPL
B
GCL
Cx57
ONL
OPL
INL
C
Cx36
ONL
OPL
INL
D
Cx57
ONL
OPL
E
Cx36
ONL
OPL
F

Fig. 2

Fig. 3. Localization of Cx57 in relation to calbindin-positive neurons in mouse retina. (A,B) Low magnification double immunofluorescence in the same field of a vertical section showing a continuous band of labelling for Cx57 restricted to the OPL (A, arrows), and calbindin-positive cell bodies just beneath this band at the outer edge of the INL (B, arrows). (C,D) Double immunofluorescence confocal micrograph of the same field showing dispersed punctate labelling of Cx57 in the OPL (C), and calbindin-positive horizontal cell bodies (D, arrows) in the INL, with their processes and punctate appendages distributed in the OPL. Some Cx57-immunopositive puncta overlap with calbindin-positive puncta in the OPL (corresponding arrowheads). Scale bars: A,B, 100 μm; C,D, 10 μm.

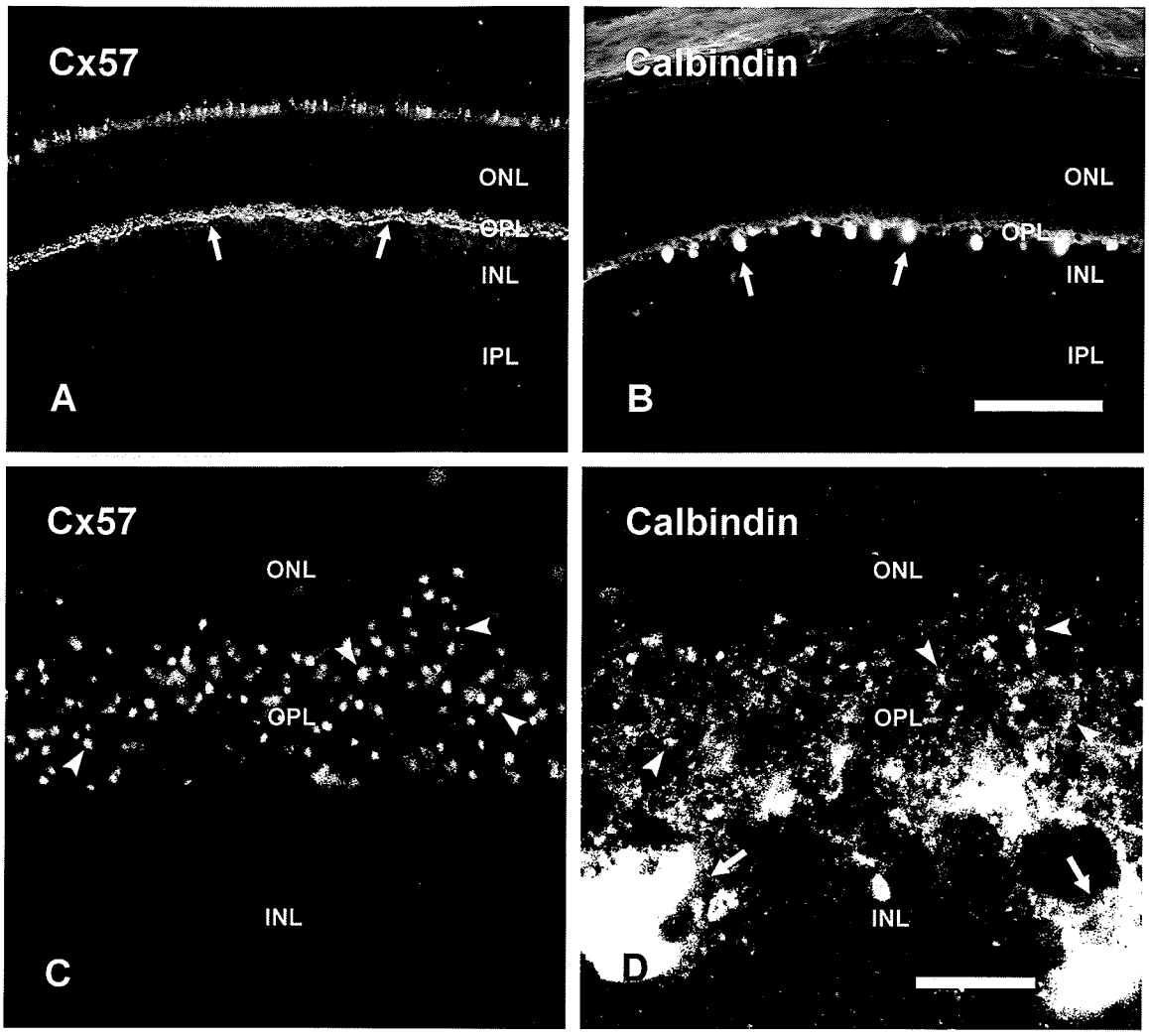
Cx57
ONL
OPL
INL
IPL
A
Calbindin
ONL
OPL
INL
IPL
B
Cx57
ONL
OPL
INL
C
Calbindin
ONL
OPL
INL
D

Fig. 3

Fig. 4. Confocal double immunofluorescence comparing the distribution of Cx57 and Cx36 in the OPL of mouse retina. Sections were labelled with polyclonal anti-Cx57 40-4800 and monoclonal anti-Cx36 37-4600. (A,B) Double immunolabelling in vertical (A) and near vertical (B) sections. Labelling of Cx57 appears as dispersed puncta throughout OPL (A1, arrows), and as intermittent bars in the inner OPL (A1, arrowheads). In the same field, labelling of Cx36 is similarly distributed, and is often seen adjacent to the Cx57-positive bars (A2, arrowheads), as seen in overlay (A3, arrowheads) and at higher magnification in inset (A3). In double-labelled sections tilted slightly off the vertical plane, Cx57-positive bars appear as round aggregates of puncta (B1, arrowheads), intermingled with fewer Cx36-positive puncta (B2, arrowheads), as seen in overlay (B3, arrowheads). (C,D) Higher magnifications showing Cx57 in relation to Cx36 in horizontal sections through OPL. Round aggregates of Cx57-positive puncta (C1, arrowheads) display largely a lack of overlap with Cx36-positive puncta associated with these aggregates (C2, arrowheads), as seen in overlay (C3, arrowheads). Dispersed Cx57-positive puncta located outside of the round aggregates (D1, arrows) rarely show co-localization with Cx36, but are often seen closely adjacent to Cx36-positive puncta (D2, arrows), as seen in overlay (D3, arrows) and at higher magnification in inset (D3). Scale bars: A-C, 10 μm; D, 20 μm.

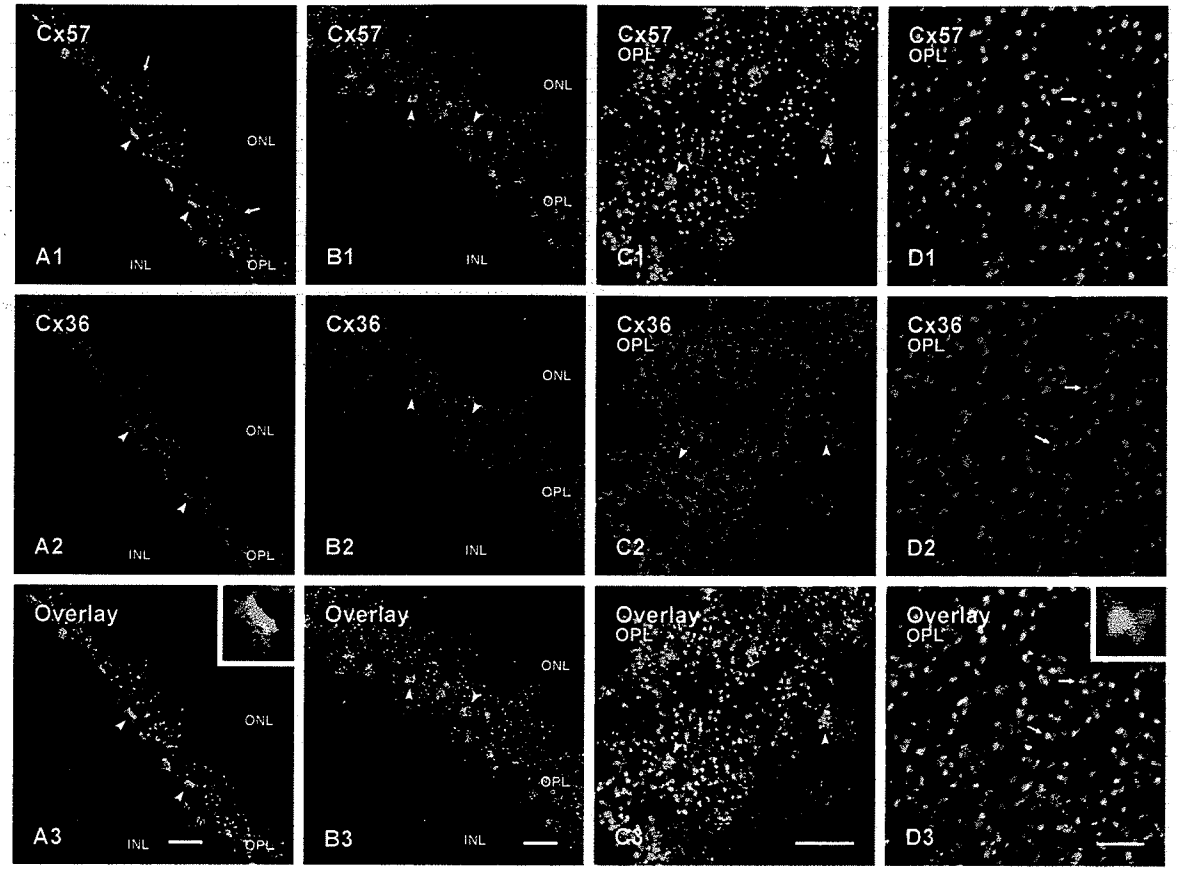
Cx57
ONL
A1
INL
OPL
Cx57
ONL
OPL
B1
INL
Cx57
OPL
C1
Cx57
OPL
D1
Cx36
ONL
A2
INL
OPL
Cx36
ONL
OPL
B2
INL
Cx36
OPL
C2
Cx36
OPL
D2
Overlay
ONL
A3
INL
OPL
Overlay
ONL
OPL
B3
INL
Overlay
OPL
C3
Overlay
OPL
D3

Fig. 4

Fig. 5. Laser scanning confocal double immunofluorescence comparing the localization of Cx36 and Cx57 to that of ZO-1 in OPL of mouse retina. (A,B) Double labelling with polyclonal anti-Cx36 (A1,B1) and monoclonal anti-ZO-1 (A2,B2) in vertical (A) and horizontal (B) sections through the OPL. Labelling of Cx36 (A1) and ZO-1 (A2) display similar distributions in the OPL, but with ZO-1 more intensely localized to short bars of puncta (A2, arrowheads). Dispersed puncta show a high degree of Cx36/ZO-1 co-localization, as seen by yellow in overlay (B3). (C,D) Double labelling in vertical (C) and horizontal (D) sections showing Cx57 and ZO-1 in the OPL (C), their presence in round aggregates of puncta (D, arrowheads), and their close proximity along immuno-positive bars in the inner OPL (C3, insert) and among dispersed puncta (D, arrows). (E,F) Higher magnification of double-labelled horizontal sections through the OPL showing Cx36/ZO-1 co-localization of dispersed puncta (E, arrows), sparse association of Cx36 with round aggregates of ZO-1-positive puncta (E, arrowheads), and close proximity of punctate labelling for Cx57 (F1) and ZO-1 (F2), shown in overlay (F3, arrows) and at higher magnification (F3, inset). Scale bars: A,C,D, 10 μm; B,E,F, 20 μm.

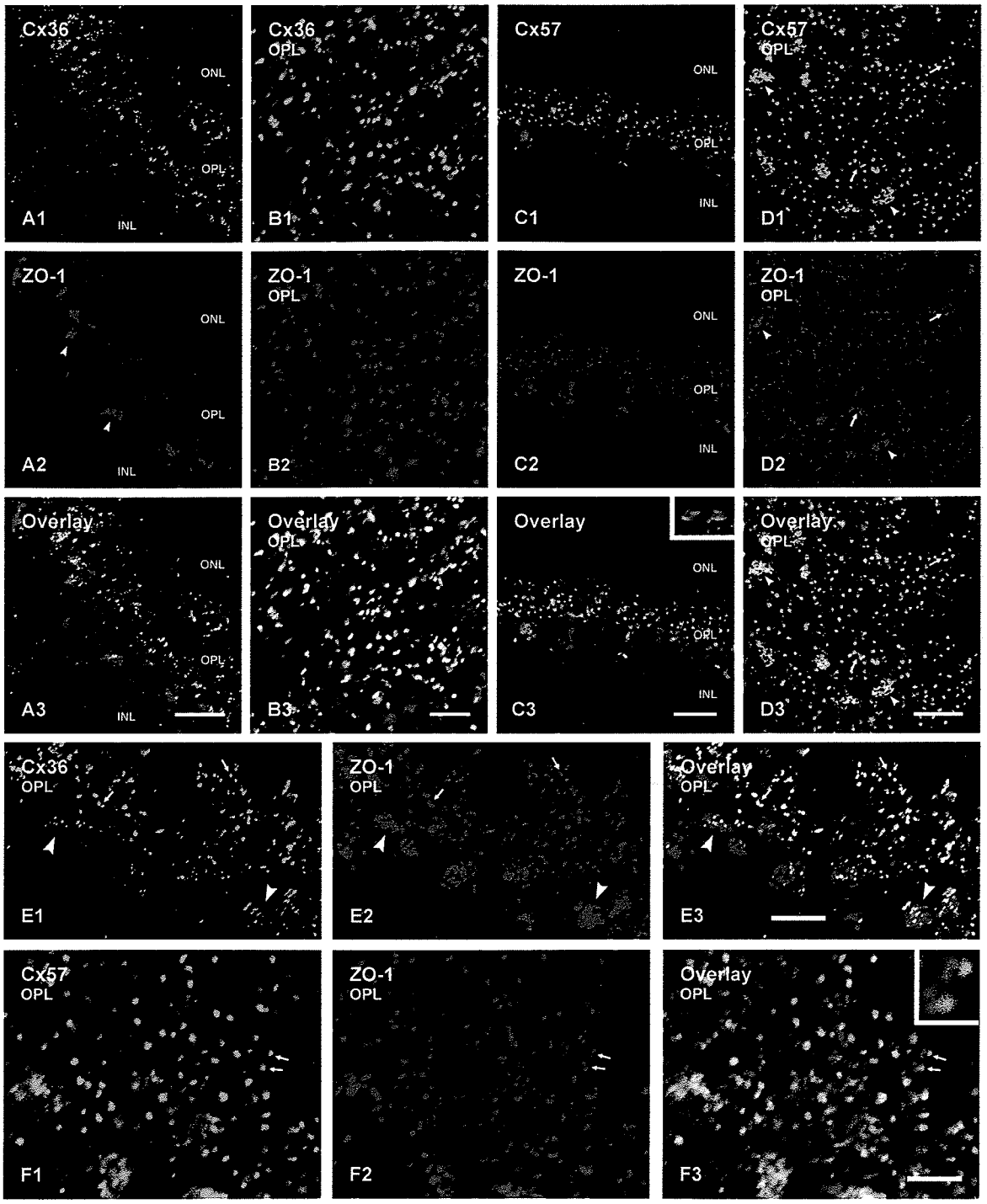
Cx36
ONL
OPL
A1
INL
Cx36
OPL
B1
Cx57
ONL
OPL
INL
C1
Cx57
OPL
D1
ZO-1
ONL
OPL
A2
INL
ZO-1
OPL
B2
ZO-1
ONL
OPL
INL
C2
ZO-1
OPL
D2
Overlay
ONL
OPL
A3
INL
Overlay
OPL
B3
Overlay
ONL
OPL
INL
C3
Overlay
OPL
D3
Cx36
OPL
E1
ZO-1
OPL
E2
Overlay
OPL
E3
Cx57
OPL
F1
ZO-1
OPL
F2
Overlay
OPL
F3

Fig. 5

Fig. 6. Low magnification immunofluorescence labelling of Cx57 and Cx36 in relation to the nerve terminal marker bassoon in vertical sections of mouse retina. (A,B) Double immunofluorescence showing a correspondence of labelling for Cx57 (A, arrows) and bassoon (B, arrows) in the OPL, and dense labelling of bassoon in IPL (double arrows), which is devoid of Cx57. (C,D) Double immunofluorescence showing a correspondence of labelling for Cx36 (C, small arrows) and bassoon (D, small arrows) in the OPL. Dense punctate labelling of Cx36 is seen in the inner IPL (C, large arrows), and sparse Cx36 labelling is seen in the outer part of the IPL (C, double arrows). Areas devoid of labelling for bassoon (D) represent tears in the section. Scale bars: 10 μm.

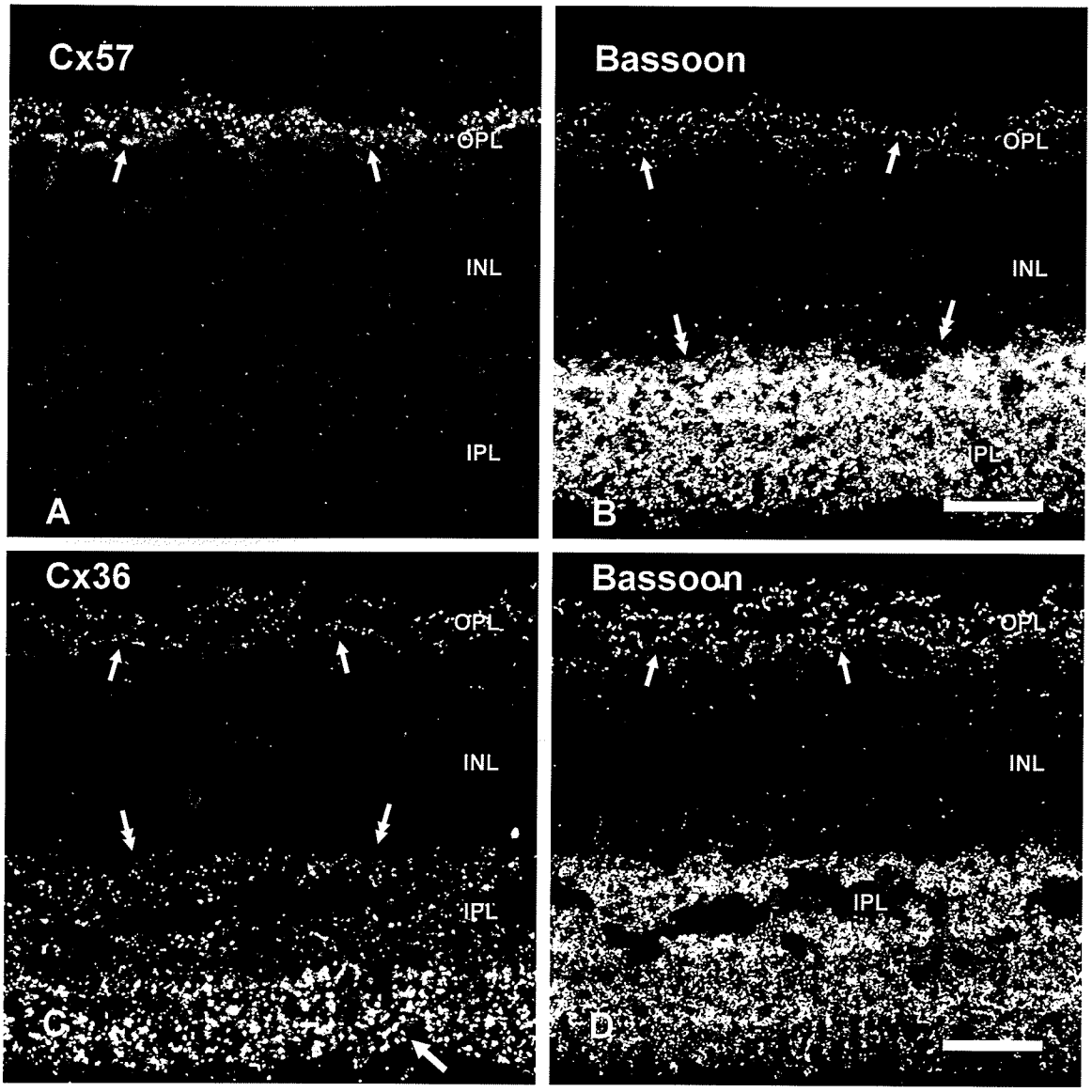
Cx57
OPL
INL
IPL
A
Bassoon
OPL
INL
IPL
B
Cx36
OPL
INL
IPL
C
Bassoon
OPL
INL
IPL
D

Fig. 6

Fig. 7. Laser scanning confocal double immunofluorescence of Cx57 and Cx36 in relation to bassoon in the OPL of mouse retina. (A) Vertical section showing close spatial relationship between bassoon-positive synaptic ribbons and labelling of Cx57 at rod spherules (dispersed puncta, arrows), and at cone pedicles (bars of aggregated puncta, arrowheads) shown at higher magnification in inset (A3). (B,C) Medium (B) and high (C) magnifications of horizontal sections through the OPL double labelled for Cx57 and bassoon. Rosette arrangements of bassoon-positive puncta representing cone synaptic ribbons (B1, arrowheads, and B3, overlay) as seen associated with dense aggregates of Cx57-positive puncta (B2, arrowheads), with minimal Cx57/bassoon co-localization in these rosettes (C, arrowheads). (D) Double labelling in a horizontal section through OPL showing lack of co-localization between bassoon-labelled cone pedicles (D1, arrowheads) and Cx36-positive puncta (D2, overlay D3, arrowheads). (E) Higher magnification of double-labelling for Cx57 (with antibody 40-4800) and bassoon in overlay showing bassoon-positive ribbon synapses in rod spherules appearing as punctate half circles (arrows), and labelling of Cx57 often appearing as round puncta (arrows) partly encompassed by, but lacking total overlap with, labelling of bassoon (arrows, shown magnified in inset). (F) Higher magnification of double-labelling for Cx57 (with antibody 40-5000) and bassoon in overlay showing similar results as that in F, with bassoon-positive ribbon synapses partly encompassing labelling for Cx57 (arrows, shown magnified in inset). (G) Higher magnification of bassoon-positive rod spherules and Cx36 showing close spatial association of often two Cx36-positive puncta with each bassoon-positive spherule (arrows, shown magnified in inset). Scale bars: A,B,E-G, 10 μm; C,D, 20 μm.

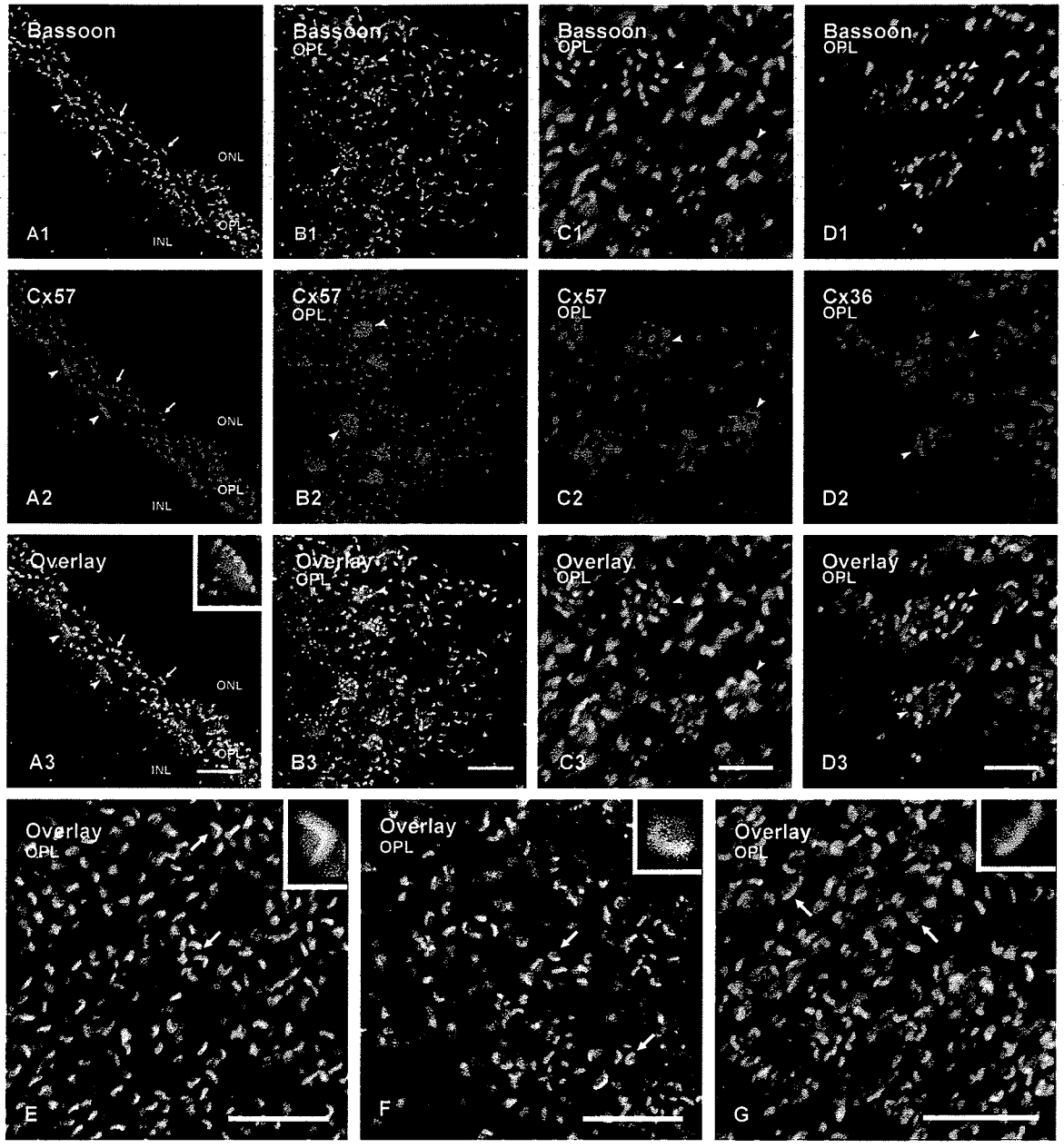
Bassoon
ONL
OPL
INL
A1
Bassoon
OPL
B1
Bassoon
OPL
C1
Bassoon
OPL
D1
Cx57
ONL
OPL
INL
A2
Cx57
OPL
B2
Cx57
OPL
C2
Cx36
OPL
D2
Overlay
ONL
OPL
INL
A3
Overlay
OPL
B3
Overlay
OPL
C3
Overlay
OPL
D3
Overlay
OPL
E
Overlay
OPL
F
Overlay
OPL
G

Fig. 7

Fig. 8. Diagrammatic representation of a rod terminal spherule. A, Spherule. B, Spherule invagination containing central and lateral elements, shown enlarged relative to the volume actually occupied by the invagination (Migdale et al., 2003). C, Central dendritic elements. D Two pairs of horizontal cell axon lateral elements (pair 1,2, and pair 3,4), with apposition of each adjacent pair (front to back) forming a ribbon synaptic unit, and some degree of presumptive apposition of elements in one unit with elemements in the other units (left to right). E,F, Synaptic ribbons (E) and arciform active zone (F), shown with a break (not evident in images) to indicate these structures as separate constituents of the left and right ribbon synaptic units. G, Processes from cone pedicles forming gap junctions (arrows) containing Cx36 at the base of spherule. H,I, Presumptive locations of Cx57-containing gap junctions at appositions between lateral axons either within a ribbon synaptic unit (H, asterisks), or between lateral axons of one unit and those of the other (I, asterisk). In this 2D-diagram, the synaptic ribbon is shown en face and was therefore placed above the spherule invagination, but would typically be located within a furrow running between the pairs (1,2 and 3,4) of lateral elements within each ribbon synaptic unit.

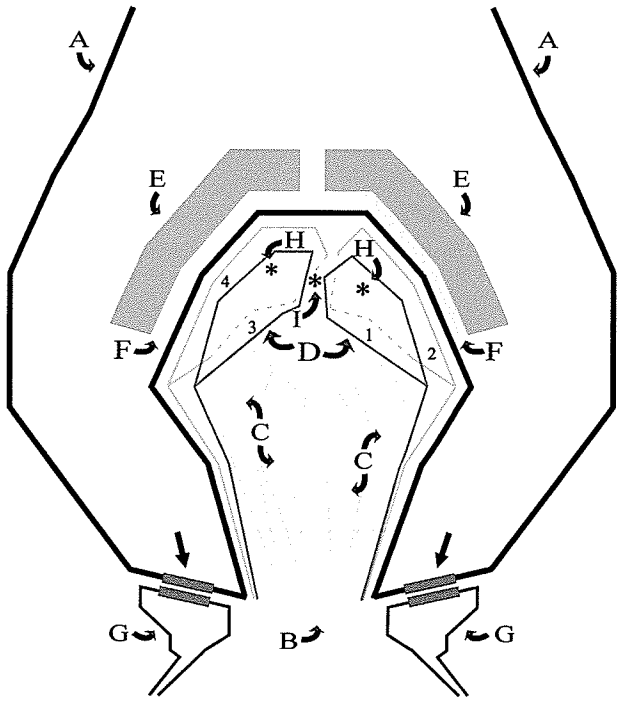

Fig. 8

VII. GENERAL DISCUSSION

Electrical coupling through gap junctions is widespread in retina, and it has been shown that the intercellular communication is the key element in retinal information processing (Vaney, 1994, 1996; Cook and Becker, 1995; Baldridge et al., 1998; Vaney et al., 1999; Weiler et al., 1996). The earliest evidence came from ultrastructural observations and showed gap junctions between photoreceptors (Raviola and Gilula, 1973); between horizontal cells (Raviola and Gilula, 1975; Kolb, 1977), between bipolar cells (Kolb, 1979; Marc et al., 1988; Cohen and Sterling, 1990), between AII amacrine cells and some types of ON-cone bipolar cells (Famiglietti and Kolb, 1975; Cohen and Sterling, 1990; Strettoi et al., 1992) and between ganglion cells and wide-field amacrine cells (Penn et al.,1994; Jacoby et al., 1996). Electrophysiological recordings as well as dye and tracer coupling experiments provided support for many of the previous findings, and in addition, suggested evidence of gap junctions between ganglion cells (Mastronarde, 1983). With the discovery and characterisation of electrical coupling in most neuronal structures of the retina, questions were raised as to the exact nature of the mechanisms responsible for such a coordinated neuronal activity. Retina is a good example in illustrating the importance of interneuronal communication in the overall process of vision regulation.

In order to be able to understand retinal functions, a detailed analysis of the proteins expressed here, their cellular and subcellular localization as well as their interaction capabilities is required. In the search for the anatomical substrate and molecular interaction of such proteins, the purpose of the current studies was to further investigate

major neuronal connexins (Cx36, Cx45 and Cx57) expressed in mouse retina, and the connexin-associated proteins believed to modulate the regulation of gap junctional communication.

Cx57, Cx45 and Cx36 expression in retina

Following identification and characterization of Cx57 in mouse retina (Manthey et al., 1999), lacZ reporter gene analyses indicated that horizontal cells express the gap junction forming protein Cx57 (Hombach *et al.*, 2004). Furthermore, it has been reported that in Cx57-defective mice, 99% of tracer coupling between horizontal cells was abolished, indicating that Cx57 is probably the major connexin expressed in this cell type. Previous studies done in mammals showed presence of gap junctions between axons and between dendrites of horizontal cells but failed to provide additional information as to their exact subcellular distribution (Raviola and Gilula, 1975; Kolb, 1977; Vaney, 1993; He et al., 2000). Here, by employing newly developed anti-Cx57 antibodies, we were able to show for the first time using immunoflourescence approaches, the presence of Cx57 protein in mouse horizontal cells. Our results showed a remarkable association of a single, large Cx57-positive puncta with rod spherules and cone pedicles, indicating its presence within gap junctions probably at the tips of horizontal cells axons and dendrites (invaginating the spherules and the pedicles, respectively). These results indicate the appositions between lateral elements either within a ribbon synaptic unit or between lateral elements of one unit and those of the second unit as possible locations of Cx57-containing gap junctions. Extensive EM analyses are further required to investigate

these presumptive locations, as well as to quantify the number of Cx57-containing gap junctions present at this location.

Besides its role in forming GJIC between HC terminal processes, the functional/physiological contribution of Cx57 in retina is not completely understood. It has been shown that the development and the morphology of horizontal cells are not affected in Cx57-deficient mice, but lack of Cx57 expression leads to a premature onset of horizontal cells migration, therefore indicating that Cx57 is involved in the regulation of horizontal cell patterning.(Hombach *et al.*, 2004).

A fundamental characteristic of the first synapse in the retina is a negative feedback pathway from the second order neurons to the cones (O'Bryan, 1973; Dowling, 1987; Wu, 1991), having as an effect the adjustment of light stimuli properties. Feedback to the cones is now proposed to occur by means of electrical synapses consisting of gap junctions thought to be formed between horizontal cell lateral elements invaginating photoreceptor terminals at triad ribbon synapses. Feedback signals from the IPL are transmitted via substances like dopamine, which activates D1 and D2 dopamine receptors distributed throughout retina. Dopamine causes the gap junctions among horizontal cells to become uncoupled, therefore reducing the size of their receptive fields. The presence of gap junctions at pedicle- as well as spherule-invaginating lateral elements further suggests the involvement of horizontal cells in retinal adaptation to stimuli under bright light and/or dim light conditions through, processing of visual information coming from both rods and cones.

The identification and characterisation of the remaining connexin genes expressed in mouse horizontal cells is key for a complete understanding of the properties of gap junctions present at this level, and it would provide further information for understanding the characteristics and functions of horizontal cells.

In the mouse retina, we found Cx36 in both synaptic layers, which is consistent with previous studies (Feigenspan, 2001, 2004; Lee et al., 2003; Li et al., 2004a). Presence of Cx36 in IPL was initially attributed to AII amacrine cells (Mills et al., 2001; Feigenspan et al., 2001). Comparing the pattern of labelled AII amacrine cell dendrites with that of Cx36, it was suggested that Cx36 staining originates from at least one additional cell population. A recent report (Schubert et al., 2005) showed that alpha-ganglion cells also express Cx36, which explains the presence of Cx36-positive puncta in the OFF-sublamina of IPL, which do not associate with the lobular appendages of AII amacrine cells present at that level (Feigenspan et al., 2001).

In OPL, the identity of all connexin proteins present at gap junctions between photoreceptor cells of the mammalian retina is largely unknown. So far, Cx36 was identified at cone pedicles (Lee et al., 2003; Feigenspan et al., 2004) while Deans (2002) showed that Cx36 was abundantly expressed in rods. Also, it has been shown that dendrites of OFF-cone bipolar cells express Cx36 (Feigenspan et al., 2004).

The physiological function of Cx36 has so far been only studied in AII amacrine cells. Here, Cx36-containing gap junctions mediate visual processing in its very early stage, being directly involved in the interaction between rod and cone systems. The role of Cx36 in visual transmission was examined by using Cx36-deficient mice (Güldenagel et al., 2001) and electroretinogram (ERG) recordings, which indicated a decrease in the b-

wave amplitude, leading to impairment of visual signal transmission under scotopic conditions.

By its presence in different types of neurons, Cx36 is an essential element of all three rod pathways known so far. In the primary pathway, rod bipolar cells receive input from rods and transmit the signals to AII amacrine cells, which are responsible for transmitting rod signals to the cone pathway by electrical synapses involving Cx36. The second rod pathway uses the Cx36-positive gap junctions between rods and cones (Raviola and Gilula, 1973) for the rod signal to enter the ON- and OFF-cone bipolar cells. For the third rod pathway, (Hack et al., 1999, 2001, Tsukamoto et al., 2001), it was proposed that Cx36-positive OFF-cone bipolar cells directly contact 5-20% of the rod terminals and are responsible for transmitting rod signals to ganglion cells.

Another important result of our studies was to employ newly developed Cx45 antibodies to confirm Cx45 protein expression in IPL of retina. Furthermore, we show Cx36/Cx45 co-localization, confirming the results obtained by Maxeiner et al (2005). Using two lines of Cx45-deficient mice, they showed that Cx45 is a neuronal connexin expressed by ON- and OFF-cone bipolar cells and amacrine cells, the latter of which are different from AII type that do not express Cx45 (Maxeiner et al., 2005).

By its presence at Cx36/Cx45 heterotypic gap junctions formed between AII amacrine cells and ON-cone bipolar cells, Cx45 is an essential element of the first rod pathway, and it has been shown that deletion of Cx45 in mouse retinal neurons disrupts this pathway, leading to impaired visual transmission (Maxeiner et al., 2005). Because the subcellular localization of Cx45 is not known, a functional role for Cx45 in OFF-bipolar cells and amacrine cells is difficult to assign.

Also, it has been shown that gap junctional coupling between these two cell types forms the basis of neurotransmitter coupling (Vaney et al., 1998), with glycine being transported from the glycinergic AII cells to ON-cone bipolar cell by means of gap junctions established between these cells. In Cx36- and Cx45-deficient mice (Güldenagel et al., 2001; Maxeiner et al., 2005), it was demonstrated that the level of glycine in ON cone bipolar cell is highly reduced, clearly indicating that both Cx36 and Cx45 participate in the formation of functional heterotypic gap junctions between these two types of neurons.

The study of retinal connexins is currently in progress, with the identity of all the connexin proteins expressed as well as the exact cellular types expressing them still needing further clarification.

The rigorous characterization of connexin-deficient mice can help us understand and learn a lot about the function of these intercellular channels in mammals and in retina in particular. Furthermore, these mouse models could be used for studying the physiological consequences of inherited connexin-defects in patients.

ZO-1 and ZONAB at retinal gap junctions

Initially, ZO-1 has been described in a wide variety of tissues at tight junctions (Stevenson et al., 1986; Gonzales-Mariscal et al., 2003). Also, its presence has been identified at adherens junctions (Itoh et al., 1991, 1993; Howarth et al., 1992) as well as at gap junctions between cells *in vivo* and *in vitro*, where ZO-1 has been shown to interact with various connexins (Giepmans et al., 1998; Toyofuku et al., 1998; Kausalaya et al., 2001; Laing et al., 2001; Kojima et al., 2001; Giepmans et al., 2001; Nielsen et al., 2001, 2002, 2003; Li et al., 2004a,b,c; Penes et al., 2005). Among all the connexins

known to interact with ZO-1, only Cx36 binds to the first PDZ domain (Li et al., 2004a,b), whereas the others (Cx30, Cx31.9, Cx43, Cx46, Cx47, Cx50) bind exclusively to the second PDZ domain of ZO-1. The significance of connexin/ZO-1 interaction as well as the exact implications of connexins binding to first or second PDZ domain have not been elucidated yet. A better assessment of ZO-1 functions in retina could be achieved by modifications of the PDZ binding motifs of connexins shown to associate with ZO-1 at this level or by blocking the corresponding PDZ domain at the ZO-1 molecule. This could show whether binding to ZO-1 is important in the early stages of connexin trafficking or assembly and whether the cells expressing these connexins can still form functional channels with their neighbors.

In our studies we showed that in retina ZO-1 is widely expressed in IPL and OPL. In IPL, consistent with our previous study (Li et al., 2004a), ZO-1 was found to co-localize with Cx36. Moreover, by immunofluorescence and co-IP, we demonstrated that Cx45 associates with ZO-1 and interacts with its second PDZ domain. Our demonstration that only a small proportion of Cx36- and of Cx45-positive puncta participate in forming heterotypic gap junctions and that Cx36 and Cx45 are not expressed by the same cell type, co-association of ZO-1 with each of these proteins indicates its expression in alpha-ganglion cells, AII amacrine cells, ON- and OFF-cone bipolar cells, as well as in other Cx36- or Cx45- positive cell types which have not yet been identified. Furthermore, we observed that the numerous ZO-1-positive puncta in IPL outnumbered the Cx36- and Cx45-positive puncta, suggesting that besides its association with these two proteins, ZO-1 is present at other structures as well as gap junctions composed of different, yet

unknown connexins in retina, which could be either expressed in different neuronal types or in glia.

In OPL, co-localisation of ZO-1 and Cx36 was present as expected (Li et al., 2004), but it was restricted to Cx36-positive puncta associated with the rod spherules. At cone pedicles, co-association between ZO-1 and Cx36 was very rare, suggesting a possible association of ZO-1 with different cell types and subcellular structures present in the OPL, besides the Cx36-expressing cells.

In our attempt to determine whether Cx57 is another ZO-1-interacting connexin, we demonstrated that only minor co-localization can be established between the two.

Furthermore, knowing that at tight junctions ZO-1 is associated with numerous proteins (Gonzales-Mariscal et al., 2003) and that ZO-1 is present at gap junctions, we investigated the possibility that some of these proteins are also expressed at gap junctions. One of these proteins is ZONAB, a Y-box transcription factor that has previously been reported to interact with the SH3 domain of ZO-1 at tight junctions in canine MDCK cells (Balda and Matter, 2000; Balda et al., 2003). Our results clearly indicate presence of ZONAB in IPL and OPL of retina, and we show a high degree of co-localization between Cx36 and ZONAB in both plexiform layers, whereas Cx45 showed minimal and Cx57 no co-localization with ZONAB.

In Cx36 KO mice, ZO-1/ZONAB co-localized puncta persisted in IPL, especially in the outer part of the layer, in a pattern matching that in wild type mice, suggesting the possible association of these proteins with gap junctions composed of an as yet unidentified connexin. Further ultrastructural analyses in retina of Cx36 KO mice as well

as detailed molecular studies are required to establish the presence and association of ZO-1/ZONAB with these junctions.

Also, future characterization of functional proteins interacting with connexins and/or ZO-1 in retina could provide additional information as to possible regulatory mechanisms of retinal gap junctions that would have implications regardind the regulation of retinal development and function. Developmental studies could be used to examine changes in ZO-1/ZONAB/Cx expression during embryogenesis and after birth, and their possible involvement in key regulatory events.

VII. REFERENCES

Balda MS, Matter K (2000) The tight junction protein ZO-1 and an interacting transcription factor regulate ErbB-2 expression. EMBO J 19:2024-2033.

Balda MS, Matter K (2003) Epithelial cell adhesion and the regulation of gene expression. Trends Cell Biol 13:310-318.

Balda MS, Garrett MD, Matter K (2003) The ZO-1-associated Y-box factor ZONAB regulates epithelial cell proliferation and cell density. J Cell Biol 160:423-432.

Baldridge WH, Vaney DI, Weiler R (1998) The modulation of intercellular coupling in the retina. Semin Cell Dev Biol 9:311-318.

Becker D, Bonness V, Mobbs P (1998) Cell coupling in the retina: patterns and purpose. Cell Biol Internal 22:781-792.

Bennett MVL (1997) Gap junctions as electrical synapses. J Neurocytol 26:349-366.

Bennett MV, Contreras JE, Bukauskas FF, Saez JC (2003) New roles for astrocytes: gap junction hemichannels have something to communicate. Trends Neurosci 26:610-617.

Bennett MVL (2004) Electrical coupling and neuronal synchronization in the mammalian brain. Neuron 41:495-511.

Bermingham-McDonogh O, McCabe KL, Reh TA (1996) Effects of GGF/neuregulins on neuronal survival and neurite outgrowth correlate with erbB2/neu expression in developing rat retina. Development 122:1427-1438.

Bloomfield SA, Xin D, Osborne T (1997) Light-induced modulation of coupling between AII amacrine cells in the rabbit retina. Vis Neurosci 14:565-576.

Brandstätter JH, Fletcher EL, Garner CC, Gundelfinger ED, Wässle H (1999) Differential expression of the presynaptic cytomatrix protein bassoon among ribbon synapses in the mammalian retina. Eur J Neurosci 11:3683-1393.

Bruzzone R, White TW, Goodenough DA (1996) The cellular Internet: on-line with connexins. Bioessays 9:709-718.

Butterweck A, Elfgang C, Willecke K, Traub O (1994) Differential expression of the gap junction proteins connexin45, -43, -40, -31, and -26 in mouse skin. Eur J Cell Biol 65:152-163.

Casalini P, Iorio MV, Galmozzi E, Menard S (2004) Role of HER receptors family in development and differentiation. J Cell Physiol 200:343-350.

Casini G, Rickman DW, Brecha NC (1995) AII amacrine cell population in the rabbit retina: identification by parvalbumin immunoreactivity. J Comp Neurol 35:132-142.

Ciolofan C, Wellershaus K, Willecke K, Nagy JI (2005) Spatial relationships of connexin57, connexin36 and zonula occludens-1 (ZO-1) in the outer plexiform layer of mouse retina. Eur J Neurosci Submitted.

Cohen E, Sterling P (1990) Demonstration of cell types among cone bipolar neurons of cat retina. Philos Trans R Soc Lond B Biol Sci 330:305-321.

Condorelli DF, Parenti R, Spinella F, Trovato Salinaro A, Belluardo N, Cardile V, Cicirata F (1998) Cloning of a new gap junction gene (Cx36) highly expressed in mammalian brain neurons. Eur J Neurosci 10:1202-1208.

Connors BW, Long MA (2004) Electrical synapses in the mammalian brain. Annu Rev Neurosci 27:393-418.

Cook JE, Becker DL (1995) Gap junctions in the vertebrate retina. Microsc Res Tech 31:408-419.

Dang L, Pulukuri S, Mears AJ, Swaroop A, Reese BE, Sitaramayya A (2004) Connexin 36 in photoreceptor cells: studies on transgenic rod-less and cone-less mouse retinas. Mol Vis 11:323-327.

Davies HG, Giorgini F, Fajardo MA, Braun RE (2000) A sequence-specific RNA binding complex expressed in murine germ cells contains MSY2 and MSY4. Dev Biol 221:87-100.

Deans MR, Paul DL (2001) Mouse horizontal cells do not express connexin26 or connexin36. Cell Commun Adhes 8:361-366.

Deans MR, Volgyi B, Goodenough DA, Bloomfield SA, Paul DL (2002) Connexin36 is essential for transmission of rod-mediated visual signals in the mammalian retina. Neuron 36:703-712.

Dermietzel R, Spray DC (1998) From neuro-glue ('Nervenkitt') to glia: a prologue. Glia 24:1-7.

DeVries SH, Baylor DA (1995) An alternative pathway for signal flow from rod photoreceptors to ganglion cells in mammalian retina. Proc Natl Acad Sci U S A 92:10658-10662.

tom Dieck S, Sanmarti-Vila L, Langnaese K, Richter K, Kindler S, Soyke A, Wex H, Smalla KH, Kampf U, Franzer JT, Stumm M., Garner CC, Gundelfinger ED (1998) Bassoon, a novel zinc-finger CAG/glutamine-repeat protein selectively localized at the active zone of presynaptic nerve terminals. J Cell Biol 142:499-509.

Dowling JE, Boycott BB (1966) Organization of the primate retina: electron microscopy. Proc R Soc Lond B Biol Sci 166:80-111.

Duffy HS, Delmar M, Spray DC (2002) Formation of the gap junction nexus: binding partners for connexins. J Physiol Paris 96:243-249.

Eiberger J, Degen J, Romualdi A, Deutsch U, Willecke K, Sohl G (2001) Connexin genes in the mouse and human genome. Cell Commun Adhes 8:163-165.

Evans WH, Martin PE (2002) Gap junctions: structure and function. Mol Membr Biol 19:121-136.

Famiglietti EV Jr, Kolb H (1975) A bistratified amacrine cell and synaptic cirucitry in the inner plexiform layer of the retina. Brain Res 84:293-300.

Famiglietti EV Jr, Kolb H (1976) Structural basis for ON-and OFF-center responses in retinal ganglion cells. Science 194:193-195.

Feigenspan A, Teubne B, Willecke K, Weiler R (2001) Expression of neuronal connexin36 in AII amacrine cells of the mammalian retina. J Neurosci 21:230-239.

Feigenspan A, Janssen-Bienhold U, Hormuzdi S, Monyer H, Degen J, Sohl G, Willecke K, Ammermuller J, Weiler R (2004) Expression of connexin36 in cone pedicles and OFF-cone bipolar cells of the mouse retina. J Neurosci 24:3325-3334.

Filippov MA, Hormuzdi SG, Fuchs EC, Monyer H (2003) A reporter allele for investigating connexin 26 gene expression in the mouse brain. Eur J Neurosci 18:3183-3192.

Frankel P, Aronheim A, Kavanagh E, Balda MS, Matter K, Bunney TD, Marshall CJ (2005) RalA interacts with ZONAB in a cell density-dependent manner and regulates its transcriptional activity. EMBO J 24:54-62.

Gabriel R, Straznicky C (1992) Immunocytochemical localization of parvalbumin- and neurofilament triplet protein immunoreactivity in the cat retina: colocalization in a subpopulation of AII amacrine cells. Brain Res 595:133-136.

Gao Y, Spray DC. 1998. Structural changes in lenses of mice lacking the gap junction protein connexin43. Invest Ophthalmol Vis Sci 39:1198–1209.

Giepmans BN, Moolenaar WH (1998) The gap junction protein connexin43 interacts with the second PDZ domain of the zonula occludens-1 protein. Curr Biol 8:931-934.

Giepmans BN, Verlaan I, Moolenaar WH (2001) Connexin-43 interactions with ZO-1 and alpha- and beta-tubulin. Cell Commun Adhes 8:219-223.

Giepmans BN (2004) Gap junctions and connexin-interacting proteins. Cardiovasc Res 62:233-245.

Giorgini F, Davies HG, Braun RE (2002) Translational repression by MSY4 inhibits spermatid differentiation in mice. Development 129:3669-3679.

Giorgini F, Davies HG, Braun RE (2001) MSY2 and MSY4 bind a conserved sequence in the 3' untranslated region of protamine 1 mRNA in vitro and in vivo. Mol Cell Biol 21:7010-7019.

Gong XQ, Nicholson BJ (2001) Size selectivity between gap junction channels composed of different connexins. Cell Commun Adhes 8:187-192.

Gonzalez-Mariscal L, Betanzos A, Nava P, Jaramillo BE (2003) Tight junction proteins. Prog Biophys Mol Biol 81:1-44.

Goodenough DA, Goliger JA, Paul DL (1996) Connexins, connexons, and intercellular communication. Annu Rev Biochem 65:475-502.

Gonzalez-Mariscal L, Namorado MC, Martin D, Luna J, Alarcon L, Islas S, Valencia L, Muriel P, Ponce L, Reyes JL (2000) Tight junction proteins ZO-1, ZO-2, and occludin along isolated renal tubules. Kidney Int 57:2386-2402.

Güldenagel M, Söhl G, Plum A, Traub O, Teubner B, Weiler R, Willecke K (2000) Expression patterns of connexin genes in mouse retina. J Comp Neurol 425:193-201.

Güldenagel M, Ammermuller J, Feigenspan A, Teubner B, Degen J, Söhl G, Willecke K, Weiler R (2001) Visual transmission deficits in mice with targeted disruption of the gap junction gene connexin36. J Neurosci 21:6036-6044.

Hack I, Peichl L, Brandstätter JH (1999) An alternative pathway for rod signals in the rodent retina: rod photoreceptors, cone bipolar cells, and the localization of glutamate receptors. Proc Natl Acad Sci USA 96:14130-14135.

Haverkamp S, Wässle H (2000) Immunocytochemical analysis of the mouse retina. J Comp Neurol 424:1-23

Haverkamp S, Grunert U, Wässle H (2001) The synaptic architecture of AMPA receptors at the cone pedicle of the primate retina. J Neurosci 21:2488-2500.

He S, Weiler R, Vaney DI (2000) Endogenous dopaminergic regulation of horizontal cell coupling in the mammalian retina. J Comp Neurol 418:33-40.

He S, Dong W, Deng Q, Weng S, Sun W (2003) Seeing more clearly: recent advances in understanding retinal circuitry. Science 302:408-411.

Herve JC, Bourmeyster N, Sarrouilhe D (2004) Diversity in protein-protein interactions of connexins: emerging roles. Biochim Biophys Acta 1662:22-41.

Hidaka S, Kato T, Miyachi E (2004) Expression of gap junction connexin36 in adult rat retinal ganglion cells. J Integr Neurosci 1:3-22.

Holbro T, Hynes NE (2004) ErbB receptors: directing key signaling networks throughout life. Annu Rev Pharmacol Toxicol 44:195-217.

Hombach S, Janssen-Bienhold U, Sohl G, Schubert T, Bussow H, Ott T, Weiler R, Willecke K (2004) Functional expression of connexin57 in horizontal cells of the mouse retina. Eur J Neurosci 19:2633-2640.

Hornstein EP, Verweij J, Schnapf JI (2004) Electrical coupling between red and green cones in primate retina. Nat Neurosci 7:745-750.

Howarth AG, Hughes MR, Stevenson BR (1992) Detection of the tight junction-associated protein ZO-1 in astrocytes and other non-epithelial cell types. Am J Physiol 262:C461-C469.

Hu EH, Bloomfield SA (2003) Gap junctional coupling underlies the short-latency spike synchrony of retinal alpha ganglion cells. J Neurosci 23:6768-6777.

Huang H, Li H, He SG (2005) Identification of connexin 50 and 57 mRNA in A-type horizontal cells of the rabbit retina. Cell Res 3:207-211.

Inoko A, Itoh M, Tamura A, Matsuda M, Furuse M, Tsukita S (2003) Expression and distribution of ZO-3, a tight junction MAGUK protein, in mouse tissues. Genes to Cells 8:837-845.

Itoh M, Yonemura S, Nagafuchi A, Tsukita S, Tsukita S (1991) A 220-kD undercoat-constitutive protein: Its specific localization at cadherin-based cell-cell adhesion sites. J Cell Biol 115:1449-1462.

Itoh M, Nagafuchi A, Yonemura S, Kitani-yasuda T, Tsukita S, Tsukita S (1993) The 220-kD protein colocalizing with cadherins in nonepithelial cells is identical to ZO-1, a tight junction-associated protein in epithelial cells: cDNA cloning and immunoelectron microscopy. J Cell Biol 121:491-502.

Jacoby R, Stafford D, Kouyama N, Marshak D (1996) Synaptic inputs to ON parasol ganglion cells in the primate retina. J Neurosci 16:8041-8056.

Janssen-Bienhold U, Dermietzel R, Weiler R (1998) Distribution of connexin43 immunoreactivity in the retinas of different vertebrates. J Comp Neurol 396:310-321.

Janssen-Bienhold U, Schultz K, Hoppenstedt W, Weiler R (2001) Molecular diversity of gap junctions between horizontal cells. Prog Brain Res 131:93-107.

Janssen-Bienhold U, Schultz K, Gellhaus A, Schmidt P, Ammermuller J, Weiler R (2001) Identification and localization of connexin26 within the photoreceptor-horizontal cell synaptic complex. Vis Neurosci 18:169-178.

Johansson K, Bruun A, Ehinger B. 1997. Expression of connexin43 immunoreactivity in the rabbit retina (abstract). Mol Biol Cell 8:552.

Jones CR, Becker DL, Cook JE. 1992. Gap junctions in the rat retina: immunoreactivity with antisera raised to oligopeptides of connexins Cx32 and Cx43. Neurosci Lett 42:S34.

Johnson RG, Meyer RA, Li XR, Preus DM, Tan L, Grunewald H, Paulson AF, Laird DW, Sheridan JD (2002) Gap junctions assemble in the presence of cytoskeletal inhibitors, but enhanced assembly requires microtubules. Exp Cell Res 275:67-80.

Kamermans M, Fahrenfort I, Schultz K, Janssen-Bienhold U, Sjoerdsma T, Weiler R (2001) Hemichannel-mediated inhibition in the outer retina. Science 292:1178-1180.

Kausalya PJ, Reichert M, Hunziker W (2001) Conneixn45 directly binds to ZO-1 and localizes to the tight junction region in epithelial MDCK cells. FEBS lett 505:92-96.

Kolb H (1970) Organization of the outer plexiform layer of the primate retina: electron microscopy of Golgi-impregnated cells. Philos Trans R Soc Lond Ser B Biol Sci 258:261- 283.

Kolb H. (1974) The connections between horizontal cells and photoreceptors in the retina of the cat: electron microscopy of Golgi preparations. J Comp Neurol 155:1-14.

Kolb, H. (1977) The organization of the outer plexiform layer in the retina of the cat: electron microscopic observations. J Neurocytol 6:131–153.

Kolb H (1979) The inner plexiform layer in the retina of the cat: electron microscopic observations. J Neurocytol 8:295-329.

Kolb H, Nelson R (1984) Neural architecture of the cat retina. Prog Ret Res 3:21-60.

Kojima T, Kokai Y, Chiba H, Osanai M, Kuwahara K, Mori M, Mochizuki Y, Sawada N (2001) Occludin and claudin-1 concentrate in the midbody of immortalized mouse hepatocytes during cell division. J Histochem Cytochem 49:333-340.

Kolb H, Nelson R (1985) Functional circuitry of amacrine cells in the cat retina. In: Neurocircuitry of the Retina: a Cajal Memorial (Eds Gallego A, Gouras P) Elsevier Press, New York 215-232.

Kumar NM, Gilula NB (1996) The gap junction communication channel. Cell 84:381-388.

Laing JG, Manley-Markowski RN, Koval M, Civitelli R, Steinberg TH (2001) Connexin45 interacts with zonula occludens-1 and conneixn43 in osteoblastic cells. J Biol Chem 276:23051-23055.

Laing JG, Chou BC, Steinberg TH (2005) ZO-1 alters the plasma membrane localization and function of Cx43 in osteoblastic cells. J Cell Sci Epub Ahead of Print.

Lee EJ, Han JW, Kim HJ, Kim IB, Lee MY, Oh SJ, Chung JW, Chun MH (2003) The immunocytochemical localization of connexin 36 at rod and cone gap junctions in the guinea pig retina. Eur J Neurosci 18:2925-2934.

Li X, Olson C, Lu S, Kamasawa N, Yasumura T, Rash JE, Nagy JI (2004a) Neuronal connexin36 association with zonula occludens-1 protein (ZO-1) in mouse brain and interaction with the first PDZ domain of ZO-1. Eur J Neurosci 19:2132-2146.

Li X, Olson C, Lu S, Nagy JI (2004b) Association of connexin36 with zonula occludens-1 in HeLa cells, βTC-3 cells, pancreas and adrenal gland. Histochem Cell Biol 122:485-498.

Li X, Ionescu AV, Lynn BD, Lu S, Kamasawa N, Morita M, Davidson KG, Yasumura T, Rash JE, Nagy JI. (2004c) Connexin47, connexin29 and connexin32 co-expression in oligodendrocytes and Cx47 association with zonula occludens-1 (ZO-1) in mouse brain. Neuroscience 126:611-630.

Li W, Keung JW, Massey SC (2004c) Direct synaptic connections between rods and OFF cone bipolar cells in the rabbit retina. J Comp Neurol 474:1-12.

Li W, DeVries SH (2004) Separate blue and green cone networks in the mammalian retina. Nat Neurosci 7:751-756.

Lindqvist N, Vidal-Sanz M, Hallbook F (2002) Single cell RT-PCR analysis of tyrosine kinase receptor expression in adult rat retinal ganglion cells isolated by retinal sandwiching. Brain Res Protoc 10:75-83.

Manthey D, Bukauskas F, Lee CG, Kozak CA, Willecke K (1999) Molecular cloning and functional expression of the mouse gap junction gene connexin-57 in human HeLa cells. J Biol Chem 274:14716-14723.

Marc RE, Liu WL, Muller JF (1988) Gap junctions in the inner plexiform layer of the goldfish retina. Vision Res 28:9-24.

Mariani AP (1984) The neuronal organization of the outer plexiform layer of the primate retina. Int Rev Cytol 86:285-320.

Marmor MD, Skaria KB, Yarden Y (2004) Signal transduction and oncogenesis by ErbB/HER receptors. Int J Radiat Oncol Biol Phys 58:903-913.

Massey SC, Mills SL (1999) Antibody to calretinin stains AII amacrine cells in the rabbit retina: double-label and confocal analyses. J Comp Neurol 411:3-18.

Massey SC, O'Brien JJ, Trexler EB, Li W, Keung JW, Mills S, O'Brien J (2003) Multiple neuronal connexins in the mammalian retina. Cell. Commun Adhes 10:425-430.

Mastrangelo MA, Kleene KC (2000) Developmental expression of Y-box protein 1 mRNA and alternatively spliced Y-box protein 3 mRNAs in spermatogenic cells in mice. Mol Hum Reprod 6:779-788.

Mastronarde DN (1983) Interactions between ganglion cells in cat retina. J Neurophysiol 49:350-365.

Matesic D, Tillen T, Sitaramayya A (2003) Connexin 40 expression in bovine and rat retinas. Cell Biol Int 27:89-99.

Maxeiner S, Kruger O, Schilling K, Traub O, Urschel S, Willecke K (2003) Spatiotemporal transcription of connexin45 during brain development results in neuronal expression in adult mice. Neuroscience 119:689-700.

Maxeiner S, Dedek K, Janssen-Bienhold U, Ammermuller J, Brune H, Kirsch T, Pieper M, Degen J, Kruger O, Willecke K, Weiler R (2005) Deletion of connexin45 in mouse retinal neurons disrupts the rod/cone signaling pathway between AII amacrine and ON cone bipolar cells and leads to impaired visual transmission. J Neurosci 25:566-576.

McMahon DG, Knapp AG, Dowling JE (1989) Horizontal cell gap junctions: single-channel conductance and modulation by dopamine. Proc Natl Acad Sci USA 86:7639-7643.

Migdale K, Herr S, Klug K, Ahmad K, Linberg K, Sterling P, Schein S (2003) Two ribbon synaptic units in rod photoreceptors of macaque, human and cat. J Comp Neurol 455:100-112.

Missotten, L. (1965) The Ultrastructure of the Retina. Brussels: Editions Arscia SA.

Mills SL, Massey SC (1995) Differential properties of two gap junctional pathways made by AII amacrine cells. Nature 377:734-737.

Mills SL, O'Brien JJ, Li W, O'Brien J, Massey SC (2001) Rod pathways in the mammalian retina use connexin 36. J Comp Neurol 436:336-350.

Mobbs P, Brew H, Attwell D (1988) A quantitative analysis of glial cell coupling in the retina of the axolotl (Ambystoma mexicanum). Brain Res 460:235-245.

Nagy JI, Li W, Hertzberg EL, Marotta CA (1996) Elevated connexin43 immunoreactivity at sites of amyloid plaques in Alzheimer's disease. Brain Res 717:173-178.

Nagy JI, Rash JE (2000) Connexins and gap junctions of astrocytes and oligodendrocytes in CNS. Brain Res Brain Res Rev 1:29-44.

Nagy JI, Li X, Rempel J, Stelmack G, Patel D, Staines WA, Yasumura T, Rash JE (2001) Connexin26 in adult rodent central nervous system: demonstration at astrocytic gap junctions and colocalization with connexin30 and connexin43. J Comp Neurol 441:302-323.

Nagy JI, Ionescu AV, Lynn BD, Rash JE (2003) Coupling of astrocyte connexins Cx26, Cx30, Cx43 to oligodendrocyte Cx29, Cx32, Cx47: Implications from normal and connexin32 knockout mice. Glia 44:205-218.

Nagy JI, Dudek FE, Rash JE (2004) Update on connexins and gap junctions in neurons and glia in the nervous system. Brain Res Brain Res Rev 47:191-215.

Nelson R (1977) Cat cones have rod imput: a comparison of the response properties of cones and horizontal cell bodies in the retina of the cat. J Comp Neurol 172:109-135.

Nelson R, Famiglietti EV Jr, Kolb H (1978) Intracellular staining reveals different levels of stratification for on- and off-center ganglion cells in cat retina. J Neurophysiol 41:472-483.

Nielsen PA, Baruch A, Giepmans BN, Kumar NM (2001) Characterization of the association of connexins and ZO-1 in the lens. Cell Commun Adhes 28:213-217.

Nielsen PA, Beahm DL, Giepmans BN, Baruch A, Hall JE, Kumar NM (2002) Molecular cloning, functional expression, and tissue distribution of a novel human gap junction-forming protein, connexin31.9. Interaction with zona occludens protein-1. J Biol Chem 277:38272-38283.

Nielsen PA, Baruch A, Shestopalov VI, Giepmans BN, Benedetti EI, Kumar NM (2003) Lens connexins Cx46 and Cx50 interact with Zonula Occludens Protein-1 (ZO-1). Mol Biol Cell 14:2470-2481.

Paffenholz R, Kuhn C, Grund C, Stehr S, Franke WW (1999) The ARM-repeat protein NPRAP (Neurojungin) is a constituent of the plaques of the outer limiting zone in the retina, defining a novel type of adhering junction. Exp Cell Res 250:452-464.

Paul DL (1995) New functions for gap junctions. Curr Opin Cell Biol 7:665-672.

Penes M, Li X, Nagy JI (2005) Expression of zonula occludens-1 (ZO-1) and the transcription factor ZO-1-associated nucleic acid-binding protein (ZONAB/MsY3) in glial cells and co-localization at oligodendrocyte and astrocyte gap junctions in mouse brain. Eur J Neurosci Accepted.

Penn AA, Wong RO, Shatz CJ (1994) Neuronal coupling in the developing mammalian retina. J Neurosci 14:309-324.

Piccolino M, Neyton J, Gerschenfeld HM (1984) Decrease of gap junction permeability induced by dopamine and cyclic adenosine 3':5'-monophosphate in horizontal cells of turtle retina. J Neurosci, 4:2477-2488.

Pottek M, Hoppenstedt W, Janssen-Bienhold U, Schultz K, Perlman I, Weiler R (2003) Contribution of connexin26 to electrical feedback inhibition in the turtle retina. J Comp Neurol 466:468-477.

Rash JE, Staines WA, Yasumura T, Patel D, Furman CS, Stelmack GL, Nagy JI (2000). Immunogold evidence that neuronal gap junctions in adult rat brain and spinal cord contain connexin-36 but not connexin-32 or connexin-43. Proc Natl Acad Sci USA 97:7573-7578.

Rash JE, Yasumura T, Dudek FE, Nagy JI (2001) Cell-specific expression of connexins and evidence of restricted gap junctional coupling between glial cells and between neurons. J Neurosci 15:1983-2000.

Rash JE, Pereda A, Kamasawa N, Furman CS, Yasumura T, Davidson KGV, Dudek FE, Olson C, Li X, Nagy JI (2004) High-resolution proteomic mapping in the vertebrate central nervous system: Close proximity of connexin35 to NMDA glutamate receptor clusters and co-localization of connexin36 with immunoreactivity for zonula occludens protein-1 (ZO-1). J Neurocytol 33:131-151.

Raviola E, Gilula NB (1973) Gap junctions between photoreceptor cells in the vertebrate retina. Proc Natl Acad Sci USA 70:1677-1681.

Raviola E, Gilula NB (1975) Intramembrane organization of specialized contacts in the outer plexiform layer of the retina. A freeze-fracture study in monkeys and rabbits. J Cell Biol 65:192-222.

Reed KE, Westphale EM, Larson DM, Wang HZ, Veenstra RD, Beyer EC (1993) Molecular cloning and functional expression of human connexin37, an endothelial cell gap junction protein. J Clin Invest 91:997-1004.

Robinson SR, Hampson EC, Munro MN, Vaney DI (1993) Unidirectional coupling of gap junctions between neuroglia. Science 262:1072-1074.

Rohr S (2004) Role of gap junctions in the propagation of the cardiac action potential. Cardiovasc Res 162:309-322.

Röhrenbeck J, Wässle H, Boycott BB (1989) Horizontal cells in the monkey retina: immunocytochemical staining with antibodies against calcium binding proteins. Eur J Neurosci 1:407–420.

Rouach N, Avignone E, Meme W, Koulakoff A, Venance L, Blomstrand F, Giaume C (2002) Gap junctions and connexin expression in the normal and pathological central nervous system. Biol Cell 94:457-475.

Rozental R, Carvalho AC, Spray DC (2000) Gap junctions in the cardiovascular and immune systems. Braz J Med Biol Res 33:365-368.

Saez JC, Contreras JE, Bukauskas FF, Retamal MA, Bennett MV (2003) Acta Physiol Scand 179:9-22.

Scadding JW (1981) Development of ongoing activity, mechanosensitivity, and adrenaline sensitivity in severed peripheral nerve axons. Exp Neurol 73:345-364.

Schubert T, Degen J, Willecke K, Hormuzdi SG, Monyer H, Weiler R (2005) Connexin36 mediates gap junctional coupling of alpha-ganglion cells in mouse retina. J Comp Neurol 485:191-201.

Segretain D, Falk MM (2004) Regulation of connexin biosynthesis, assembly, gap junction formation, and removal. Biochim Biophys Acta 1662:3-21.

Simon AM, Goodenough DA (1998) Diverse functions of vertebrate gap junctions. Trends Cell Biol 8:477-483.

Schutte M, Chen S, Buku A, Wolosin JM. 1998. Connexin50, a gap junction protein of macroglia in the mammalian retina and visual pathway. Exp Eye Res 66:605–613.

Sharpe LT, Stockman A (1999) Rod pathways: the importance of seeing nothing. Trends Neurosci 22:497-504.

Smith RG, Freed MA, Sterling P (1986) Microcircuitry of the dark-adapted cat retina: functional architecture of the rod-cone network. J Neurosci 6:3505-3517.

Sohl G, Guldenagel M, Traub O, Willecke K (2000) Connexin expression in the retina. Brain Res Brain Res Rev 32:138-145.

Sohl G, Guldenagel M, Beck H, Teubner B, Traub O, Gutierrez R, Heinemann U, Willecke K (2000) Expression of connexin genes in hippocampus of kainate-treated and kindled rats under conditions of experimental epilepsy. Brain Res Mol Brain Res 83:44-51.

Sohl G, Willecke K (2004) Gap junctions and the connexin protein family. Cardiovasc Res 62:228-232.

Sterling P (1995) Vision. Tuning retinal circuits. Nature 377:676-677.

Stevenson BR, Siliciano JD, Mooseker MS, Goodenough DA (1986) Identification of ZO-1: a high molecular weight polypeptide associated with the tight junction (zonula occludens) in a variety of epithelia. J Cell Biol 103:755-766.

Strettoi E, Raviola E, Dacheux RF (1992) Synaptic connections of the narrow-field, bistratified rod amacrine cell (AII) in the rabbit retina. J Comp Neurol 325:152-168.

Suchyna TM, Nitsche JM, Chilton M, Harris AL, Veenstra RD, Nicholson BJ (1999) Different ionic selectivities for connexins 26 and 32 produce rectifying gap junction channels. Biophys J 77:2968-2987.

Sun W, Li N, He S (2002) Large-scale morphological survey of mouse retinal ganglion cells. J Comp Neurol451:115-126.

Suzuki H, Pinto LH (1986) Response properties of horizontal cells in the isolated retina of wild-type and pearl mutant mice. J Neurosci 6:1122-1128.

Teranishi T, Negishi K, Kato S (1983) Dopamine modulates S-potential amplitude and dye-coupling between external horizontal cells in carp retina. Nature 301:243-246.

Teubner B, Degen J, Sohl G, Guldenagel M, Bukauskas FF, Trexler EB, Verselis VK, De Zeeuw CI, Lee CG, Kozak CA, Petrasch-Parwez E, Dermietzel R, Willecke K (2000) Functional expression of the murine connexin 36 gene coding for a neuron-specific gap junctional protein. J Membr Biol 176:249-262.

Thomas MA, Huang S, Cokoja A, Riccio O, Staub O, Suter S (2002) Chanson M. Interaction of connexins with protein partners in the control of channel turnover and gating. Biol Cell 94:445-56.

Toyofuku T, Yabuki M, Otsu K, Kuzuya T, Hori M, Tada M (1998) Direct association of the gap junction protein connexin-43 with ZO-1 in cardiac myocytes. J Biol Chem 273: 12725-12731.

Tserentsoodol N, Shin B-C, Suzuki T, Takata K (1998) Colocalization of tight junction proteins, occludin and ZO-1, and glucose transporter GLUT1 in cells of the blood-ocular barrier in the mouse eye. Histochem Cell Biol 110:543-551.

Tsukamoto Y, Morigiwa K, Ueda M, Sterling P (2001) Microcircuits for night vision in mouse retina. J Neurosci 21:8616-8623.

Vaney DI (1991) Many diverse types of retinal neurons show tracer coupling when injected with biocytin or Neurobiotin. Neurosci Lett 125:187-190.

Vaney DI (1993) The coupling pattern of axon-bearing horizontal cells in the mammalian retina. Proc Biol Sci 252:93-101

Vaney DI (1994) Patterns of neuronal coupling in the retina. Prog Ret Eye Res 13:301-355.

Vaney DI (1997) Neuronal coupling in rod-signal pathways of the retina. Invest Ophthalmol Vis Sci 38:267-273.

Vaney DI, Nelson JC, Pow DV (1998) Neurotransmitter coupling through gap junctions in the retina. J Neurosci 18:10594-602.

Vaney DI (1999) Neuronal coupling in the central nervous system: lessons from the retina. Novartis Found Symp 219:113-125.

Vaney DI, Weiler R (2000) Gap junctions in the eye: evidence for heteromeric, heterotypic and mixed-homotypic interactions. Brain Res Brain Res Rev 32:115-120.

Veenstra RD (2001) Determining ionic permeabilities of gap junction channels. Methods Mol Biol 154:293-311.

Vinken M, Vanhaecke T, Rogiers V (2003) The role of intercellular communication via "gap junctions" in disease. Ned Tijdschr Geneeskd 147:2463-2466.

Vis JC, Nicholson LF, Faull RL, Evans WH, Severs NJ, Green CR (1998) Connexin expression in Huntington's diseased human brain. Cell Biol Int 22:837-847.

Vorbrodt AW, Dobrogowska DH (2003) Molecular anatomy of intercellular junctions in brain endothelial and epithelial barriers: electron microscopist's view. Brain Res Rev 42:221-242.

Xin D, Bloomfield SA (1997) Tracer coupling pattern of amacrine and ganglion cells in the rabbit retina. J Comp Neurol 383:512-528.

Yancey SB, Biswal S, Revel JP. 1992. Spatial and temporal patterns of distribution of the gap junction protein connexin43 during mouse gastrulation and organogenesis. Development 114:203–212.

Wang Y, Rose B (1995) Clustering of Cx43 cell-to -cell chanells into gap junction plaques: regulation by cAMP and microfilaments. J Cell Sci 108:3501-3508.

Wassle H, Grunert U, Rohrenbeck J (1993) Immunocytochemical staining of AII-amacrine cells in the rat retina with antibodies against parvalbumin. J Comp Neurol 332:407-420.

Wassle H, Grunert U, Chun MH, Boycott BB (1995) The rod pathway of the macaque monkey retina: identification of AII-amacrine cells with antibodies against calretinin. J Comp Neurol 361:537-551.

Wei CJ, Xu X, Lo CW (2004) Connexins and cell signaling in development and disease. Annu Rev Cell Dev Biol 20:811-838.

Weiler R, He S, Vaney DI (1999) Retinoic acid modulates gap junctional permeability between horizontal cells of the mammalian retina. Eur J Neurosci 11:3346-3350.

Weiler R, Pottek M, He S, Vaney DI (2000) Modulation of coupling between retinal horizontal cells by retinoic acid and endogenous dopamine. Brain Res Brain Res Rev 32:121-129.

White TW. (2003) Nonredundant gap junction functions. News Physiol Sci 18:95-99.

Willecke K, Eiberger J, Degen J, Eckardt D, Romualdi A, Guldenagel M, Deutsch U, Sohl G (2002) Structural and functional diversity of connexin genes in the mouse and human genome. Biol Chem 383:725-737.

Williams CD, Rizzolo LJ (1997) Remodeling of junctional complexes during the development of the outer blood-retinal barrier. Anat Rec 249:380-388.

Williams RW, Strom RC, Goldowitz D (1998) Natural variation in neuron number in mice is linked to a major quantitative trait locus on Chr 11. J Neurosci 18:138-146.

Wolburg H, Lippoldt A (2002) Tight junctions of the blood-brain barrier: Development, composition and regulation. Vascul Pharmacol 38:323-337.

Zahraoui A (2004) Tight junctions, a platform regulating cell proliferation and polarity. Med Sci 20:580-585.

Zahs KR, Kofuji P, Meier C, Dermietzel R (2003) Connexin immunoreactivity in glial cells of the rat retina. J Comp Neurol 455:531-546

Zoidl G, Bruzzone R, Weickert S, Kremer M, Zoidl C, Mitropoulou G, Srinivas M, Spray DC, Dermietzel R (2004) Molecular cloning and functional expression of zfCx52.6: a novel connexin with hemichannel-forming properties expressed in horizontal cells of the zebrafish retina. J Biol Chem 279:2913-2921.